PORE-WATER FEEDBACKS AND RESILIENCE TO DECAY IN PEAT-FILLED BEDROCK DEPRESSIONS OF THE CANADIAN SHIELD

PORE-WATER FEEDBACKS AND RESILIENCE TO DECAY IN PEAT-FILLED BEDROCK DEPRESSIONS OF THE CANADIAN SHIELD

By Alex Furukawa, B.Sc

A Thesis Submitted to the School of Graduate Studies in Partial Fulfillment of the Requirements for the Degree of Master of Science

McMaster University Master of Science (2018) Hamilton, Ontario

(School of Geography and Earth Sciences)

TITLE: Pore-water Feedbacks and Resilience to Decay in Peat-filled Bedrock Depressions of the Canadian Shield

AUTHOR: Alex Furukawa, B.Sc

SUPERVISOR: Dr. J.M. Waddington

OF PAGES: 127

ABSTRACT

Northern peatlands are able to persist on the landscape and continue to accumulate carbon in the long-term thanks to a suite of ecohydrological feedbacks that confer resilience to disturbance such as the drier and warmer conditions associated with climate change. One feedback of particular interest operates between peat pore-water residence time and chemistry, whereby changes in hydraulic structure with depth restrict turnover in deeper layers, allowing decay end-products to accumulate and thermodynamically suppress decomposition. In this way, the burial of peat facilitates its continued recalcitrance. While this feedback has been observed in more extensive northern peatlands, at least on the side of carbon dynamics and geochemistry, there has been no observational study of profiles of pore-water residence time nor has it been assessed in smaller peat-forming systems. The peat-filled bedrock depressions of the Canadian Shield offered a unique opportunity to study this feedback in systems where primary peat formation occurs under geological constraints on growth in the form of the largely impermeable bedrock. These systems play important hydrological, biogeochemical and ecological roles on the landscape. Understanding their resilience on the landscape may reveal key insights into their evolution and their response to disturbance, which is increasing in the eastern Georgian Bay region. These systems have previously exhibited a hydrological feedback between water table depth and specific yield that varies with depression size. To assess the hydraulic structure that constrains pore-water transport to support continued recalcitrance, profiles of hydrophysical properties and pore-water residence time in four deep (>0.4 m mean depth) and five intermediate (<0.4 m) depressions. Hydraulic structure varied by depression size and depth in the profile, with very low hydraulic conductivities measured in the catotelms of deep sites. The two classes of depressions exhibited distinct hydrology, in the form of dampened water table fluctuations and hydraulic gradients in the deeper sites. Stable isotope analysis of δ^2H and $\delta^{18}O$ was used to estimate relative pore-water residence times using the simplified inverse transit time proxy (ITTP) for samples collected from May-August 2017. These estimates were observed to have similar controls to hydraulic structure and a close relationship with depth-averaged conductivity on a whole-site basis. While it was hypothesized that the catotelms of deeper depressions would have less pore-water turnover than that of shallower depressions, the ITTP was only able to differentiate between catotelm-acrotelm and deep-intermediate individually. The relative residence time of pore-water in deep catotelms based on δ^2H was longer than in intermediate

catotelms, but not significantly. These results broadly supported previous pore-water residence time work despite the likely ubiquitous promotion of turnover in the wetter-than-average study period. Carbon accumulation was quantified from extracted peat cores and pore-water chemistry was assessed as dissolved organic matter (DOM) quality using fluorescence spectrometry of monthly pore-water samples. Fluorescence and absorption indices varied by the same depression characteristics as hydraulic structure of site size and depth, but only the humification index exhibited significant temporal variation. Characterization of pore-water DOM was somewhat unclear across the seven indices calculated, although the DOM of intermediate sites appeared to be less humified, more recently produced and autochthonous in nature compared to deep sites Carbon accumulation was predominantly driven by the waterlogged, relatively stable carbon stored deep in the catotelm. Total carbon accumulated in the profile, and even more so the amount stored in the catotelm, were strongly related to depression depth. The thickness and carbon storage of the acrotelm was insensitive to depression morphology, with some intermediate sites being considered all acrotelm based on their water table behaviour. Overall, deeper peat-filled depressions showed stronger signs of the pore-water residence time-chemistry feedback, suggesting the carbon stored in their deep peat layers is more resilient to decay, by way of less conductive deep peat, longer relative pore-water residence times and more humified, less biologically active DOM. In order to comprehensively assess this feedback, longer stable isotope records are essential to ensure robust residence time estimates through differing moisture conditions, and a greater variety of depression sizes may allow for elucidation of threshold depression sizes where hydrological behaviours diverge. This study, at least on a categorical basis, can be used to inform conservation strategies of the relative vulnerability of these important reptile habitats and carbon stores, as well as guide restoration efforts to construct sufficiently deep, resilient systems.

TABLE OF CONTENTS

ACKNOWLEDGEMENTS

I would first like to thank my supervisor, Mike, for his support, openness to ideas and understanding throughout my time with the McMaster Ecohydrology Group. His undergraduate courses and invitation to join the lab opened my eyes to the opportunities of this interdisciplinary field. I would not be at this point in my academic career if not for his encouragement, amicable approach to supervision and patience throughout the development of this thesis. I appreciate allowing me to direct myself on a large part of this project, while helping lead me to the key questions to answer as well as to ask. Thank you for believing in me, even when our equipment was not always inspiring. I would like to say thank you to Paul, who also played a close supervisory role and always made time to consult him on matters of field logistics, lab analysis, statistics and the bigger picture as well. I might still be struggling to sort and analyze all of my data in Excel if not for your MATLAB expertise. It's safe to say that all of us owe much to your aid on matters covering the wide scope of the lab.

This work would not have been possible without all who contributed to the 2017 field season. Thank you all for your patience along the way as I figured things out and for sticking it out through the heat, bugs and rain to collect my many water samples. Every piezometer pumped, water level checked and sample filtered (sometimes frustrating slowly) deserves a 'thank you' in their own. To my fellow M.Sc students Jess, Danielle and Nicole, who made staying at good old Isabella far from gloomy (unlike the weather we often had). Thank you Jess for always keeping me on my toes with questions and lending so much of your time up in NOBEL and in the lab. Thank you Danielle, for not only offering transportation for the first month of the season but being there every step of the way, even as you had to tend to your auto-chambers for your work. To Nicole, for helping out during the early stages of piezometer installation and filling in for me as I figured out the Aqualog back at McMaster. To our undergraduate assistants Waverley and Taylor as well, thank you for the helping hands as you worked to elevate iWetland from its humble beginnings. In the following fall-winter, I would like to thank my undergraduate lab assistants Greg, Michelle and Becky for their help with K_{sat} and LOI.

Thanks go to our lab technicians, past and present. Cam, your help got my project off the ground in NOBEL, me headed in the right direction (literally) and the Picarro off on its first repair. You

always brought a good humour to your work, even when we had to put down our old lab van. To Craig, although your time with the lab was relatively short, you always brought a great attitude to the myriad of tasks you were given, including a big helping hand in some late, autumn field work and an expertise in all things GIS. To our GWF technicians Ian and Keegan, thank you for your lab assistance and troubleshooting of tech problems from the most delicate to deceptively simple. A big thank you goes out to my fellow lab mates, past and present. To Ben, who laid the groundwork in NOBEL and the Picarro as well as to Rebekah, Patrick and Kristyn for their valuable lab meeting input. To Sophie, our lone PhD student, but really so much more: acclaimed orator and Alberta coordinator, I'm always impressed by what you've accomplished in but a few years here. To Alanna, for introducing me to the NOBEL and the wonders of the Parry Sound region in my first year as your assistant, your passion for snakes and turtles has always underpinned just how important our work is in these systems. To our lab's other post docs and their guidance. Lorna, I thank you for your vegetation expertise and insight on the development of these peat-forming systems; the identification of my mosses is all thanks to you. To Chantel, who also guided me through my undergraduate thesis work and continues to pose thoughtful questions while never ceasing her crucial work with the turtles that call our sites home. Thanks go out to my collaborators outside of the McMaster Ecohydrology Group as well. To the McMaster Watershed Hydrology group, I would like to thank Nadine and Supriya for teaching me on all things fDOM, from running the Aqualog to calculating indices, and Dr. Sean Carey, an instructor on many occasions as well as an invaluable consult on residence time and commissioning our rainfall collectors. To the McMaster Research Group for Stable Isotopologues, Dr. Sang-Tae Kim and Martin, for their advice and patience as I got started with isotopic analysis to working with standards and running some our lab working standards. I would like to thank Dr. Carl Mitchell and Dr. April James for their references on IRIS and LMWL.

To my family and friends, thank you for your love and support behind following this path in science and putting up with my frequent absences throughout the summer whereupon I returned with bug bites and dirty field gear. To my parents, who provided care packages to fuel this research, permitted me to borrow the family van when the need arose and to store my peaty water samples in the fridge. Thank you to you all. I only hope that this work may do your collective contributions justice.

LIST OF TABLES

Table 3.2: General linear model of two variables of peat carbon related to site parameters of size, microtopography and depth. Three two-way interactions were included. Carbon accumulation failed to meet model assumptions and so had to be $\log_{10}$-transformed. P-values are **bolded** where significant to $p<0.01$, *italicized* where significant to $p<0.05$ and model performance was assessed as adjusted R^2.

Table 3.3: General linear models were used to assess the relationships of fDOM indices with parameters of site (deep or intermediate), microtopography (hollow or hummock), depth in the profile (acrotelm or catotelm), and the month of collection (May to August). Six two-way interactions were included. Freshness index, E2/E3 and BIX were $\log_{10}$- transformed to meet model assumptions, whereas HIX 2002 had to undergo a Box-Cox transformation ($\lambda=7$). P-values are **bolded** where significant to $p<0.01$, *italicized* where significant to $p<0.05$ and model performance was assessed as adjusted R^2.

Table 3.4: Spearman rank correlation was used to investigate relationships between site carbon accumulation measures and site morphological parameters. Spearman's ρ is displayed, **bolded** where significant to $p<0.001$ and *italicized* where significant to $p<0.05$.

LIST OF FIGURES

outliers. Letters denote significant differences (to $p<0.05$, by Tukey HSD) between groups not sharing a letter.

Figure 2.9: Boxplots depict differences in K_{Total} with depth and its interactions with depression size and microform (top to bottom). Boxes display the interquartile range, with crosses indicating outliers. Letters denote significant differences (to $p<0.05$, by Tukey HSD) between groups not sharing a letter.

Figure 2.10: Boxplots depict differences in porosity with depth and its interactions with depression size and microform (left to right). Boxes display the interquartile range, with crosses indicating outliers. Letters denote significant differences (to $p<0.05$, by Tukey HSD) between groups not sharing a letter.

Figure 2.11: Linear regressions were developed between site depth averaged K for hollow and hummock profiles with parameters of overall site size depicted top to bottom; mean depth (R^2=0.604, $p<0.01$ and R^2 = 0.666, $p<0.005$, respectively), maximum depth (R^2=0.63, $p<0.01$ and R^2= 0.765, $p<0.005$, respectively) and area (R^2= 0.597, $p<0.01$ and R^2= 0.388, $p<0.05$, respectively). Depth averaged K was the K_{total} at the most basal layer measured and was $\log_{10}$-transformed.

Figure 2.12: Boxplots depict differences in $ITTP_{\delta 18O}$ with microform, depth, site size x microform, site size x depth and three-way interactions between them all (left to right, top to bottom) Boxes display the interquartile range, with crosses indicating outliers. Letters denote significant differences (to $p<0.05$, by Tukey HSD) between groups not sharing a letter.

Figure 2.13: Boxplots depict differences in $ITTP_{\delta 2H}$ with site size, microform, depth, site size x microform, site size x depth and three-way interactions between them all (left to right, top to bottom) Boxes display the interquartile range, with crosses indicating outliers. Letters denote significant differences (to $p<0.05$, by Tukey HSD) between groups not sharing a letter.

Figure 2.14: Orthogonal regression was used to investigate the significant correlations between $ITTP_{\delta 2H}$ and measured hydrophysical properties. Bulk density was significant to $p<0.005$ whereas the measures of hydraulic conductivity were significant to $p<0.001$. Adjusted-R^2 values were 0.1254, 0.3504, and 0.3933 (top to bottom).

Figure 2.15: Profiles of relative pore water residence time, as estimated by the inverse transit time proxy (ITTP) from δ^2H are compared by microform (Hol and Hum) across four deep sites (234, 301, 408 and 415) and five intermediate sites (313, 405, 410, 416 and 502). Also plotted in cyan are the $ITTP_{\delta 2H}$ of outflow collected at the outlet of sites 234, 301, 313, 408, 410 and 415, which were observed to be 'spilling' for a majority of the 16-week study period.

Figure 3.1: Duplicate pore-water samples (n=5) were compared by all seven fDOM indices by orthogonal regression analysis to discern if one day storage in amber HDPE bottles had any appreciable impact on the fluorescence and absorbance signals measured. 'Field' denotes the sample originally collected and filtered in the field in June-August whereas 'Apt' denotes samples intentionally stored refrigerated in HDPE. Orthogonal regression equations are

displayed below each plot, where 95% confidence intervals all contained 1 for slope and 0 for the intercept.

Figure 3.2: Boxplots depict differences LOI of peat with site size, depth, the interactions between the two and the interaction between site size and microform (left to right, top to bottom) Boxes display the interquartile range, with asterisks indicating outliers. Letters denote significant differences (to $p<0.05$, by Tukey HSD) between groups not sharing a letter.

Figure 3.3: Boxplots depict differences of carbon accumulation to a given depth with depth in profile and its interaction with site size (left to right). Boxes display the interquartile range, with asterisks indicating outliers. Letters denote significant differences (to $p<0.05$, by Tukey HSD) between groups not sharing a letter.

Figure 3.4: Boxplots depict differences in pore-water DOM character by seven fDOM indices with site size. Boxes display the interquartile range, with asterisks indicating outliers. All comparisons displayed were significantly different by Tukey HSD ($p<0.05$).

Figure 3.5: Boxplots depict differences in pore-water DOM character by seven fDOM indices with depth in the peat profile. Boxes display the interquartile range, with asterisks indicating outliers. All comparisons displayed were significantly different by Tukey HSD ($p<0.05$).

Figure 3.6: Boxplots depict differences in pore-water DOM character by five fDOM indices determined by general linear model analysis to vary significantly by the interaction between site size and depth.. Boxes display the interquartile range, with asterisks indicating outliers. Letters denote significant differences (to $p<0.05$, by Tukey HSD) between groups not sharing a letter.

Figure 3.7: Boxplots depict differences in the degree of humification of pore-water DOM using the humification index (HIX 2002) with month of sampling in 2017. Boxes display the interquartile range, with asterisks indicating outliers. Letters denote significant differences (to $p<0.05$, by Tukey HSD) between groups not sharing a letter.

Figure 3.8: Linear regressions between carbon accumulation (in kg m^{-2}) and the maximum depth measured in each depression are displayed as totals ($p<0.001$, $R^2=0.826$) and divided up into the respective site's acrotelm ($p=0.463$, $R^2=0$) and catotelm ($p<0.001$, $R^2=0.855$). This analysis was repeated for the subsets of the hollow and hummock microforms for total carbon ($p<0.001$, $R^2=0.818$ and $p<0.001$, $R^2=0.825$, respectively), acrotelm carbon ($p=0.316$, $R^2=0.02$ and $p=0.888$, $R^2=0$, respectively) and catotelm carbon ($p<0.001$, $R^2= 0.821$ and $p<0.001$, $R^2=0.894$, respectively).

Figure 3.9: The proportion of total carbon stored in the acrotelm was related to site depth for all peat profiles ($p<0.001$, $R^2=0.583$) and when considering hollows ($p<0.01$, $R^2=0.644$) and hummocks ($p<0.05$, $R^2=0.464$) separately.

CHAPTER 1: INTRODUCTION

1.1 Northern peatlands

Northern peatlands are significant carbon sinks that are estimated to have stored 455 Pg of carbon globally (Gorham, 1991) and regionally cover 17% of Canada's land area (Kuhry et al., 1993). However, their continued role in sequestering carbon is uncertain in the face of disturbances such as climate change (Belyea and Malmer, 2004) due to the effect of higher temperatures and evaporation promoting carbon loss by peat decomposition (Bragg, 2002; Moore et al., 2007). Peatlands can be considered fairly resilient thanks to a number of autogenic, hydrological feedbacks that modulate their response to external forcings, as well-discussed in Waddington et al. (2015). These feedbacks intimately link the carbon and water balances of peatlands with hydrological measures, namely water table depth (WTD). While the synthesis of Waddington et al. (2015) articulated a number of these feedbacks as well as their direction and relative magnitude, the authors highlighted a need to assess these feedbacks quantitatively among varying peatland types and climatic regions. Addressing this need is crucial in order to identify peatlands that may be particularly vulnerable to intensifying external forcings of climate and anthropogenic activity, and those that are resilient enough to persist on the landscape long-term.

1.2 Peat-filled bedrock depressions

The majority of studies relevant to peatland hydrology and their carbon dynamics have focused on larger northern peatland systems (Belyea and Malmer, 2004; Bubier et al., 2003; Charman et al., 1994; Vitt et al., 2000), but considerably less attention has been given to smaller peat deposits. The bedrock depressions of the Canadian Shield comprise a landscape of ongoing primary peat formation on the bare rock, offering a unique opportunity to study small-scale peat formation (Devito et al., 1989; Phillips et al., 2011). While individually small in areal coverage, the Canadian Shield that underlies these peat-accumulating depressions spans approximately one-third of Canada's land surface (Spence and Woo, 2008). These systems play a significant role in the hydrology of the landscape, may be considered important points of biogeochemical activity and serve as habitat for a wide variety of fauna. Bedrock depression wetlands differ from conventional northern peatlands through the constraints imposed by their geology by the fact that the bedrock limits the minimum WT. It serves as a largely impermeable boundary that limits any

water input to precipitation and lateral inflow from its catchment area, which may include upslope depressions (Spence and Woo, 2006). Preliminary work on water storage dynamics (Didemus, 2016; Smolarz, 2017) has been undertaken on the depressions found on the rock barrens of eastern Georgian Bay (Catling and Brownwell, 1999), a particular hotspot for the ecological significance of these systems. These systems are of concern due to encroaching anthropogenic development and the sensitivity of their WT to climatic conditions (Didemus, 2016), which may leave them more vulnerable to predicted increases in droughts (Meehl and Tebaldi, 2004).

1.2.1 Hydrological function

The peat-forming bedrock depressions of the Canadian Shield serve as an intermittently connected network of water storage basins in northern catchments that exhibit what has been named "fill and spill" (Spence and Woo, 2006, 2003). By this mechanism, a depression will store received water from rainfall or surface flow until a threshold capacity is reached. After this point any further supplied water becomes runoff that may contribute to downslope depressions (Oswald et al., 2011; Spence and Woo, 2006, 2003). The hydrophysical properties of the largely organic material filling the depressions act as controls on the capacity and responsiveness of the storage basins to input, in addition to the vegetation (Brooks and Hayashi, 2002). This threshold-like behaviour for hydrological connectivity acts to modulate runoff across Precambrian Shield landscapes (Allan and Roulet, 1994; Frisbee et al., 2007; Phillips et al., 2011). These landscapes consist of complex, heterogeneous basins that make streamflow prediction difficult, but these bedrock depressions may provide insights with regards to controls on hydrological connectivity (Bracken and Croke, 2007) and potentially broader frameworks of topography, topology and typology (Buttle, 2006).

1.2.2 Biogeochemical function

While the role of larger northern peatlands in biogeochemical cycling is well understood (Bullock and Acreman, 2003; Gorham, 1991), relatively less attention (and protection) has been given to smaller organic deposits, in particular those that lack persistent connectivity to surface water systems. The peat-forming bedrock depression of the Canadian Shield are considered "geographically isolated wetlands" (GIW) as defined by Tiner (2003). Contrary to the name, this

classification encompasses wetlands across a continuum of landscape connectivity despite being surrounded by uplands locally (Mushet et al., 2015; Rains et al., 2016). Hydrological, biogeochemical and ecological functions of GIWs are asserted in the review by Cohen et al. (2016); most apply to wetlands in general but the characteristics of GIWs make them particularly powerful in their biogeochemical role. Their nutrient retention capabilities are facilitated by high primary production and prevalence of anaerobic soils (Jordan et al., 2011; Marton et al., 2015), abundance and position on the landscape to interact with runoff first (Cohen et al., 2016; Whitmire and Hamilton, 2005), small size (Ghermandi et al., 2010), and longer residence times stemming from their inherently less consistent connectivity (Holland et al., 2004; Werner and Kadlec, 2000). Rather than being purely "hot spots" of biogeochemical activity, GIWs and especially peat-forming bedrock depressions may be considered "cold spots" in some important respects, so the recent concept of ecosystem control points (Bernhardt et al., 2017) may be a more appropriate descriptor for their influence on ecosystem fluxes. While their connectivity by means of water may be intermittent, the ecological connectivity of these wetlands may not abide by the same criteria (Leibowitz, 2009), but if the two are intimately linked, it presents a significant collaboration opportunity between the fields of ecology and hydrology.

1.2.3 Ecological function

GIWs, such as those considered ponds and pools, are important ecologically not only for their plurality across landscapes, but for the diversity contained within each of them (De Meester et al., 2005). From a conservation perspective, this is further highlighted by their relevance to their crucial role in the life cycle of many herpetofauna (Gibbons, 2003; Johnson, 2000), the group of animals including reptiles and amphibians that is facing widespread decline (Gibbon et al., 2000). In a regional context in Ontario, the peat-filled depressions found on the Canadian Shield rock barrens serve as crucial hibernation habitat for the threatened Eastern Massasauga Rattlesnake (*Sistrurus catenatus*) (Harvey and Weatherhead, 2006; Smolarz et al., 2018) and nesting sites for the threatened Blanding's Turtle (*Emydoidea blandingi)* (Markle and Chow-Fraser, 2014; Smolarz, 2017).

1.3 Hydrological feedbacks in bedrock depression systems

The dominant role of *Sphagnum* mosses in larger boreal peatlands (Johnson et al., 2015; Turetsky, 2003) extends to the smaller bedrock depression systems, suggesting that many of the ecohydrological feedbacks associated with *Sphagnum* (Moore et al., 2015; Waddington et al., 2015) also apply. However, it remains uncertain which of these feedbacks are present amongst these smaller systems, and to what strength they operate. Previous work on investigating one of these feedbacks in peat-filled bedrock depressions focused on the feedback between WTD and specific yield, whereby shallower depressions exhibited lower specific yield and greater WT variability, highlighting depression depth as a potential control on the systems' resilience (Didemus, 2016).

1.3.1 Pore-water chemistry- residence time feedback

The feedback identified by Waddington et al. (2015) that is of particular relevance to smaller peat-forming systems is the WTD-peat decomposition feedback (Figure 1.1), specifically the interaction between water residence time and pore-water chemistry. As a peatland develops, underlying peat undergoes structural changes due to the weight of the added material as well as decomposition that lead to alteration of hydrophysical properties such as hydraulic conductivity (Belyea and Clymo, 2001; Grover and Baldock, 2013; Ivanov, 1981). Pore-water movement by advection is thus progressively slowed with depth which facilitates conditions in deeper peat layers that thermodynamically suppress further decomposition (Beer et al., 2008; Beer and Blodau, 2007). In effect, increases in decomposition at the surface by drier or warmer conditions lead to longer pore-water residence time in deeper peat layers that slow any further decay in the catotelm, the deeper, permanently saturated layers as defined by Ingram (1978). Simplified hydrological modelling work by Morris and Waddington (2011) in theoretical peatlands suggest that larger peatlands experience less pore-water turnover in their deeper layers, conferring a greater resilience to external forcings that may enhance decomposition. This feedback, however, is not well observed in natural peatland systems apart from the original pore-water chemistry work conducted by Beer et al. (2008), let alone any assessment of the influence of peatland size on its strength.

1.4 Thesis Objectives

Most research effort on carbon accumulation and hydrological feedbacks in peatlands have focused on more extensive northern peatland systems compared to the smaller organic deposits such as those found on the rock barrens of the Canadian Shield, despite sharing a foundation in *Sphagnum* moss as their respective ecosystem engineers. These bedrock depression-based wetlands play an important hydrological role in runoff generation and connectivity on the landscape and act as ecosystem control points with regards to biogeochemical cycling and ecological significance to locally threatened reptile species at risk. In the eastern Georgian Bay region, peat-filled depressions face direct loss by anthropogenic development and as smaller systems may be more vulnerable to climate forcings. An understanding of the hydrological feedbacks present within peat-filled depressions is needed to assess their vulnerability to future climate change as well as to inform habitat restoration initiatives on the key parameters that control feedback strength to build resilient, cost-effective habitats. This study focuses on the residence time-chemistry feedback identified by Waddington et al. (2015) as it plays a crucial role in long-term persistence and carbon accumulation on the landscape by suppressing further peat decomposition. Peat-filled bedrock depressions present a unique opportunity to observe primary peat formation and the development of hydrological feedbacks across depressions limited by their size and depth. The peat hydrophysical properties that control water movement and thereby pore-water turnover were quantified through peat profiles of varying depth. A stable isotope approach was employed to estimate pore-water residence time with depth in order to assess relationships with peat properties as well as higher order controls at the site level in Chapter 2. Carbon accumulation among different sized depressions was quantified and the pore-water chemistry through these peat profiles was characterized through the lens of dissolved organic matter (DOM) quality by fluorescence spectroscopy in Chapter 3.

1.5 FIGURES

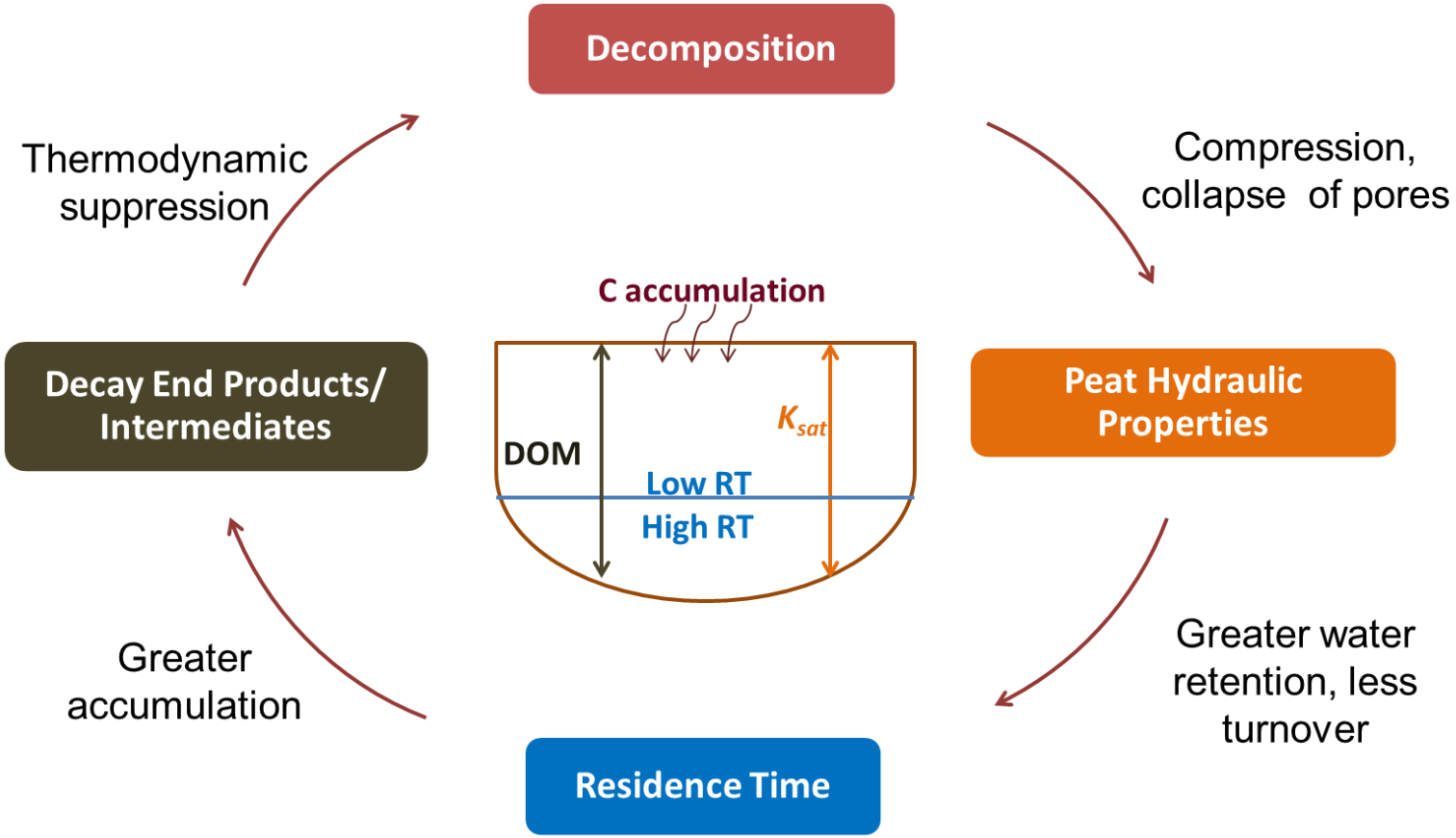

Figure 1.1: A conceptual model of the feedback between pore-water residence time and chemistry that confers a biogeochemical resilience to decay to northern peatlands. From top, clockwise, a forcing that enhances decay at the surface will lead to deposition of the decayed litter as peat in lower layers (catotelm). This decay and burial alters the hydraulic properties of the underlying peat by the compression and collapse of pores. Lower hydraulic conductivities in the catotelm result in reduced advective transport of pore-water and less turnover, observed as longer residence times with depth. Since the pore-water remains largely stagnant in the waterlogged conditions of the catotelm, end-products of decay may accumulate, which in turn thermodynamically suppress anaerobic decay by making them less energetically favourable (based on the work of Beer and Blodau (2007), Beer et al. (2008) and Morris and Waddington (2011).

CHAPTER 2: PEAT HYDROPHYSICAL PROPERTIES AND ISOTOPIC CHARACTERIZATION

2.1 INTRODUCTION

2.1.1 Peat hydrophysical properties and water movement in peatlands

The evidence for a biogeochemical resilience to decomposition in peatlands by Beer et al. (2008) is largely hydrological in basis; the accumulation of decay end products to thermodynamically suppress decay in deeper peat layers is facilitated by the dominance of slow diffusive pore-water transport over advective mechanisms (Beer and Blodau, 2007). Slowed movement of pore-water and thus, longer residence times, is crucial to allow for the accumulation of these end-products that permit the continued recalcitrance of peat. If pore-water is permitted to reach these deeper layers by vertical flux, as has been observed in peatlands (e.g. Siegel et al., 1995), the accumulation of decay—limiting phenolics, DIC and other end-products (Conrad, 1999; Ivarson, 1977) would not be possible. Furthermore the depletion of nutrients and electron terminal acceptors (Wickland and Neff, 2008) would be disrupted by the influx of more labile organic material from higher in the peat profile, which could instead stimulate microbial activity (Aravena et al., 1993; Charman et al., 1994).

Peatland hydraulic structure (as per Baird et al., 2008) serves as one of the primary controls on pore-water residence time, as modelled by Morris and Waddington (2011), where variation in hydraulic conductivity (K) among model peatlands of the same size yielded contrasting residence time distributions. Profiles of K with depth can vary considerably from the intuitive decrease with depth (Price et al., 2003; Whittington et al., 2007); Chason and Siegel (1986) observed no correlation between the two. Non-linear decreases up to four orders of magnitude have been measured in a Canadian peatland by Fraser et al. (2001), while contrasting C-shaped profiles were observed in European peatlands (Waddington and Roulet, 1997). Pore-water movement in the catotelm of northern peatlands is typically limited by very low K (Beckwith et al., 2003), but there is potential for macropore-mediated flow deep in peat (Chason and Siegel, 1986) to cause such patterns. Since peat-forming bedrock depression systems only receive input from rainfall

and runoff inflow, the K of the deep peat layers as well as through the flow path from the surface to these layers should influence pore-water turnover, or lack thereof.

Peat hydraulic structure is not limited to variation with depth; it may also vary spatially across peatlands, namely between microforms (Johnson et al., 1990). Microforms are features typically 1-10 m in length that comprise a continuum of higher elevation hummocks to low –lying hollows that have characteristic vegetation (Andrus et al., 1983) and play important roles in peatland hydrological and biogeochemical function (Baird et al., 2013). Lateral spatial variability has been observed in peatlands (Surridge et al., 2005) that has been attributed to plant communities (Whittington et al., 2007) and the differing ability of *Sphagnum* species to maintain their pore size structure (Johnson et al., 1990). Vascular plants also present a potentially powerful control on K due to the dominance of macropores for water flow (Carey et al., 2007; Holden et al., 2001). In raised bogs, the hydraulic conductivity has been found to be significantly lower at the margins compared to its middle (Baird et al., 2008). Branham and Strack (2014) investigated the variation of hydrophysical properties across several peatlands and discerned climate, peatland type, microform, and depth to significantly explain variation in K, which was related to other physical parameters such as bulk density, macropore frequency and degree of humification (von Post).

The driver of pore-water movement, the hydraulic gradient, should also exert a control on residence time and itself is driven by seasonal climate conditions (Siegel et al., 1995; Waddington and Roulet, 1997) and limited by hydraulic properties of the medium, namely K. With regards to pore-water chemistry, climate driven flushing has been noted to be significant when hydraulic gradients shift in the long term (Romanowicz et al., 1993).

2.1.2 Isotope hydrology

Isotope hydrology entails the use of isotopes of water or its solutes as tracers for the estimation of the age of water, its sources and movement throughout the hydrological cycle. The stable isotopes of oxygen and hydrogen that comprise water are ideal conservative tracers as they are not reactive (Clark and Fritz, 1997); the most commonly used are ^{18}O and ^{2}H, respectively. The only way that the isotopic composition of some water may change is by the isotopic fractionation

that accompanies processes such as evaporation/condensation whereby lighter isotopes are preferentially evaporated, leading to enrichment of remaining water (with the converse for condensation) (Hoefs, 2009) and if that water undergoes mixing with water of differing isotopic composition (Ferronsky and Polyakov, 2012). In a northern peatland context, stable isotopes of water have previously been used to trace the hydrological functions of land cover in peat-dominated catchments (Hayashi et al., 2004) as well as seasonal groundwater recharge in northern fens and bogs from dual-isotope vertical profiles of pore-water (Levy et al., 2014).

2.1.2.1 Stable isotope analysis of water

Stable isotope analyses of water have been conducted by traditional isotope ratio mass spectrometry (IRMS) for decades (Brand, 2004; Werner and Brand, 2001), providing a high degree of precision and accuracy that has been invaluable to the field of isotope hydrology in addition to other earth and aquatic sciences. However, these systems carry the caveats of high start-up and operational costs, large size and the requirement of stringent climate control that may render them unsuitable for many laboratories that are not sufficiently equipped or specialized in isotopic analysis. Additionally, IRMS requires that hydrogen and oxygen be measured separately and in their gaseous phases. While techniques for simultaneous extraction (into H_2 and CO) exist (Gehre et al., 2004), equilibration techniques typically are needed to convert water to CO_2 (Epstein and Mayeda, 1953) and H_2 (Ohsumi and Fujino, 1986) separately.

An alternative method was published by Kerstel et al. (1999) that enabled the simultaneous measurement of $\delta^{18}O$ and $\delta^{2}H$ in water vapour based on low-pressure gas-phase infrared absorption spectra that are assigned to unique isotopic species, which came to be known as stable isotope ratio infrared spectroscopy (IRIS) (Chesson et al., 2010). This technique does not require the sample preparation steps associated with IRMS, permitting the direct measurement of water vapour (or liquid water that is flash-vaporized) on instruments that are comparably inexpensive and compact compared to IRMS systems, while offering comparable accuracy and precision (Chesson et al., 2010; Gupta et al., 2009; Lis et al., 2008; Penna et al., 2010). These systems do carry trade-offs, as IRIS measurements have been observed to be sensitive to organic contamination (Brand et al., 2009), requiring that natural water samples in particular be screened to detect potential contamination (such as the software tool ChemCorrect by Picarro, Inc),

appropriate corrections be applied or the sample be treated to otherwise reduce the organic contaminants (Chang et al., 2016; Schmidt et al., 2012). Additionally, memory effects from previously injected samples and drift of the isotopic signal over time are both concerns that require analysis to include appropriate processing of raw data in order to correct for these effects and normalize to the standard Vienna standard mean ocean water (VSMOW) (van Geldern and Barth, 2012).

2.1.2.2 Applications: Residence time

Pore-water turnover rates, and residence time, were both originally asserted to be crucial to permitting the biogeochemical resilience to decay observed by Beer et al. (2008) and Beer and Blodau (2007). The residence time refers to the length of time a molecule of pore-water would spend in a particular reservoir and was modelled as a tracer half-life by Morris and Waddington (2011). The use of stable isotopes as tracers to model residence times has received considerable attention (de Dreuzy and Ginn, 2016; McGuire and McDonnell, 2006) in the field of hydrology due to its nature as a composite metric of a system, providing insights into flow paths, storage and biogeochemical activity (Burns et al., 2003). Modelling approaches vary, but typically entail the use of parallel time series of input (precipitation) and output with lumped parameter models that use convolution integrals to account for the dampening and time lag of input to output tracer signal. This method, as well as numerous examples of applications of this technique, are reviewed in McGuire and McDonnell (2006). Most instances of this approach are geared towards streamflow, or assessing residence time on a catchment scale (McGuire et al., 2005; Soulsby and Tetzlaff, 2008; Tekleab et al., 2014). For peatlands, other tracers such as iodide (Postila et al., 2015) and tritium (^{3}H) (Cartwright and Morgenstern, 2016; Mažeika et al., 2009) have been applied in a similar manner. Stable isotopes of water have indeed been used to investigate the hydrology of peatlands (Carrer et al., 2016; Levy et al., 2014), but observational studies of peat pore-water residence time profiles have been notably absent from the literature (Morris and Waddington, 2011).

2.1.2.3 Applications: Meteoric water and hydrologic partitioning

One of the key relationships in isotope hydrology is the linear correlation, $\delta^2H = 8\ \delta^{18}O + 10$ which describes the relationship between isotopes of hydrogen and oxygen in natural waters, reported by Craig (1961) as the global meteoric water line (GMWL). On a local scale, precipitation typically delineates its own local meteoric water line (LWML) whose slope and intercept may differ from the GMWL as a function of altitude, latitude, precipitation amount and continental effects (Clark and Fritz, 1997; Gat and Tzur, 1967). As previously stated, evaporative processes are the dominant source of isotopic enrichment in natural waters, with the potential to influence both source and surface waters and cause them to plot to the right of the LWML (Clark and Fritz, 1997). The LMWL may be treated as a reference point, upon which surface water may plot along a local evaporative line (LEL) away from the meteoric line to indicate evaporative processes had occurred along its flow path (Rock and Mayer, 2007). Plotting in this δ^2H -$\delta^{18}O$ space may also be used to assess spatiotemporal patterns in source-water contributions of surface water (Mountain et al., 2015). Long-term monitoring of isotopes of water for this purpose may be especially valuable to elucidate watershed input timing and patterns that may not be picked up by regular hydrometric analysis (England, 2017).

2.1.3 Hypotheses

To further understanding of resilience to decomposition in peat-filled depressions by way of the pore-water residence time, we characterized the hydrophysical properties of peat profiles in two microforms in two sets of depressions constituting deep and intermediate size classes. It was hypothesized that site size and depth act as controls on hydraulic structure, whereby deeper depressions should slow vertical pore-water flux by way of lower K and porosities. Stable isotope characterization was performed for pore-water, rainfall and outflow collected weekly for the bulk of the growing season (May through August) to estimate the residence times that permit biogeochemical resilience to decay in deep peat layers. Residence times were hypothesized to be controlled by depth and site size in accordance with hydraulic structure, whereby less turnover takes place in deep depressions to allow decay end-products to accumulate and suppress further decay in the catotelm.

2.2 METHODS

2.2.1 Study area

This research was undertaken in the Dinner Lake area of the Northern Ontario Barrens and Bog Ecosystems Landscape (NOBEL). This area is located approximately 20 km north of the town of Parry Sound, ON (Figure 2.1) and has been the site of previous research including the investigation of water table dynamics of peat-filled bedrock depressions (Didemus, 2016) as well as habitat suitability for reptile species-at-risk (Smolarz, 2017). The NOBEL is characterized by granite barrens with moss or lichen cover (Catling and Brownwell, 1999) and is located in the Georgian Bay fringe physiographic region (Chapman and Putnam 1984). While the upland ridges feature these bedrock barrens, the lowland valleys may consist of mixed forest, expansive peatlands and beaver ponds The terrain at NOBEL is comprised of a system of ridges and trenches that span roughly east to west and serve as the basis for site numbering, whereby site names range from 200 (most northerly) to 500 (most southerly) for the ridges.

The climate of the NOBEL consists of warm summers (daily average temperature from 16.2 to 18.9°C) that often include periodic drought and mild to cool winters (daily average temperature from -11.1 to -6.7°C), as well as a wet spring and fall (237 mm and 347 mm of rainfall, respectively) (Environment Canada, 2018). The growing season is relatively long at 190-200 days. There is evidence of past fire on the landscape in the form of ash layers at the bottom of intermediate depressions (Didemus, 2016); these natural and anthropogenic fires are believed to have played a role in the vegetation cover of this landscape, though there has not been a major fire recorded in nearly 60 years (Catling and Brownwell, 1999) As a result of these conditions, soils, if present, are generally slow-to-accumulate, shallow and nutrient-poor Brunisols that along with the moisture conditions, limit vascular vegetation growth (Catling and Brownwell, 1999). Deciduous trees, such as oak and red maple, are typically limited to woodland patches within the deeper mineral soils found in the wetter valleys or bedrock cracks. *Pinus backsiana* (Jack Pine), however, is found among the driest areas as well as along the margins of, and sometimes within, the depression-based wetlands scattered throughout the landscape (Catling and Brownwell, 1999).

The wetlands in the NOBEL range from small pits on the ridges with up to 0.2 m of soil, overlain by lichen and *Polytrichum* moss, to extensive permanent peatlands found in the valleys between ridges. While these wetlands vary in size, depth, moisture regime and vegetation, they are all essentially bedrock depressions that serve as important interception reservoirs on this landscape (Didemus, 2016). They are assumed to have negligible drainage through the bedrock itself due to the low permeability of the smooth granite and gneiss of the Canadian Shield with minimal fracturing (Freeze and Cherry, 1979). The impervious nature of the bedrock is responsible for moisture extremes of both kinds; periodic summer drought in the most shallow depressions and moisture retention in deeper depressions that facilitates peat accumulation (Catling and Brownwell, 1999). The peat-filled bedrock depressions of interest for this study include five sites with a mean depth under 0.4 m (hereafter referred to as "intermediate" sites) and four deeper depressions greater than 0.4 m average peat depth that could be considered small bogs (hereafter referred to as "deep" sites) (Table 2.1).

The deep sites (234, 301, 408 and 415) were typically dominated by a cover of *Sphagnum* mosses throughout their interiors, with some mosses of the genus *Polytrichum* were found along the margins. Trees were not common within the depression itself but instead were largely found in and around the margins, with the majority being *Pinus Backsiana* along with a smaller fraction of *Pinus strobus* (Eastern White Pine) and some individuals of *Larix laricina* (Tamarack). The shrub cover in these sites consisted largely of *Chamaedaphne calyculata* (Leatherleaf) along with some *Vaccinium angustifolium* (lowbush blueberry) and *Kalmia polifolia* (bog-laurel) (Didemus, 2016). The intermediate sites (313, 405, 410, 416 and 502) varied considerably in their vegetation patterns. While sites 410, 416 and 502 were structured relatively similarly to the deep sites in having trees largely restricted to their margins, sites 313 and 405 were more like wet woodlands with trees found throughout the site. Moreover, the smaller sites had a much greater cover of *Polytrichum* mosses and their shrub cover was largely restricted to smaller species such as blueberry and graminoids. Specifics of the moss species cover at the two microforms of interest based on surface samples collected (see 2.2.4) are included in Table 2.2.

2.2.2 Site characterization

The perimeter and area of each depression was initially mapped using the perimeter-walk feature on a Garmin eTrex 20 handheld GPS (Garmin Ltd., Olathe, KS, USA, accuracy: 4 m) by walking around each peat-filled bedrock depression along its sill. However, the finest distance interval for plotting tracks was 10 m, which proved too coarse for the smaller sites. As such, the site perimeters were delineated digitally using an ArcGIS Web Application by the West Parry Sound Geography Network (WPSGN), which uses 0.2 m resolution aerial imagery from the 2016 Central Ontario Orthophotography Project. Triplicate perimeters were drawn and the resulting measurements averaged to account for any inconsistencies with manual digitization Perimeter and area were computed using the application's measurement tool. These estimates were generally in agreement with those derived by GPS and so were used going forward given the greater precision for perimeter delineation.

The distribution of peat depths at each site was surveyed using two pairs of orthogonal transects, with the first intended to capture the longest dimension of the bedrock depression at each site. At one meter intervals for intermediate sites and two meter intervals for deep sites, peat depth was measured with a rebar inserted into the peat until the bedrock was reached, and the relative elevation was measured with a Smart Leveler digital water level (Digital Leveling Systems Inc., Smyrna, TN, accuracy: 2.5 mm). A stable reference, either in the center, or on the margins of the depression, was measured at the beginning and end of each transect to establish a datum for each site and correct for any drift as one moved across the site. The Smart Leveler was also used to measure the relative elevations of the installed piezometers and groundwater wells (see 2.2.4) in order to compare their measurements to the same datum. The largest site, 408, was only surveyed for peat depth and at a coarser resolution of four meters, as its size was beyond the lateral measurement range of the Smart Leveler. For site 234, depths were taken from previous work by Didemus (2016), as the high water table presented logistical problems for surveying without damaging the peat or equipment.

2.2.3 Field hydrological data

Groundwater wells constructed of 0.05 m diameter PVC were installed in all nine sites to continuously monitor water table depth (WTD) every ten minutes using Solinst Levelogger

Junior pressure transducers (Solinst Canada Ltd, Georgetown, ON) for which data was available since May 2016, corrected for variation in atmospheric pressure using a Barologger Edge barometric logger (Solinst Canada Ltd, Georgetown, ON). WTD data from a relatively dry year in 2016 was used to discern the portions of the peat profile in each depression that could be considered acrotelm or catotelm, as being within the range of variation of the WT or continuously saturated, as per the traditional diplotelmic model (Ingram, 1978). The boundary between the layers in this case was considered to be one standard deviation below the mean water table of each site for the growing season (May to October).

Tipping bucket rain gauges (TE525M-Campbell Scientific, Logan, UT, USA) connected to Campbell Scientific CR10X or CR100 dataloggers were used to monitor rainfall at sites 234 and 415.

In late April to early May 2017, piezometer nests were installed in a representative hollow and hummock microform at each site to enable sampling of peat pore-water at discrete depths and also facilitated monitoring of the relative hydraulic head. Piezometers were constructed from 0.025 m diameter PVC with approximately 0.1 m of slotted openings centered on the depth of interest below the surface, covered with a sediment screen and installed to sample depth intervals of 0.2 m below the surface (Table 1). Exceptions to these increments were made to accommodate sampling the deepest point possible in each microform in sites 301 (deepest piezometer installed to a depth of 0.87 m in the hollow microform), 408 (deepest piezometer installed to a depth of 1.6 m after the 1.2 m depth in the hummock microform), and 502 (deepest piezometer in the hollow microform was installed to 0.3 m. Relative hydraulic head was measured weekly using a Solinst Model 107 TLC (Temperature, Water Level and Conductivity) Meter; these were then referenced to each site's common datum. Hydraulic gradients through the peat profile in each microform were then calculated for each week simply by the slope of the linear regression between hydraulic head and depth.

Saturated hydraulic conductivity (K_{sat} in m s^{-1}) was measured in-situ by performing a slug test in each piezometer whereby a solid slug was introduced by addition of a Solinst Levelogger Junior pressure transducer which was then used to monitor the water level. The Levelogger induced a

change in hydraulic head of 0.095 m that was monitored at a frequency of 1-2 Hz for near-surface (0.2-0.4 m) piezometers and 0.1-1 Hz for deeper (>0.4 m) piezometers. Slug tests for deeper piezometers sometimes spanned over a day to allow for adequate recovery, in which case another Levelogger was suspended in air in piezometer casing nearby to measure the atmospheric pressure to correct for diurnal variation. Slug test data was analyzed using the Hvorslev (1951) method:

$$K_{sat} = \frac{r^2 \ln (L/R)}{2\, L\, T_L}$$

Where: r is the effective (inner) radius of the piezometer (in meters), L is the screen length, R is the outer radius of the piezometer (in meters) and T_L is the time lag when the normalized displacement $h_t/h_0 = 0.37$, where h_t is the displacement at time t and h_0 is the initial displacement.

The total or depth-averaged hydraulic conductivity (K_{Total}, in m s^{-1}) through each microform was estimated using a derivation of Darcy's law for conductivity through soil layers of differing hydraulic conductivity; K_{sat}: $K_{eff} = \Sigma L/\Sigma(L_i/K_i)$ where L_i is the thickness (in meters) of each layer, i represented by the piezometers and K_i is the corresponding saturated conductivity derived from the slug test(s) performed in that piezometer. In cases where multiple successful slug tests were conducted, the arithmetic mean was used. Layer thicknesses were generally 0.2 m in accordance with the depth increments installed, but were either smaller in the case of the piezometers installed at 0.3 m in site 502, or 0.87 m in site 301. In cases where slug tests could not be performed successfully, data was supplemented with K_{sat} for the same depth measured ex-situ by the falling or constant head method from extracted peat cores (see 2.2.6); this was the case for a few near-surface (0.2 m) piezometers. In the case of the deepest piezometer at 1.6 m at site 408, it was simply assumed that the hydraulic conductivity was equivalent to the layer above where data was available, as the two shallower depths were also within an order of magnitude. The purpose of this K_{Total} for each profile was to obtain a measure of the total resistance to any new infiltrating water (rainfall or run-in) to reach a certain depth in the peat profile, where the deepest piezometer increment was treated as the basal layer.

Ceramic cup suction lysimeters (Soilmoisture Equipment Corp., Goleta, CA, USA) were also installed starting from late May alongside some of the near-surface piezometers (Table 2.1) in order to continue to sample the peat pore-water when the water table periodically fell below these depths. These lysimeters were first 'primed' by pressurizing to -60 kPa and emptying three times after installation before being used for sampling.

2.2.4 Peat core collection

Near-surface peat cores were extracted by hand-cutting from each site as approximately 0.1 m x 0.1 m blocks of varying height and stored in Tupperware containers to maintain peat structure. These blocks were used to sample the top 0.4 m, including the living moss layer. A Russian peat corer (AMS, Inc., American Falls, ID, USA) was used to extract samples at greater depths. If intact, the hemispherical cores were transferred to 0.05 m diameter PVC casing and wrapped in plastic wrap. Otherwise, peat samples that were too small or lacked the structure for the aforementioned options were simply bagged. All samples were kept cool before being frozen back at the McMaster University Ecohydrology Lab. Intact surface samples were retained at each site-microform to identify the moss species cover (Table 2.2). The larger near-surface cores were cut into ~0.05 m thick slices, thawed, and cut to fit into 0.08 m diameter stainless steel rings made by METER Group (METER Group, Inc., Pullman, WA, USA). These samples underwent the following analyses: saturated hydraulic conductivity, bulk density, and loss on ignition (LOI) (see 2.2.6 for methods). The PVC-bound cores underwent the same analyses except for saturated hydraulic conductivity. Bagged peat samples were analyzed for bulk density, von Post, and LOI.

2.2.5 Peat hydrophysical properties laboratory analyses

In addition to the K_{sat} assessed in-situ via slug tests conducted in installed piezometers, it was also measured ex-situ, by falling and constant head tests performed on intact peat cores on the KSAT device (METER Group, Inc., Pullman, WA, USA).

Cores for ex-situ K_{sat} analysis were first saturated for at least 48 hours before being run on the KSAT. This device uses Darcy's Law to measure hydraulic conductivity as a column of water is passed through the sample by continuously measuring pressure head (to nearest 1 Pa) using the

falling head technique, or for at least three data points using the constant head technique. The manufacturer specifies a typical statistical inaccuracy of 2-10% given constant soil and environmental and flow parameters. The falling head technique was initially conducted for all samples whereby the pressure head difference (*H(t)*) was measured every second and fit to an exponential function and used to calculate K_{sat} as:

$$K_{sat} = A_{bur}/A_{sample} * L * b$$

Where: A_{bur} is the cross-sectional area of the burette holding the water column (cm^2), A_{sample} is the cross-sectional area of the sample (cm^2), L is the length of the sample (cm) and b if the coefficient of the fitted exponential function. A run was considered successful if the exponential fit had an R^2 of at least 0.99. Three successful runs were performed and the arithmetic average was taken for each sample.

Following the falling head technique, the constant head technique was employed for peat cores which had too high K_{sat} for the device to detect the changes in pressure head automatically. In these cases, the column of water passed through too quickly for the system to take hydraulic head readings on its own. Instead, measurements were taken by the operator at up to five specified pressure heads, which are used by the KSAT VIEW software along with the cumulative percolated water volume to determine the steady-state flow rate ($Q = \Delta V/\Delta t$) and the average hydraulic gradient between the inlet and outlet, H by linear regression. The saturated hydraulic conductivity was then calculated as:

$$K_{sat} = (Q/A_{sample})(L/H)$$

Where: A_{sample} is the cross-sectional area of the sample (cm^2) and L is the length of the sample (cm). Three successful runs were performed for each sample analysed under this technique and averaged, where successful was considered to be when the linear regression had an R^2 of at least 0.99.

Following the previous analyses, samples were oven-dried at 65°C for at least 48 hours until they ceased to lose mass (to the nearest 0.1 g) to calculate bulk density, ρ_b (g cm^{-3}). Volumes of intact cores were calculated based on their dimensions whereas the less structured cores were measured volumetrically.

The organic matter content (expressed as a percentage) of peat samples was determined by loss on ignition. Crucibles filled with about 5 cm^3 of peat from each 5 cm increment were weighed and then burned in a muffle oven at 550℃ for 4 hours (Payne et al., 2016) before being weighed again. The proportion of organic matter content was then calculated as:

(weight of peat pre-LOI – weight of ash post-LOI)/ weight of peat pre-LOI

The porosity, φ of each sample was estimated using the equation:

$$\varphi = 1 - \rho_b/\rho_s$$

Where ρ_b is the measured bulk density (kg m^{-3}) and ρ_s is the particle density (kg m^{-3}) of the peat which was estimated based on the relative organic/inorganic fractions based on the LOI analysis as well as organic/inorganic particle densities of 1470 kg m^{-3} and 2650 kg m^{-3}, respectively (Redding and Devito, 2006).

2.2.6 Field water chemistry collection

Rainfall for isotopic analysis was collected at least weekly for sampling period of May to August, with the aim to collect on an event-by-event basis. The collectors used were based on the design of Gröning et al. (2012) which minimize evaporation and are suitable for up to monthly sample collection. Collectors were installed at six sites (234, 301, 405, 408, 415 and 502) near the center to avoid canopy cover and were paired with manual rain gauges to measure the size of rainfall events collected. Rainfall data at the remaining sites was derived from the nearest rainfall collector; 301 also served to collect rain for 313 and 415 also served to collect rain for 410 and 416. Mesh was placed over the opening of the collector to keep out debris. Each sample was

coarsely filtered using a paper coffee filter before being transferred into HDPE vials of 7 or 20 mL in size with conical cap inserts.

Peat pore-water for isotopic analysis was collected from the installed piezometers and lysimeters on a weekly basis from the second week of May to the third week of August 2017 to comprise a 16-week sampling campaign. Before collection, a Solinst TLC was used to first measure the temperature (in °C), electrical conductivity (EC in µS/cm) and level of the water before the piezometer was purged of a full casing and allowed to recover. This was done to ensure that stagnant water was not collected that may have been subject to evaporation (and thus fractionation) in the casing and repeated until the EC was within 10% of the previous measurement. This was loosely based on EPA guidelines for 5% variance for purging before groundwater sampling, (Vail, 2013) but modified for our purposes due to the precision of our instrumentation and for the sake of our focus on isotopes. Any stagnant water residing in the piezometer case could have undergone evaporation and thus isotopic fractionation that it would not have as pore-water. This was sometimes performed the day prior to sampling to account for longer recovery times, but piezometers were always purged at least once on the sampling day prior to collection. Once considered 'stabilized' by this criterion, pore-water was pumped up using Tygon tubing into 125 mL HDPE field collection bottles, first into a waste bottle to clear the tubing of any residual water and then into the designated sample bottle. Sample bottles were environmentalized with collected water and then filled as much as possible (to minimize head space) before being put into a cooler in the field and then a refrigerator. For piezometers that had run dry, suction lysimeters were used to collect pore-water by pressurizing to -60 kPa the day prior to sampling and collecting the resulting water from the body of the lysimeter. If water was collected from both the piezometer and lysimeter of a given depth, both were collected and underwent isotopic analysis, but only the piezometer-derived values in these cases were used towards estimating residence time. Collected pore-water was transferred into smaller 7 or 20 mL HDPE vials within 48 hours of collection where headspace could be better minimized. Samples were preferentially filtered using 0.2 or 0.45 µm polyethersulfone syringe filters if they appeared to have high amounts of suspended solids after settling for 2-6 hours. Between sampling weeks, the field collection bottles were washed with Liquinox detergent and placed in a bath of 5% HCl for 30 minutes before being rinsed thoroughly with reverse osmosis water and dried. Duplicates

were intentionally collected for random samples in order to assess them for consistency of isotopic analysis.

In the same weekly sampling schedule as pore-water, outflow was also collected from sites when present, which included sites 234, 313, 301, 408, 410, 415 and 502 that were 'spilling' at least some of the time. Of these sites, 415 was sampled both for water flowing into and out of the depression. This surface water was sampled by hand using 20 mL plastic syringes which were first rinsed with sample water and used to transfer water into 7 or 20 mL HDPE vials that were environmentalized three times. Filtering by 0.45 µm polyethersulfone syringe filter was only occasionally necessary as discharge was typically quite clear. The status of the outflow on a weekly basis was used to make an estimate of the relative elevation of the depression sill, over which the site would 'spill' if the WT exceeded it. This was estimated based on the minimum WTD observed on the weeks that there was no appreciable outflow, as one could deduce that during these instances that the WT was below the sill.

2.2.7 Stable isotopes of water analysis

Pore-water, rainfall and surface water samples were analyzed for stable isotopes of hydrogen ($\delta 2H$) and oxygen ($\delta^{18}O$) on a Picarro L-1102-i cavity ring-down spectroscopy (CRDS) isotopic water analyzer (Picarro, Inc., Santa Barbara, CA, USA) paired with a V1102-I vaporizer module and a HTC-PAL auto-sampler by CTC Analytics (Leap Technologies, Carrboro, NC, USA). The CRDS technique is a type of IRIS that uses a series of high reflectivity mirrors to create a long (up to 10 km) absorption path length for an infrared spectrum laser, whereby the light intensity in the cavity is measured for exponential decay during the 'ring-down' measurement when the laser is quickly shut off (Berden et al., 2000; O'Keefe and Deacon, 1988; Wahl et al., 2006). In this manner, the absorption of this light by the common isotopologues of water ($^{1}H^{1}H^{16}O$, $^{1}H^{2}H^{16}O$, and $^{1}H^{1}H^{18}O$) is treated as a kinetic phenomenon, where the optical loss of the ring-down and laser wavelength are measured to generate spectral profiles of each sample (Brand et al., 2009). The concentration of each isotopologue (and thus the isotopic ratios) may then be measured based on the area under spectral absorption features that are specific to each isotopologue, given that low pressures are maintained and temperature kept constant in the cavity (Brand et al., 2009).

First, working standards were calibrated on November 23, 2017 to the international standards, Vienna Mean Ocean Water 2 (VSMOW2) and Standard Light Antarctic Precipitation 2 (SLAP2) acquired from the International Atomic Energy Association (IAEA, Vienna, Austria) by analyzing 10 injections of each in the following sequence; VSMOW2, DSH, MDI, BSB305-DI, IWL, SLAP2 and taking the mean of injections 9-10 as the measured values that may be free of memory effects of the previous water. The established delta values (Gonfiantini, 1978) of δ^2H = 0‰ and $\delta^{18}O$ = 0‰ for VSMOW2 and δ^2H = -427.5‰ and $\delta^{18}O$ = -55.50‰ for SLAP2 were used to develop a linear relationship between the measured and known values to calibrate the working standards. This was conducted similarly to the methods employed by Kerrigan (2015). The working standards DSH, MDI, BSB305-DI and IWL were also analyzed on February 7, 2018 using IRMS with the McMaster Research Group for Stable Isotopologues for calibration of $\delta^{18}O$ values. While measuring similarly to our CRDS-based calibration, these IRMS values were the 'known' values going forward for $\delta^{18}O$ (Table 2.3). DSH was sourced from bottled deep sea water and IWL was sourced from bottled iceberg water from Newfoundland, Canada whereas MDI and BSB305-DI were sourced from mixtures of reverse osmosis water from McMaster University. All working standards were homogenized prior to calibration and subsequently stored in sealed amber glass bottles with conical cap inserts in a refrigerator afterwards.

The methods used for subsequent sample analysis were based on those described by van Geldern and Barth (2012) for optimal performance and post-measurement corrections; in the context of these methods, DSH and IWL served as heavy and light standards for calibration to the VSMOW2 scale whereas MDI, of isotopic composition similar to samples, was injected throughout the sample run for the purposes of quantifying the effects of drift and memory in order to apply appropriate corrections. BSB305-DI was also similar in isotopic composition to samples and treated as a sample of known isotopic signature and served as a quality control to quantify precision across runs (Table 2.4).

When running collected water samples, they were allowed to equilibrate to room temperature before 1.85 mL was transferred to glass auto-sampler vials with septa lids and arranged in a tray in the manner of Table 2.4, with 19 samples analyzed per sampler run over the course of approximately 19 hours. The HTC-PAL auto-sampler handled sample transfer from vial to

analyzer (by way of the vaporizer). Injection volumes of approximately 1.5 µL were adjusted with each run to achieve an ideal H_2O concentration of 20000 ppmv for analysis as per the manufacturer's operating range of 17000-23000 ppmv. Isotope analysis was conducted from December 2017 to April 2018. Post-processing of data consisted of flagging samples contaminated with organics and applying the corrections and calibrations included in the methods of van Geldern and Barth (2012).

The influence of organics found in samples was a concern because the presence of certain compounds have been found to cause optical interference with IRIS measurements, particularly volatile organic compounds in waters extracted from plants (Chang et al., 2016; Schmidt et al., 2012). Dissolved organic matter was certainly present in our pore-water samples, but only a general characterization was undertaken in Chapter 3, rather than quantification of specific compounds. Peat pore-water may fall somewhere in-between the plant-extracted water, which is typically determined to contain significant optically interfering compounds, and soil water, which may not (Schultz et al., 2011). The filtering of many samples was undertaken partly in an effort to mitigate potential organics contamination as well as remove suspended solids. We elected further to screen all samples using the analyzer's ChemCorrect software (Picarro, Inc, Santa Barbara, CA, USA), which assesses organics contamination based on the variability between injections of the same sample and known spectra of interfering organics such as methane and simple alcohols. In all but a few cases, the ChemCorrect software determined that there was no contamination of the waters by organics. For these few cases, they appeared to be caused by a missed injection or bearing an abnormally high or low H_2O concentration that artificially elevated the between-injection variability. When they were re-analyzed, these issues were resolved with appropriate injection numbers and volumes, as the software did not detect any significant organics contamination on their second run. The ChemCorrect software is capable of applying corrections for organics contamination, and this post-processing strategy has been somewhat successful in flagged samples in similar instruments (Schultz et al., 2011) but since all remaining samples were cleared by the software, we elected to trust the software's determination that the measured values of δ^2H and $\delta^{18}O$ would not be subject to significant interference.

Post-processing on raw data from the Picarro analyzer as outlined in van Geldern and Barth (2012) to correct for memory and drift effects were performed by means of a provided Microsoft Excel™ spreadsheet from the authors with their suggested modifications to the manufacturer standard protocols for CRDS isotopic analysis. The authors' approach to correcting for memory effects used the first four standards injected ten times (Table 2.4) involved the calculation of memory coefficients, *m* to quantify the carry-over of one sample to the next*:*

$$m_i^n = \frac{\delta_t^{(n-1)} - \delta_i^n}{\delta_t^{(n-1)} - \delta_t^n}$$

Where *i* is the injection number for a sample *n* for each injection and δ_t indicates the true value (in ‰) of the sample, around which it stabilizes after numerous injections. In this manner, an *m* of 0.95 indicates that the analyzed isotopic value represents 95% of the true isotopic value, or influenced by 5% of the previous sample. Using the iterative "solver" function of Microsoft Excel™ to minimize the weighted mean of the combined standard deviation of the sample:

$$c.s.d. = \sqrt{\sum_{n=1}^{i} (s.d.)_n^2}$$

Where $(s.d.)^2$ is the variance of the isotopic ratio of all injections *i* of vial number *n*. This *c.s.d.* is high before corrections are applied because the first few injections of a sample are more strongly influenced by the previous than after several injections. It was assumed the last injection of each set of ten would be best representative of the true isotope value, so m_{10} was set to 1.0. With these coefficients, subsequent injections, *i* of each vial, *n* could be corrected as follows:

$$\delta_{memory\ corrected} = \delta_{i(raw)}^n + (1 - m_i) \times (\delta_{i(raw)}^n - \delta_t^{(n-1)})$$

Where m_i is the memory coefficient for appropriate injection number and $\delta_t^{(n-1)}$ is the true isotopic value (in ‰) of the previous sample.

Drift was monitored throughout each sample run by repeated analysis of the lab standard MDI throughout the run at approximately equidistant spacing (Table 2.4) at four injections each. For this purpose, the first six injections of the first vial of MDI were discarded as "warm-up injections". The slope of the linear regression line of the memory-corrected isotopic values of MDI through time was then used to apply a drift correction:

$$\delta_{drift\ corrected} = \delta_{memory\ corrected} + (slope \times n)$$

Where *n* is an injection's position in the sequence that correlates to the analysis time.

Both memory and drift corrections were calculated and applied for each run and for $\delta^{18}O$ and $\delta^{2}H$ separately, as the effects can vary run-to-run and between the two isotopes. Afterwards, the memory and drift-corrected delta values were then normalized to the VSMOW/SLAP scale by calibrating to the heavy and light working standards DSH and IWL to yield the final isotopic values used. All results are reported in δ-notation relative to the VSMOW in permil (‰) (Gat, 2010; Gonfiantini, 1978).

2.2.8.1 LMWL development

A local meteoric water line (LMWL) was developed for the NOBEL area using the rainfall collected from May to August 2017 and a later collection in early October, from the sites where rainfall collectors were installed. This limited the applicability of the meteoric water line to spring and summer precipitation and notably was lacking any influence of winter precipitation. In a similar manner to Benjamin et al. (2004), the deuterium excess = $\delta^{2}H - 8\ \delta^{18}O$ (Dansgaard, 1964) was computed to compare to the global expected range of d-excess values. Generally, one expects to see *d*-excess values of -2 to 10-15 ‰, with larger values in the winter and smaller values in the summer (Kreutz et al., 2003) Samples with d-excess values outside of this range were treated as outliers and removed as abnormally low values in particular may indicate partial evaporation of the sample during storage. Each of the six collection sites had 18 samples collected that ranged from coverage of 1-4 rainfall events, capturing from 1-82 mm at a time.

Linear regression analysis was used to develop the LMWL using the relationship between $\delta^{18}O$ and $\delta^{2}H$ to produce an equation of the format:

$$\delta\ ^{2}H = m\ \delta^{18}O + b$$

Where *m* is the slope of the regression line and *b* is the deuterium-excess (intercept).

2.2.8.2 ITTP: residence time estimation

Due to this study's relatively limited coverage of four months in one year, traditional residence time modelling approaches (reviewed in McGuire and McDonnell (2006)) were avoided due to the complications associated with data availability and sampling frequency, since the data record would have to be artificially extended (Hrachowitz et al., 2011; Stockinger et al., 2016). Instead, the residence time of pore-water was estimated using a simplified metric, the inverse transit time proxy (ITTP) published by Tetzlaff et al. (2009). The ITTP was originally calculated as the ratio of the standard deviation of $\delta^{18}O$ of the output of a catchment over the study period, to the standard deviation of $\delta^{18}O$ of inputs over the study period. While a much simpler measure than more conventional modelling techniques, there have been strong relationships observed between mean transit time (MTT) by lumped parameter models and this ITTP (DeWalle et al., 1997; Maloszewski et al., 1983; McGuire et al., 2005; Soulsby & Tetzlaff, 2008). This measure, however, correlates negatively with transit time and so a higher ITTP means less dampening of the input isotopic signal from precipitation (a lower residence time) and a lower ITTP infers the converse (a longer residence time) (Tetzlaff et al., 2009). The original formulation of the ITTP was adapted for use to estimate relative residence times of pore-water and outflow:

$$ITTP_{\delta X} = \frac{\sigma_{output}}{\sigma_{input}}$$

Where δX refers to whether the ITTP is calculated with $\delta^{18}O$ or $\delta^{2}H$, since both are measured simultaneously by CRDS. σ_{output} is the standard deviation for the isotopic ratio (in permil) for a given point of measurement for pore-water or outlet for outflow, through the 16 week study period. ITTPs were calculated for outflow surface waters that were observed for the majority of

the study period (234, 301, 313, 408, 410 and 415). σ_{intput} is the standard deviation for the isotopic ratio (in permil) for rainfall collected for a given site (see 2.2.6) through the 16 week study period.

The original ITTP was designed for quick inter-comparison among catchments, with the caveats of being subject to differences depending on the sampling interval and length of the isotopic record (Tetzlaff et al., 2009). One of the complications that arise in residence time estimation, including this simplified metric, is from interannual variation in the stable isotopes of water in precipitation and differences between data records (Hrachowitz et al., 2009). Since each site-microform-depth was sampled weekly for the same 16 week study period, they should be free of differences stemming from differing lengths and sampling frequencies of their data records. However, the major limitation of this approximation is the relatively short length of the data record, as it limits the length of residence time that may be captured (Hrachowitz et al., 2011)..

2.2.9 Statistical analyses

Data management and statistical analyses were undertaken in MATLAB R2018a (Mathworks, Natick, MA, USA) and Minitab 18 (Minitab Inc., State College, PA, USA). A general linear model was used to assess the relationships between measured hydrophysical variables (K_{sat}, K_{Total}, bulk density, porosity, and ITTP estimates) with parameters of site (deep or intermediate), microtopography (hollow or hummock) and depth in the profile (acrotelm or catotelm). The depths of each piezometer were treated as the increments of measure for each variable. These variables were based on measurements from peat cores or from piezometer-based measures at particular depths. K_{Total} however, could be considered the average or sum up to a given depth. The model compared the three predictor variables individually as well as three two-way interactions between them. The three-way interaction between the predictor variables was included if it improved model performance (as R^2-adjusted). Models were developed for each response variable and the residuals were assessed visually to determine whether they met model assumptions of normality (histogram and normal probability plot) and constant variance (residuals vs. fits). K_{sat}, K_{Total} and bulk density failed to meet model assumptions and so had to be $\log_{10}$-transformed. Where site parameters (and interactions) were significant with regard to the

variation in each variable, pairwise comparisons using Tukey HSD 95% confidence intervals were used to determine specific categorical (and category interaction) differences.

Spearman correlation was used to investigate relationships between all previously mentioned hydrophysical variables and residence time estimates. For the pairs of variables where significant correlations were found, orthogonal regression was used to investigate the relationship between them to account for measurement error on each variable. Similarly to the general linear model, $\log_{10}$-transformations were applied to K_{sat}, K_{Total} and bulk density. On a whole-site basis, the depth-averaged K was taken as the K_{Total} of the deepest layer of a site and linearly regressed against depression morphological parameters; mean depth, maximum depth and depression area.

2.3 RESULTS

2.3.1 Hydrological data

For the period of study, from May to August 2017, 385-434 mm of rainfall fell, with monthly totals of 68-100 mm in May, 133-144 mm in June, 84-92 mm in July and 98-101 mm in August (Figure 2.3). It was a considerably wetter-than-average season, as the regional climate normals for 1981-2010, available for the nearby weather station at Dunchurch, ON (located approximately 25 km NNE) are a four month total of 335 mm of precipitation, comprised of monthly averages of 93 mm in May, 74 mm in June, 79 mm in July and 88 mm in August (Environment Canada, 2018). This places the rainfall for the study period anywhere from 50 to nearly 100 mm above the recent historical average. Rain fell on nearly half (61 of 123) of the days in this study. Of these days, 32.8% received less than 1 mm of rain (contributing 1.3% of the total rainfall), 26.2% received 1-5 mm (contributing 9.6%), 26.2% received 5-20 mm (contributing 38.7%) and 11.4% received over 20 mm (contributing 49%).

2017 was considerably wetter than the previous year, 2016, which saw monthly precipitation of 52 mm in May, 31 mm in June, 58 mm in July and 140 mm in August based on data collected at site 415. Even with the excess of rain in August, stemming from a large 65 mm rainfall event, this period was still a relative drought compared to the historical average, as it received 50 mm less than the 1981-2010 climate normal (Environment Canada, 2018) and 154 mm less than 2017

for the same site of collection. The differences in rainfall input are reflected in the WTD data for 2016 and 2017 (Figure 2.2). In 2016, all of the intermediate sites and possibly the deep site 415 lost their WT at some point in the summer; that is to say it fell below the level of the bedrock. In 2017, only the intermediate site 405 appeared to lose its WT. Through May-August 2017, the mean WTD relative to the surface in the deep sites was less than 0.2 m, varying by a standard deviation as high as 6.8 cm in 408, while the deepest the WT fell was 30 cm in site 301 (Figure 2.3). In contrast, the intermediate sites were more variable relative to their total depths, with the greatest variation found in the shallow 405 (σ = 9.3 cm) (Figure 2.3). Owing to the wet conditions of 2017 and the placement of the groundwater well in wet hollow-like areas in sites 313, 410 and 416 the WT was often pooled above the peat surface, whereas in 405 and 502 it was largely below the surface, albeit not particularly deep (Figure 2.2, 2.3).

The relatively consistent rainfall and higher-than-average total rainfall kept conditions fairly wet throughout the study period in 2017, so it would not have been appropriate to draw any diplotelmic boundaries regarding the stability of the peat based on this year alone. The use of the comparably dry 2016 water table data to distinguish what could be considered the acrotelm and catotelm in the peat profiles yielded more conservative estimates (as seen in Figure 2.5). This typically resulted in the 0.2 m depth hollow piezometers and up to the 0.4 m depth hummock piezometers falling into what could be considered the active acrotelm zone, though there were a few exceptions (Table 2.1). Furthermore, even with this relatively deep boundary, in 2016, deep sites experienced 26-33 days where the WTD fell below the acrotelm, and the intermediate sites had 41-70 days. In contrast, the catotelm defined by these criteria were saturated for the whole study period with the exception of sites 405 and 502 (2.5 and 0.7 days respectively).

Site 234 was observed to have appreciable outflow at its outlet at 15 of the 16 weeks of study. Based on the WTD on the week it was not spilling, one can surmise that the sill was as deep as 0.33 m below the peat surface (or -0.69 m below the site's reference). Put another way, this includes depths to as deep as 0.26 m in the hollow and 0.31 m in the hummock monitored. Site 301 was observed to be flowing on 13 of the 16 weeks, though the water at its primary outlet was pooled and somewhat stagnant for three of these occasions. Based on the shallowest WTD observed in these no-flow instances, this water would have been coming from depths up to 0.26

m below the surface, or 1.30 m below the rock reference. This includes depths to 0.23 m in the hollow and 0.32 m in the hummock. The largest site, 408, exhibited outflow for all but two weeks, where the WTD was at least 0.24 m below the surface, or 0.75 m below the rock reference. Up to 0.30 m in the hollow and up to 0.20 m in the hummock would have contributed to the outflow. Site 415 received appreciable surface water input on 12 of 16 weeks, and had outflow for 13. The shallowest WT of these instances was 0.17 m below the peat surface, or 0.52 m below the site reference. This encompassed depths up to 0.07 m in the hollow and up to 0.17 m in the hummock.

Sites 313 and 410 were observed to be 'spilling' on 11 and 10 of the 16 weeks observed, respectively, but were also very low in magnitude for a few of those instances, particularly in late May/early June and early August. Site 313 was flowing until the WT fell below 0.05 m above the surface where the well was located (or 0.25 m below the reference). In the hollow, up to the top 0.05 m would have participated, or up to the first 0.19 m in the hummock. Site 410 had outflow until the WTD fell below 0.05 m above the peat surface where the well was located, or 0.42 m below the site reference. These depths corresponded to 0.02 m of ponded water in the hollow and up to the first 0.14 m in the hummock. The intermediate site 502 was only observed to be 'spilling' on two weeks of visits, and these were instances where the WT was over 0.05 m above the surface, or 0.04 m below the reference point. These depths meant the WT had to reach as high as 0.003 m above the hollow, or 0.04 m in the hummock.

Weekly hydraulic gradients revealed further hydrological differences between deep and intermediate sites. Gradients from 0.2 m to the bottom of peat profiles within deep sites were typically more moderate through the study period from May through August (Figure 2.6). No clear trends are apparent, though the deep sites track similarly close to having close to no gradient for much of the summer, with the exception of May experiencing some more dramatic changes. The intermediate sites, on the other hand, experience greater fluctuations, or reversals of hydraulic gradient and these tended to go more positive than any gradients observed in the deep sites.

2.3.2 Peat hydrophysical properties

Saturated hydraulic conductivity varied significantly with depth ($p<0.001$) as well as its interactions with site type ($p<0.05$) and microform ($p<0.05$), respectively (Table 2.5). The K_{sat} in the acrotelm of all sites was significantly higher than in the catotelm ($p<0.001$), which held true within deep ($p<0.001$) but not intermediate ($p=0.477$) sites and within hummocks ($p<0.001$) but not hollows ($p=0.114$) (Figure 2.8). Depth-averaged conductivity, a derivative of the previous, similarly varied significantly with depth ($p<0.001$) (Table 2.5) and its interactions with site type ($p<0.01$) and microform ($p<0.05$). The K_{Total} in the acrotelm was significantly higher than the catotelm ($p<0.001$), which again was consistent within deep sites ($p<0.001$) but not intermediate ($p=0.411$) and within hummocks ($p<0.001$) but non-significantly for hollows ($p=0.059$) (Figure 2.9). Variation in bulk density was significantly explained by site type ($p<0.001$) and depth ($p<0.001$) but not any interactions between the two or with microform (Table 2.5). Porosity also varied significantly by the same two factors ($p<0.001$) but also with the interaction between site type and depth ($p<0.05$) (Table 2.5). In this case, porosity was lower in the catotelm ($p<0.001$) and was consistently so within deep ($p<0.001$) and intermediate sites ($p<0.001$) (Figure 2.10). However, for the acrotelm there was not a significant difference in porosity between deep and intermediate ($p=0.072$) even though the intermediate site catotelm had a lower porosity than the deep site catotelm ($p<0.001$).

All hydrophysical properties and residence time estimates were correlated significantly (Spearman, $p<0.05$) to one another to some extent, except for $ITTP_{\delta 18O}$ (Table 2.6). Depth averaged K_{sat} of each site; that is, the K_{Total} of the basal peat layer, exhibited log-linear relationships with site parameters (Figure 2.11). In the hollows and hummocks, K_{Total} was log-linearly related to mean depression depth ($R^2=0.604$, $p<0.01$ and $R^2 = 0.666$, $p<0.005$, respectively), maximum depression depth ($R^2=0.63$, $p<0.01$ and $R^2= 0.765$, $p<0.005$, respectively) and depression area ($R^2= 0.597$, $p<0.01$ and $R^2= 0.388$, $p<0.05$, respectively) (Figure 2.11).

2.3.3 Isotopic characterization

The Picarro L1102-i CRDS analyzer is rated by the manufacturer for precisions of ≤0.1‰ and ≤0.5‰ for $\delta^{18}O$ and $\delta^{2}H$, respectively. Upon its last testing with the manufacturer in January

2017, it performed with precisions of 0.049‰ and 0.19‰, where precision was quantified as the standard deviation of groups with 12 injections over 24 hours. In terms of drift, the analyzer is rated for ≤0.6‰ and ≤1.8‰ of drift for $\delta^{18}O$ and $\delta^{2}H$, respectively. During the same testing, it was also assessed to exhibit drift of 0.235‰ and 0.64‰, respectively, where drift was quantified as the peak-to-peak mean of groups with 12 injections over 24 hours.

The quality control sample (BSB305-DI) in each run was used to quantify external precision over the six months of isotopic analysis as the standard deviation of this sample. Precisions of 0.03‰ for $\delta^{18}O$ and 0.17‰ for $\delta^{2}H$ (n = 66) were achieved. These precisions are within what is considered acceptable precision for traditional IRMS isotopic analysis. In this span, the deviation of BSB305-DI from the original calibrated values ranged from 0 to 0.10‰ for $\delta^{18}O$ and 0.10 to 0.84‰ for $\delta^{2}H$. Memory effect corrections according to the methods of van Geldern and Barth (2012) were always applied, whereas drift corrections were only applied when found to improve overall precision. Four runs were discarded and re-analyzed after failing precision thresholds; this was often the product of missed injections or injections exceeding accepted H_2O concentrations.

2.3.3.1 LMWL development

The LMWL developed from the 2017 rainfall collection by linear regression followed the equation $\delta^{2}H = 7.80\ \delta^{18}O + 10.03$ with an adjusted R^2 value of 0.968 (Figure 2.7, $p<0.001$). This plotted the rainfall at NOBEL very close to the GMWL, $\delta^{2}H = 8\ \delta^{18}O + 10$ (Craig, 1961) but deviated considerably compared to other meteoric water lines developed in the region, at least in terms of d-excess. In the Nipissing area, England (2017) developed a LMWL of $\delta^{2}H = 7.6\ \delta^{18}O + 8.0$ based on 2013 precipitation. A similar LMWL of $\delta^{2}H = 7.28\ \delta^{18}O + 7.5$ was developed at the Dorset Environmental Science Center (Mountain et al., 2015). The Online Isotopes in Precipitation Calculator (Bowen, 2017) uses data collected by the Global Network of Isotopes in Precipitation (GNIP) to estimate monthly precipitation isotopic signatures based on input coordinates; the modelled LMWL for the coordinates of the NOBEL study area further differed at $\delta^{2}H = 7.24\ \delta^{18}O + 1.47$. Samples of outflow and basal pore-water (from the deepest

piezometer of each site) plotted fairly close to the LMWL and GMWL, tending not to deviate any further than the rainfall samples did (Figure 2.7).

2.3.3.2 Residence time estimation

Residence time estimates based on $\delta^{18}O$ had its variation significantly explained by microform ($p<0.001$) and depth type ($p<0.05$) as well as the interactions of site type with microform ($p<0.05$) and depth type ($p<0.05$) (Table 2.5). The three-way interaction of the site parameters was also significant ($p<0.01$). It should be noted, however, the general linear model for this variable accounted for the least variation overall (R^2-adjusted = 0.3996). The $ITTP_{\delta 18O}$ was slightly higher (and therefore shorter residence time) in hummocks and the acrotelm (Figure 2.12). Intermediate site hummocks had a lower $ITTP_{\delta 18O}$ than all other site-microform combinations ($p<0.05$).

Residence time based on δ^2H varied significantly by site type ($p<0.001$), microform ($p<0.005$), depth ($p<0.001$) and all interactions except for the two-way interaction between microform and depth (Table 2.5). The pore-water had a significantly higher $ITTP_{\delta 2H}$ (shorter residence time) in intermediate sites, hummocks and the acrotelm (Figure 2.13). Within intermediate sites, hummocks had a higher $ITTP_{\delta 2H}$ ($p<0.01$) but there was no microform difference within deep sites. Within deep ($p<0.001$) and intermediate ($p<0.001$) sites, $ITTP_{\delta 2H}$ was significantly higher in the catotelm, but the intermediate catotelm did not significantly differ from the deep acrotelm ($p=0.311$). The general linear model describing the variation in $ITTP_{d2H}$ performed the best of the six (R^2 -adjusted = 0.6877). On a continuous basis for depth, $ITTP_{d2H}$ generally decreased with depth, albeit not always in a consistent (or linear) manner (Figure 2.15).

Orthogonal regression of the 'best' performing ITTP measure using δ^2H revealed significant relationships with the $\log_{10}$ of bulk density, K_{sat} and K_{Total} (Figure 2.14). The regression with bulk density was significant to $p<0.005$ whereas the measures of hydraulic conductivity were significant to $p<0.001$. The adjusted R^2 values of the orthogonal regressions were 0.1254, 0.3504, and 0.3933, respectively.

Estimates of outflow residence time for the sites that demonstrated appreciable outflow throughout the study period (234, 301, 313, 408, 410 and 415) were generally consistent with the source depths inferred from WTD on weeks that they were not spilling with the notable exception of 234. The $ITTP_{\delta 2H}$ of outflow at this site corresponded to pore-water held at a depth of 0.6 m in the hollow, yet was greater for the entire hollow profile (Figure 2.15). In site 301, the outflow's residence time matched that of pore-water 0.4 m and above in the hummock. The largest site, 408, saw the residence time of its outflow roughly correspond to the shallowest collected pore-water at 0.2 m in both microforms. For the site 415, outflow appeared to be 'younger' than any pore-water depths. This was also the case in the intermediate site 410, whereas the other, smaller depression of 313 had outflow of similar residence time to 0.2 m in the hollow, and near 0.4 m in the hummock.

2.4 DISCUSSION

2.4.1 Peat-filled bedrock depression hydrology

The wetter 2017 spring-summer season saw a greatly damped variability in WTD, particularly among deep sites that largely stayed within 0.2 m of the surface from May to October (Figure 2.2). While the intermediate sites did not lose their WT at any point as occurred in 2016, they again demonstrated their greater vulnerability to short-term drought that is indicative of the WT-specific yield feedback observed by Didemus (2016) two years prior. It is worth noting, however, that unlike the drought conditions of 2016, the intermediate sites behaved considerably differently in response to reduced moisture stress (or even moisture surplus). The sites 405 and 502, despite having similar morphometric characteristics (Table 2.1), experienced more dramatic changes in WT than 313, 410 and 416, whose WTD varied by only as high as 0.06 m throughout the study period (Figure 2.4). While partly the by-product of groundwater well placement in relative pool microforms, the latter three sites also had their WT above the surface in areas for much of the season. While the intermediate sites certainly experienced greater WT variability, both in an absolute sense and relative to their total depths, their hydrology may differ considerably in times of more favourable moisture conditions. In contrast, the four deep sites, despite differing greatly morphometrically in comparison (Table 2.1), behaved much more similarly, with WTDs nearly overlapping for much of the season (Figure 2.3). Although affected

by the greater changes in depth, the hydraulic gradients measured weekly were also more moderate in the deep sites.

With regards to the runoff observed at the outlets of these peat-filled bedrock depressions and their fill-and-spill dynamics (Spence and Woo, 2006), the two size types again demonstrated some interesting hydrological differences. Based on the estimates of discrete weekly monitoring of outflow coupled with WTD measurements, the deep sites' sills were 0.17 – 0.33 m below the peat surface at the groundwater monitoring well and largely in this range at the hollow and hummock microforms instrumented. In contrast, similar estimates for the three intermediate sites with sufficient outflow ranged from 0.05 m above the surface to 0.05 m below. This would suggest that in the deep sites, peat has grown to a considerable extent above the depression sill, whereas the peat accumulation in intermediate depressions has only just about filled the depression. As such, larger peat-forming depressions may not be as limited by the geological constraints of their bedrock container, which is relevant not only to carbon accumulation, but their hydrological behaviour on a landscape level (Allan and Roulet, 1994; Frisbee et al., 2007; Phillips et al., 2011). While shallower depressions may be more responsive to inputs such as rainfall due to their smaller storage capacity, their WT tends to be much more variable, leading to more intermittent contributions to runoff compared to deep depressions. During periods of relatively favourable moisture conditions, deep depressions may be more consistent contributors of runoff, potentially to the benefit of downslope depressions. Even in relative drought conditions of 2016 the deep depressions spend more time above their estimated sill compared to the more 'flashy' response intermediate depressions (Figure 2.2), These findings are only partially supported by residence time estimates (Figure 2.15), but may be further explored by monitoring of 'spill' from these bedrock depressions on a continuous basis in parallel with WTD, coupled with more detailed topographical data, particularly with regards to depression bathymetry.

Seasonal fluctuations in hydraulic head have been observed in larger northern boreal peatlands (Siegel et al., 1995; Waddington and Roulet, 1997). Within the deep sites, hydraulic gradients were generally fairly weak (<0.5) and tended to be slightly negative, whereas the intermediate sites experienced reversals of hydraulic gradient that were also greater in magnitude, more

frequently around ±0.5 (Figure 2.6). These gradients are of interest because of their control on the vertical movement of pore-water, potentially transporting decay-stimulating labile organics down and flushing pore-water of decay-suppressing end products (Aravena et al., 1993; Charman et al., 1994). Despite the high rainfall inputs received over the study period, these gradients were never particularly strong, especially in the deep sites. Upward flushing of pore-water has been observed in systems with strong groundwater flow systems (Siegel et al., 1995), something notably absent from these bedrock depression systems. It also tended to occur during drought periods, with downward movement more prevalent during precipitation recharge periods, which is more in line with the season observed.

2.4.2 Peat profiles and controls on hydraulic properties

As in Branham and Strack (2014), measures of K_{sat} were significantly related to other peat physical properties (Table 2.6), as well as depth (Table 2.5). Microtopography alone did not appear to exert control on peat hydrophysical properties, except in its interaction with depth, whereby K_{sat} was significantly higher in the macropore-rich acrotelms of the hummocks than deeper in the profile (Figure 2.8) and even compared to the hollow acrotelm for K_{Total} (Figure 2.9). This is again, roughly consistent with the findings of Branham and Strack (2014). However, it should be noted that the microtopography of most sites was not particularly well-developed. Microforms were selected on a functional basis of relative topographic highs and lows at the time of site selection in early spring 2017, rather than based on their vegetation. Despite considerable differences in elevation (and thus distance to WT), many microforms fell somewhere in the middle of the hummock-hollow gradient with respect to species of *Sphagnum* mosses (Table 2.2; Andrus et al., 1983). This was the case for many of the hummock microforms, which tended to be more lawn-like with sites 405, 416, 502, 234 and 415 having *S. fallax* which falls towards the hollow end of the continuum. The presence of non-*Sphagnum* species of *Polytrichum* also confounded differences. These true mosses were more prevalent among the intermediate site hummocks, which were typically located on the depression margins and raised partly with the aid of another feature such as a tree. These mosses differ in their hydrophysical behaviour from *Sphagnum*, as they exhibit stronger near-surface moisture retention and lower porosities (Didemus, 2016). Between the two types of depressions, significant differences only emerged in their combinations with depth in the profile. Catotelm

conductivity was lower in the deep sites, but not significantly (Figure 2.8, 2.9). This may be explained by the surprisingly low porosities observed in the catotelm of intermediate sites (Figure 2.10), though this may be skewed to some degree due to the smaller thickness of the catotelm in the intermediate sites (if present at all), as well as the presence of mineral soil at the base of some of the smaller depressions. On a site scale, the K_{Total}, which provides a measure of the total resistance of peat material to inflow from the surface reaching its base, was the most strongly related to depression maximum depth in a log-linear manner. The greater depths of the deep sites present a longer flow path for potential pore-water flow as well as a hydraulic structure that presents peat of orders of magnitude lower K than shallower sites due to the greater compression of overbearing material (Belyea and Clymo, 2001) and potentially, decomposition over longer time periods.

Profiles of conductivity presented mixed findings compared to the profiles modelled by Morris and Waddington (2011). The deep sites' profiles could be described to be more in line with the exponential K profiles that drastically increased modelled residence time distributions with depth, whereas the profiles of K in intermediate sites lack the spatial resolution to pick up such patterns, though they generally decrease with depth. These contrasting hydraulic structures among peat-filled depressions would suggest longer pore-water residence times should follow. However, modelled peatlands were on a significantly larger scale compared to the peat-filled bedrock depressions we studied, where their smallest (L = 100 m) was roughly the size of our largest (deep site 408).

2.4.3 Meteoric water

The similar slope of the 2017 LMWL to studies in the region (England, 2017; Mountain et al., 2015) is encouraging, but the discrepancy with regards to the *d*-excess suggests that not all of the variation in the isotopic composition of precipitation was captured, at least on a yearly basis. Having only collected in 2017, no interannual variation is captured in our LMWL and having no snowfall samples means that none of this isotopically lighter precipitation is represented. Indeed, the LMWL predominantly plots higher up on the regression line (Figure 2.7). Snowfall was fairly heavily represented by England (2017) and comprises a significant fraction (27.8%) of annual precipitation for the region, based on 1981-2010 climate normals (Environment Canada,

2018). The primary aim of the rainfall isotopic analysis undertaken was for residence time estimation, which requires parallel time series of input (precipitation) and output (pore-water). Given that spring snowmelt occurred well before the start of the study period, it was unlikely for there to be any appreciable inputs from previous precipitation. In this respect, the rainfall sampling period was deemed sufficient for this purpose, even if not considered to be so for proper LMWL development. Moving forward, however, precipitation collection throughout the whole year would be advisable to develop a more robust LMWL.

With this context regarding the limitations of our developed LMWL, the subset of data including outflow surface waters and the basal pore-water taken at the deepest piezometers of each depression did not yield any obvious trends. Given their sourcing from several different depressions, the outflow waters show the greatest variation in dual isotopic space but generally plot along the LMWL fairly closely (Figure 2.7). They do not appear to plot to the right of the LMWL in a LEL as surface waters may do due to evaporative fractionation (Clark and Fritz, 1997), which would have been a concern for outflow residence time estimates. These estimates aimed to trace back the likely source depth from the pore-water since they should have roughly the same 'age', but this could have been obscured by the evaporation signal in the more slow-flowing outlets. The basal pore-waters plot mostly along the LMWL but with some clustering in a line of lower slope, with the waters of the four deep depressions more tightly clustered (Figure 2.7). Given that the deep layers of larger depressions should experience less turnover (Morris and Waddington, 2011), this tight grouping should be expected in these poorly mixed waters. In comparison, the basal pore-waters of intermediate sites exhibit greater spread of their isotopic signatures. The total resistance to flow reaching the base of these shallower depressions is considerably less than the deep sites (Figure 2.11), and their WTs fell below the reach of the deepest piezometers in sites 405 and 502 (Figure 2.2), so they were likely subject to greater mixing with rainfall and run-in inputs in the generally wet conditions as well as the influence of evapotranspiration into the profile during drier periods. The accompanying WT drop of the latter, however, may trigger a negative feedback with moss surface resistance and albedo to reduce evapotranspiration (Waddington et al., 2015).

2.4.4 Pore-water residence time

Our results on residence time (estimated as ITTP) broadly support the modelling work by Morris and Waddington (2011), at least in terms of the influence of peatland size and depth. For estimates based on both $\delta^{18}O$ and $\delta^{2}H$, pore-water residence time was on average, longer in the catotelm but it was only significantly longer in deep sites for $\delta^{2}H$-based estimates (Figure 2.12, 2.13). Looking into the interactions between site parameters, however, there was not a significant difference between catotelm residence time in deep and intermediate sites. Though the deep and intermediate sites differed considerably in size, with the deep sites typically over twice as deep and, on average, an order of magnitude larger in area, the absolute differences pale in comparison to those modelled by Morris and Waddington (2011), which varied in lateral extent by increments of 100 m in lateral extent. As stated previously, the largest peat-filled depression studied here was about as large as the smallest peatland modelled. Most of the striking differences in residence time that the authors noted came at depths exceeding those of our deepest depression (>3 m). The fact that the deepest depths sampled typically did not differ by more than a meter between deep and intermediate sites may explain the absence of dramatic differences in the catotelms of sites. Furthermore, a limitation mentioned previously, that the catotelms of intermediate sites were very limited in sample size, compared to deep sites which averaged ITTP across as many as six depth increments, may have left intermediate catotelm ITTP sampling from very dense material that may have been at least partly mineral soil in nature. Differences were also observed among microforms, particularly with short residence times being found in the hummock acrotelms (Figure 2.12, 2.13) which shows agreement with hydraulic structure findings of higher K (Figure 2.8, 2.9).

Significant relationships between $ITTP_{\delta 2H}$ and three hydrophysical properties (Figure 2.13) support the assertion by Morris and Waddington (2011) of hydraulic structure acting as a control on pore-water residence time that illustrates a limitation of the diplotelmic model, whereby peatlands of the same WT height (and therefore catotelm thickness) may have contrasting residence time distributions if their hydraulic structures differed. While our peat-filled depressions varied in size and WT, there was still reasonably strong correlation between the two measures of K, with residence time.

2.4.5 Implications

Residence time estimates supported general differences between deep and intermediate sites, but not necessarily between their catotelms, in spite of distinct hydraulic structure. It is worth noting that the residence time estimates made by the simplified peatland groundwater residence time modelling by Morris and Waddington (2011) on a year-to-year basis suggested that increases in net rainfall rate may lead to greater pore water turnover, equivalent to 50% decrease in tracer half-life at 3 m for a 12 cm yr^{-1} increase in rainfall, roughly the increase in rainfall observed above the average for the study period in the NOBEL. In this manner, especially given the much shallower depths investigated in peat-filled depressions, it is plausible that the data underestimates longer term residence time. Prolonged rainfall was modelled to hasten pore-water turnover across peatlands and obscure differences with depth (Morris and Waddington, 2011). Though there was little evidence of rainfall-induced pore-water advection in deeper depressions, it has been observed to extend the active zone of methanogenesis in peat column experiments (Bonaiuti et al., 2017). On the geochemical side of the pore-water feedback, this would suggest a deeper zone of shorter pore-water residence times, where suppression on decay is eased. Not unlike the issue of few intermediate catotelms, this may have led to some of the shallower catotelm depths acting more acrotelm-like, at least for the wet season.

Given that our study took place merely over one year, its residence time estimates are restricted temporally (Hrachowitz et al., 2011), in addition to the challenge of spatial scaling in reference to the modelling work inspiring it and the biogeochemical feedback work preceding it (Beer et al., 2008; Beer and Blodau, 2007). The inclusion of only one year (and only the spring-summer at that) could have certainly limited the applicability of our findings in the long-term. The wetter-than-average period observed would have promoted greater-than-average pore-water turnover across all peat-filled depressions compared to previous years such as 2016. Based on the WT record, the intermediate sites lost their respective WTs during this summer. With the entire peat profile left unsaturated, the water occupying the largest pores, about 90% of the total volume (Hayward and Clymo, 1982) would have been emptied, leading to massive pore-water turnover that would more strongly affect the shallower sites due to their greater vulnerability to WT change by the specific yield feedback (Didemus, 2016). It is possible that this turnover imposed

by evapotranspiration could have a more site-specific effect on pore-water residence times, given the differing hydrologic behaviour of the categories of depressions.

Further considerations for our residence time estimates need to be given to the simplified nature of our metric of choice, the ITTP. Designed to be a transferable, simplified measure for use across a large number of catchments, the authors stressed caution for interpretation (Tetzlaff et al., 2009). While our use of it across peat profiles for the same time period and same sampling frequency alleviates some of the issues of comparability, the inclusion of only the dampening effect from input to output (via their standard deviations) leaves out some of the temporal variability that is included in lumped parameter models. Given the resolution of the peat profiles examined and the number of sites monitored, simplified measures of residence time became necessary due to logistical constraints in data collection as well as the greater data processing demands of the lumped parameter modelling approach. The ITTP appears to have value for simple comparisons such as these, but comes with the trade-off of being only a relative metric of residence time, making any comparisons to residence time estimates in absolute terms impossible. In the geochemical context, the slowdown of anaerobic decay was observed to set in after 150 days in peat column experiments (Bonaiuti et al., 2017), which suggests a pore-water residence time of at least this length may be required to achieve this 'peat inactivation'. It is unfortunately not possible with our relative estimates to draw any conclusions on whether this benchmark was achieved, so traditional modelling in absolute temporal units should be a crucial next step. The inverse relationships between ITTP and mean residence time by lumped parameter modelling has been observed to be reasonably robust for Soulsby and Tetzlaff (2008) (R^2=0.84) and McGuire et al. (2005) (R^2=0.81) despite fairly small sample sizes of catchments, but that also entails they be subject to the same challenges of the lumped parameter approach. The one problem of most concern for this study was the data record length problem (McGuire and McDonnell, 2006) whereby shorter input periods increase uncertainty of estimates. Though there is no one-size-fits-all record length, longer records are recommended on the scale of a few years to a decade to ensure greater confidence in residence time estimations.

The results of this preliminary investigation of peat pore-water residence time are informative to future applications. It is recommended that future residence time estimates be supported by a

conventional lumped parameter modelling approach enabled by more intensive and extended sampling regime in a subset of sites in order to develop empirical relationships (as done by McGuire et al., 2005; Soulsby and Tetzlaff, 2008) which may be unique to these peat-accumulating depression systems. This would allow for estimates to be made in terms of absolute units of time and permit these systems to be placed in the context of the slow turnover of groundwater systems to the more rapid flushing of surface systems. With an interannual data record, it may also be possible to elucidate if the dramatic seasonal changes in hydrology that occur under drought in smaller systems (Didemus, 2016) do indeed govern pore-water turnover as suggested.

2.6 TABLES

Table 2.1: Characteristics of the sites in the NOBEL study area. Mean and maximum depths were based on four transects per site at a resolution of 1 m for intermediate and 2 m for deep sites (with the exception of 408 at a resolution of 4 m). Piezometer nests were installed in relative hollow and hummock microforms where depth indicates the depth of the center of the screened portion (~0.1 m) below the peat surface. Depths in *italics* indicate piezometers supplemented with suction lysimeters to allow the pore-water to be sampled when the water table fell below the given depth. Depths that are underlined were considered to be in the acrotelm based on 2016 WT data, whereas the rest were considered to be in the catotelm.

Site #	Depression Size	Mean Depth (m)	Max Depth (m)	Area (m^2)	Piezometer Depths Hollows (cm)	Piezometer Depths Hummocks (cm)
313	Intermediate	0.24	0.60	678	0.2, 0.4	*0.2*, 0.4, 0.6
405	Intermediate	0.29	0.63	333	*0.2*	*0.2*, *0.4*
410	Intermediate	0.30	0.62	176	0.2, 0.4, 0.6	*0.2*, 0.4
416	Intermediate	0.26	0.60	142	0.2, 0.4	0.2, 0.4
502	Intermediate	0.25	0.57	376	*0.2*, *0.3*	*0.2*
234	Deep	0.75	1.22	2653	0.2, 0.4, 0.6, 0.8, 1.0	0.2, 0.4, 0.6, 0.8, 1.0
301	Deep	0.68	1.47	934	0.2, 0.4, 0.6, 0.8, 0.87	*0.2*, 0.4, 0.6, 0.8, 1.0, 1.2
408	Deep	1.37	2.31	12460	0.2, 0.4, 0.6, 0.8, 1.0, 1.2, 1.4	*0.2*, 0.4, 0.6, 0.8, 1.0, 1.2, 1.6
415	Deep	0.46	1.11	4052	0.2, 0.4, 0.6	0.2, 0.4, 0.6

Table 2.2: The moss species identified from the surface of extracted cores from relative hollow and hummock microforms of five intermediate and four deep depressions studied. Relative elevations are based on the average heights at the bases of piezometers installed (see Table 2.1) in the microforms, relative to a rock reference at each site.

Site #	Depression Size	Hollow Species	Hollow Relative Elevation (m)	Hummock Species	Hummock Relative Elevation (m)
313	Intermediate	*Sphagnum cuspidatum, Sphagnum fallax*	-0.20	*Polytrichum*	-0.06
405	Intermediate	*Sphagnum compactum, Polytrichum*	-0.49	*Sphagnum fallax, Sphagnum capillifolium*	-0.25
410	Intermediate	*Sphagnum compactum, Sphagnum cuspidatum*	-0.45	*Sphagnum palustre, Polytrichum*	-0.28
416	Intermediate	*Sphagnum magellanicum, Sphagnum palustre*	-0.53	*Sphagnum fallax, Sphagnum palustre, Polytrichum*	-0.39
502	Intermediate	*Sphagnum palustre, Polytrichum*	-0.04	*Sphagnum fallax, Polytrichum*	-0.01
234	Deep	*Sphagnum fallax*	-0.43	*Sphagnum fallax, Sphagnum palustre*	-0.38
301	Deep	*Sphagnum palustre*	-1.08	*Sphagnum palustre, Sphagnum rubellum*	-0.99
408	Deep	*Sphagnum fallax, Sphagnum palustre*	-0.55	*Sphagnum fuscum, Sphagnum magellanicum, Polytrichum*	-0.45
415	Deep	*Sphagnum cuspidatum, Sphagnum palustre*	-0.45	*Sphagnum fallax, Sphagnum palustre*	-0.35

Table 2.3: Four working standards were calibrated for use when running pore-water, rainfall and outflow samples on the Picarro L-1102-i CRDS analyzer. The DSH and IWL were used for normalizing to the VSMOW/SLAP scale. MDI was used throughout sample runs to first correct for memory and drift effects. BSB305-DI was treated as a sample in runs as a quality control. δ^2H values were calibrated on 23/11/2017 on the Picarro L-1102-i CRDS analyzer, whereas $\delta^{18}O$ values were calibrated on 07/02/2018 by IRMS with the McMaster Research Group for Stable Isotopologues.

Working Standard	**$\delta^{18}O$ value (‰)**	**δ^2H value (‰)**
Deep Sea Heavy (DSH)	0.10	-2.23
Iceberg Water Light (IWL)	-28.32	-212.47
BSB305-DI	-6.46	-47.17
Mixed DI water (MDI)	-6.51	-46.97

Table 2.4: Isotopic analysis sample runs on the Picarro L-1102-i CRDS analyzer were arranged according to the tray scheme suggested by van Geldern & Barth (2012) for use with their provided methods of memory and drift corrections. Sample runs typically took just over 19 hours to complete.

Vial	Identifier	Injections
1	MDI	10
2	DSH	10
3	IWL	10
4	MDI	10
5	BSB305-DI	4
6	Sample 1	4
7	Sample 2	4
8	Sample 3	4
9	MDI	4
10	Sample 4	4
11	Sample 5	4
12	Sample 6	4
13	Sample 7	4
14	Sample 8	4
15	Sample 9	4
16	Sample 10	4
17	Sample 11	4
18	MDI	4
19	Sample 12	4
20	Sample 13	4
21	Sample 14	4
22	Sample 15	4
23	Sample 16	4
24	Sample 17	4
25	Sample 18	4
26	Sample 19	4
27	MDI	4

Table 2.5: General linear model of peat hydrophysical variables and residence time estimates related to site parameters of size, microtopography and depth. Three two-way interactions between the three parameters were included in every model, whereas the three-way interaction between the parameters was only included if it improved model performance, as assessed by the adjusted R^2 values. K_{sat}, K_{Total} and bulk density failed to meet model assumptions and so had to be log_{10}-transformed. P-values are **bolded** where significant to p<0.01, *italicized* where significant to p<0.05 and model performance was assessed as adjusted R^2.

	K_{sat}		K_{Total}		Bulk Density		Porosity		$ITTP_{\delta 18O}$		$ITTP_{\delta 2H}$	
	F	*p*	*F*	*p*	*F*	*p*	*F*	*p*	*F*	*p*	*F*	*p*
Site type	1.65	0.204	1.44	0.235	35.47	**0.000**	31.33	**0.000**	1.27	0.055	18.61	**0.000**
Microform	1.52	0.223	3.20	0.079	0.07	0.787	0.56	0.458	9.05	**0.000**	12.40	**0.001**
Depth type	23.96	**0.000**	28.28	**0.000**	60.54	**0.000**	59.51	**0.000**	7.77	*0.018*	51.85	**0.000**
Site type x Microform	0.23	0.635	0.02	0.875	2.07	0.156	2.65	0.110	2.37	*0.045*	4.25	*0.044*
Site type x Depth type	6.15	*0.016*	7.37	**0.009**	0.21	0.646	4.63	*0.036*	6.69	*0.023*	5.80	*0.020*
Microform x Depth type	4.08	*0.048*	4.22	*0.045*	4.00	0.051	2.94	0.093	0.13	0.432	0.37	0.547
Site type x Microform x Depth type									8.86	**0.004**	4.87	*0.032*
R^2 (adj)	0.4983		0.5428		0.5757		0.5289		0.3996		0.6877	

Table 2.6: Spearman rank correlation analysis was used to examine relationships between peat hydrophysical properties and residence time estimates in the correlation matrix below, with the displayed values being Spearman's ρ, where **bolded** terms are significant to $p<0.05$.

	K_{sat}	K_{Total}	Bulk Density	Porosity	$ITTP_{d18O}$	$ITTP_{d2H}$
K_{sat}						
K_{Total}	**0.962**					
Bulk Density	**-0.468**	**-0.502**				
Porosity	**0.509**	**0.542**	**-0.986**			
$ITTP_{d18O}$	0.123	0.189	-0.182	0.168		
$ITTP_{d2H}$	**0.599**	**0.663**	**-0.441**	**0.462**	0.701	

2.7 FIGURES

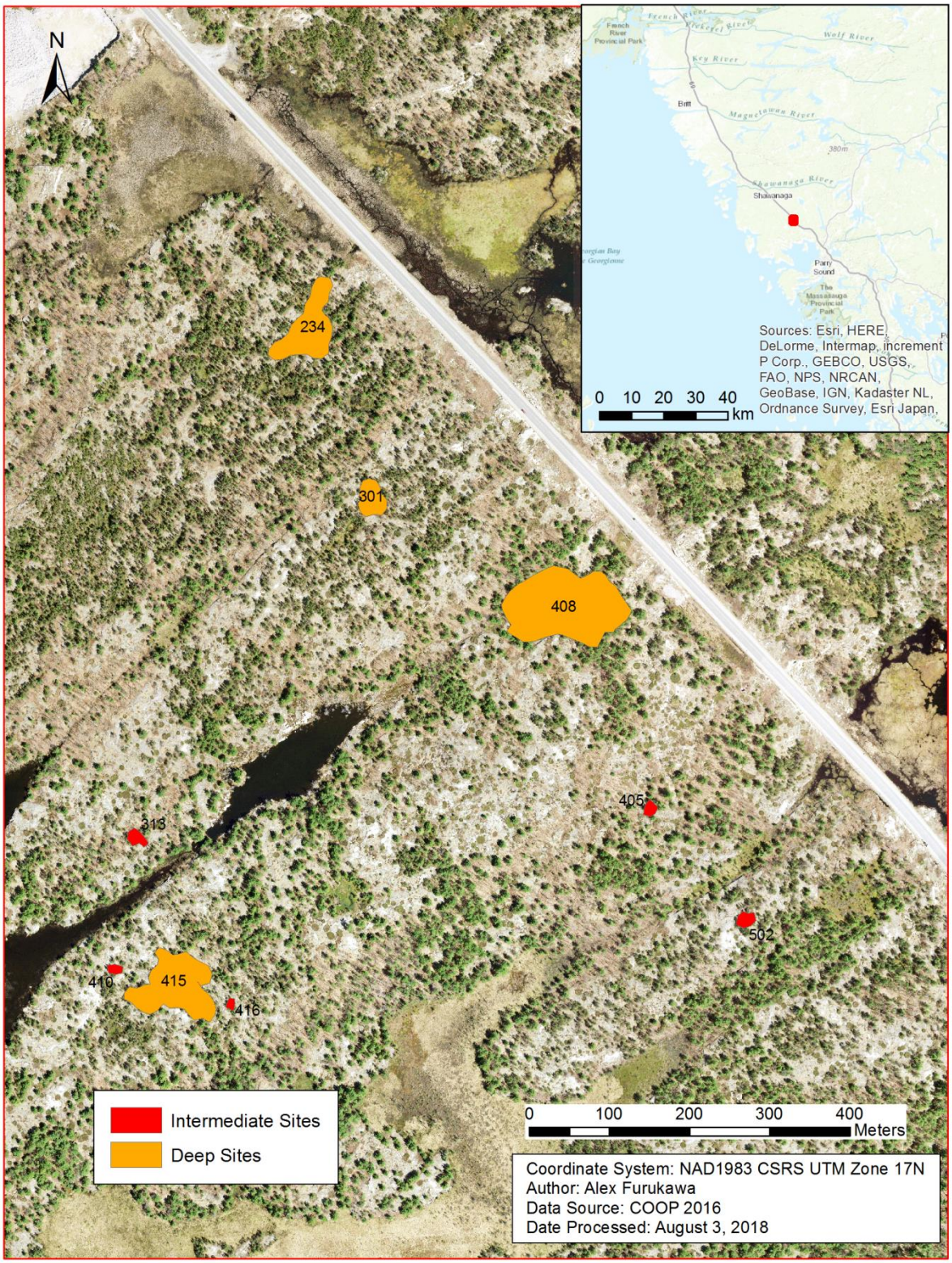

Figure 2.1: The study area of the NOBEL is located approximately 20 km north of the town of Parry Sound, ON (inset). The peat-filled bedrock depressions studied consisted of four deep sites (orange, >0.4 m mean depth) and five intermediate sites (red, <0.4 mean depth). Labels indicate the site names used when referenced.

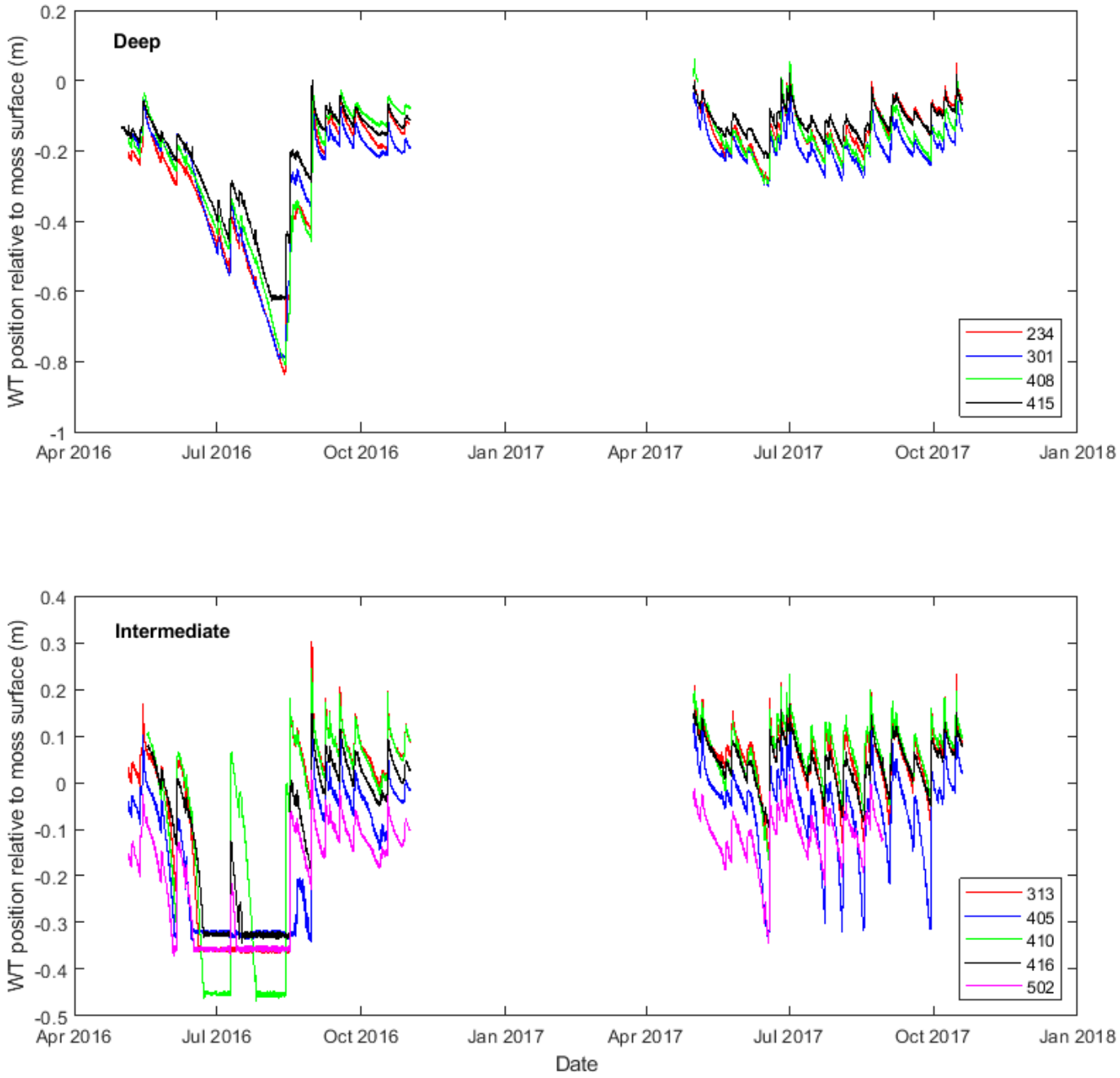

Figure 2.2: Water table depth (WTD) relative to the moss surface was measured continuously (every 10 minutes) with Solinst Levelogger Junior pressure transducers for 2016 and 2017. Displayed are the ice-free periods from each year (May through October) for the sites considered deep and intermediate in size.

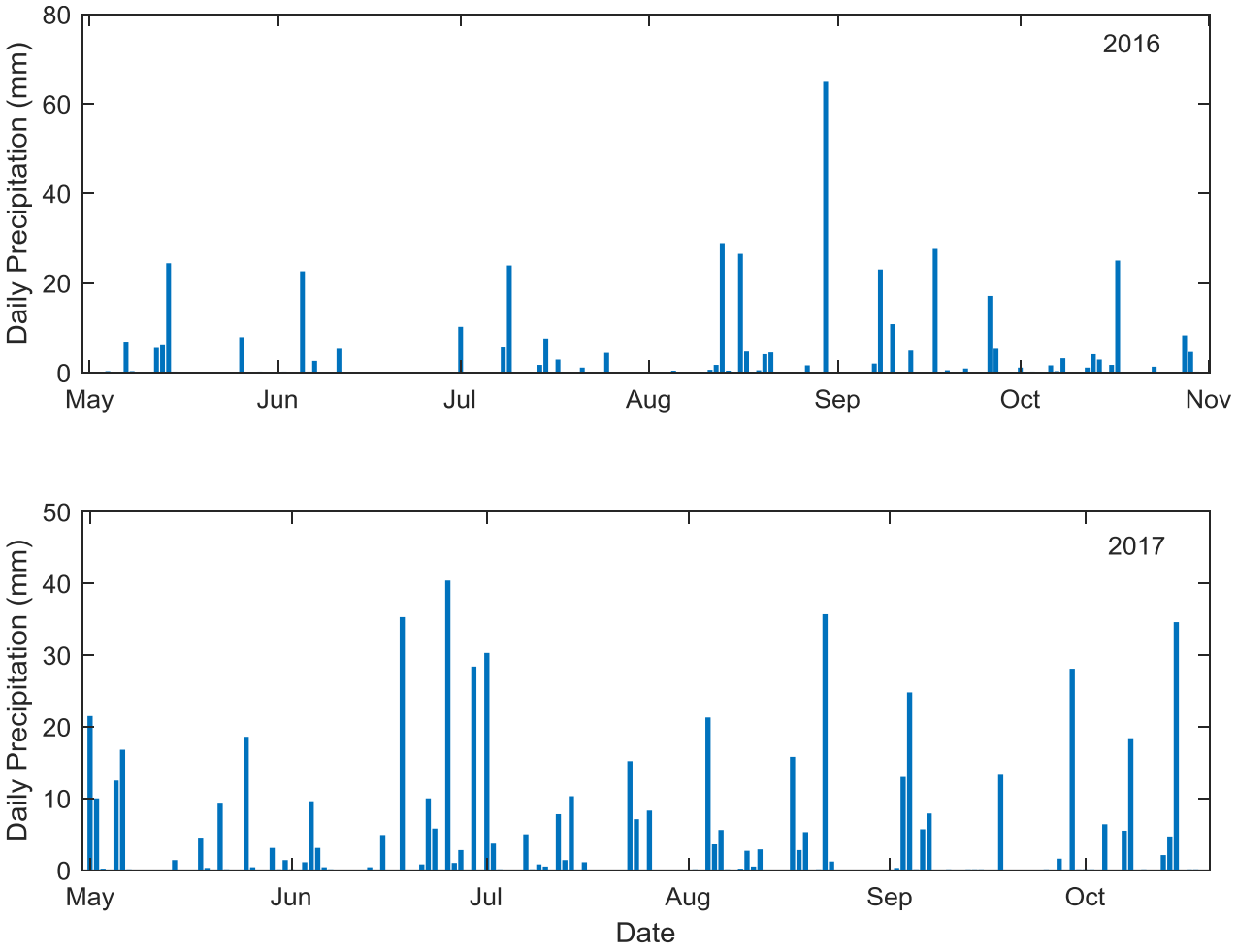

Figure 2.3: Precipitation received at site 415 in the NOBEL in May to October of 2016, a drier than average period, and 2017, which was wetter than average. Rainfall data was based on measurements collected by tipping bucket rain gauge.

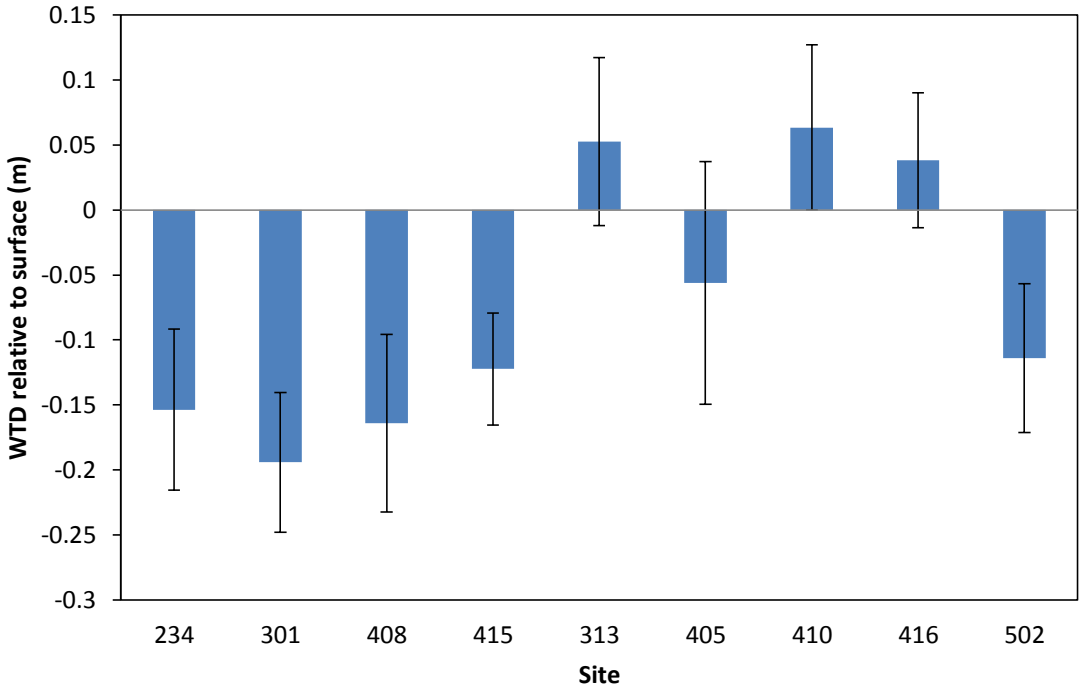

Figure 2.4: Mean WTD and standard deviation (as error bars) based on continuous measurements in groundwater wells from all sites during the study period from May to August 2017. Sites 313, 410 and 416 had a mean WTD above the surface due to their monitoring wells being located in wet, pool-like areas of the wetland.

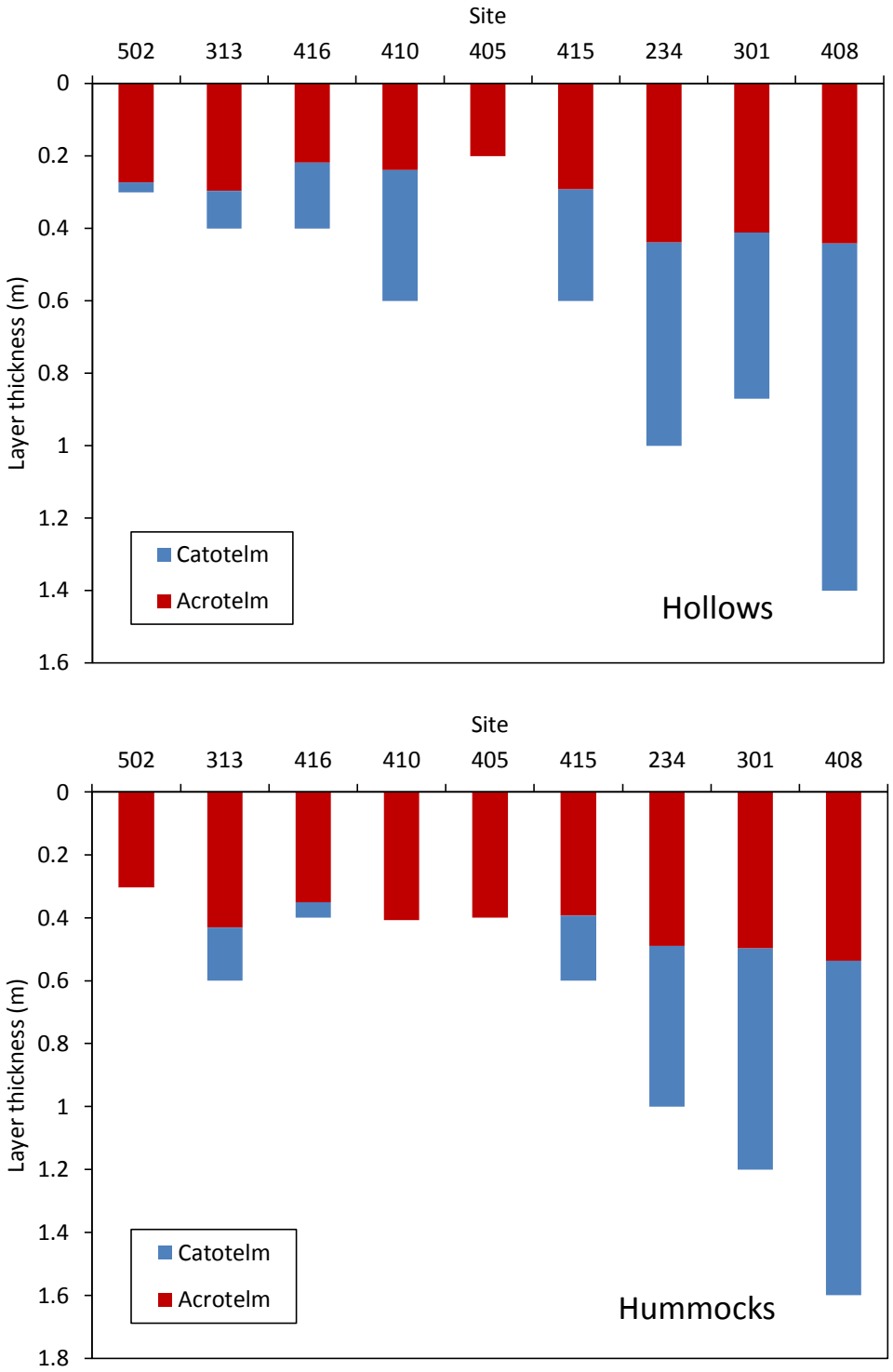

Figure 2.5: The thicknesses of the acrotelm and catotelm were based on a boundary of one standard deviation below the mean for growing season (May – October) of the relatively dry year 2016. Sites are included in order of increasing maximum depth, left to right. Layer thicknesses are displayed in reverse order in order to better visualize how depths in piezometers were classified.

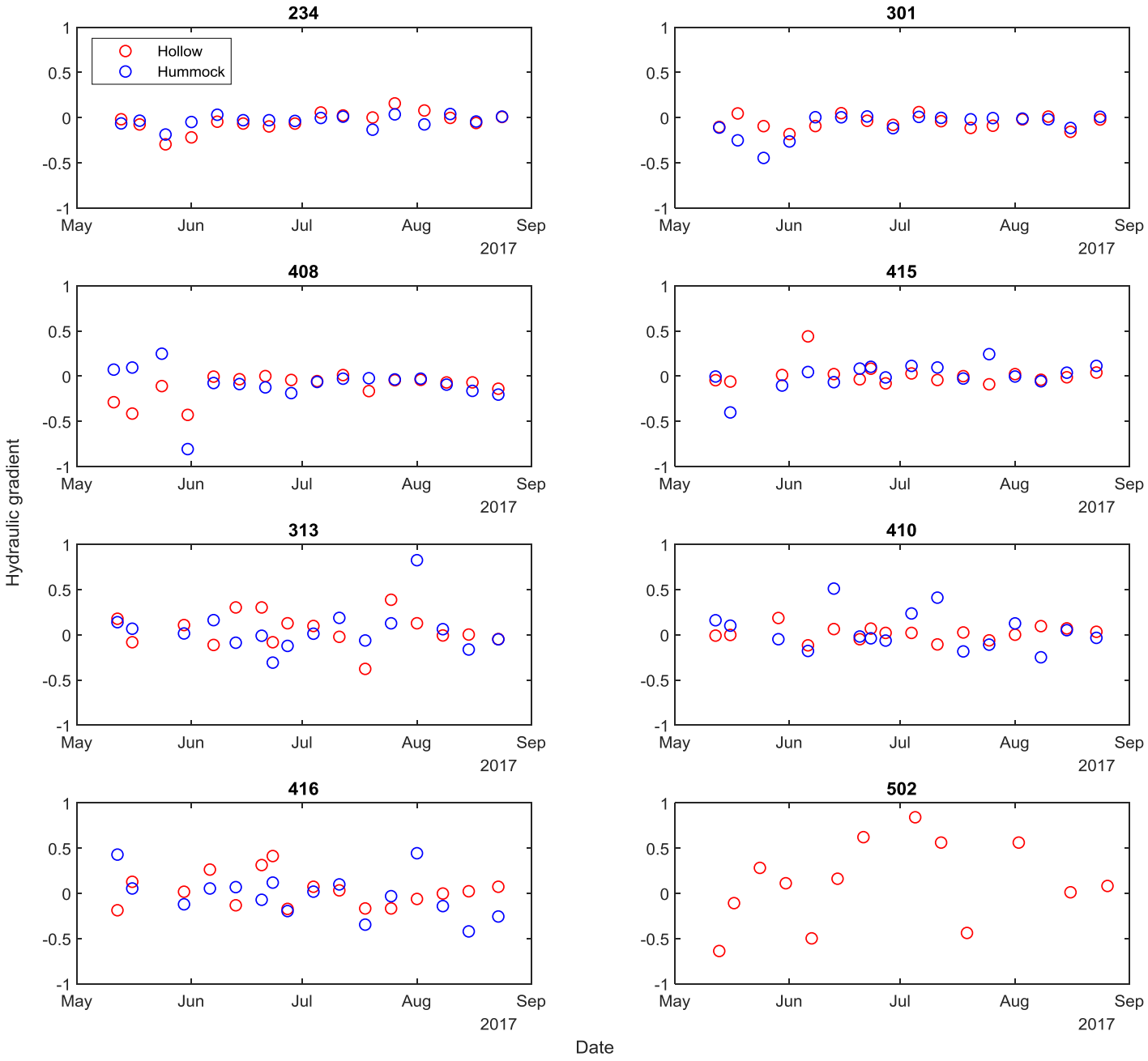

Figure 2.6: Hydraulic gradients based on weekly hydraulic head measurements made in piezometer nests relative to an arbitrary datum at each site. Gradient is measured as the slope of hydraulic heads from the shallowest piezometer increment (0.2 m) to the deepest (0.3 – 1.6 m). Site 405 is not included due to dry conditions precluding regular measurement of hydraulic head throughout the season and only one piezometer being installed in the hollow microform. Site 502 only displays data for the hollow, as the hummock only had one piezometer installed due to depth constraints.

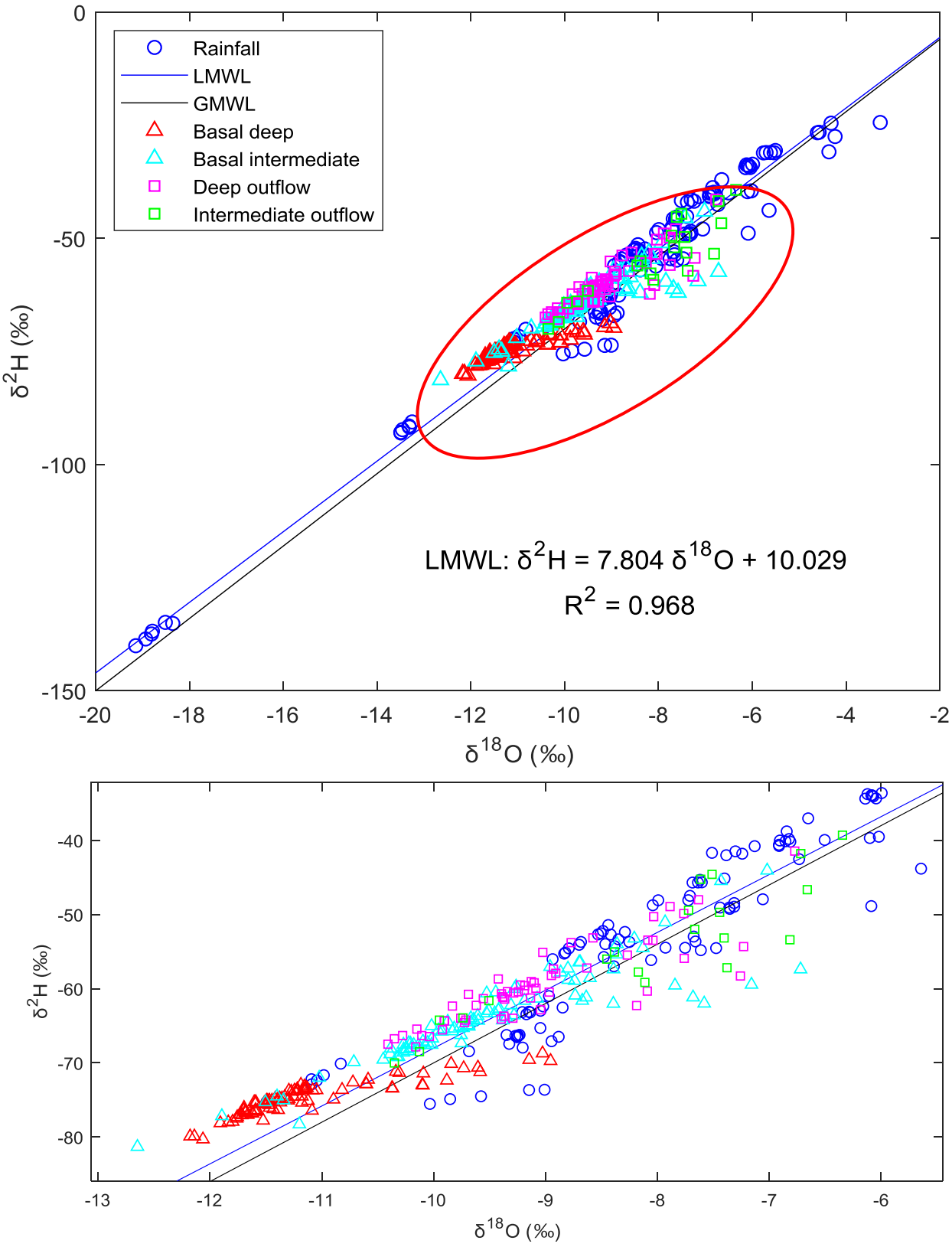

Figure 2.7: A local meteoric water line (LMWL) was developed using linear regression of δ^2H and $\delta^{18}O$ of rainfall samples collected from six sites within the NOBEL from May-August and one collection in October. The LMWL and its equation is displayed along with the global meteoric water line (GMWL), which plotted as $\delta^2H = 8\ \delta^{18}O + 10$. Also plotted are pore-water samples collected from the base of deep and intermediate sites as well as outflow from four deep and two intermediate sites. The inset below provides a closer view of the red-encircled region to allow for easier distinguishing of clusters of samples along the LMWL.

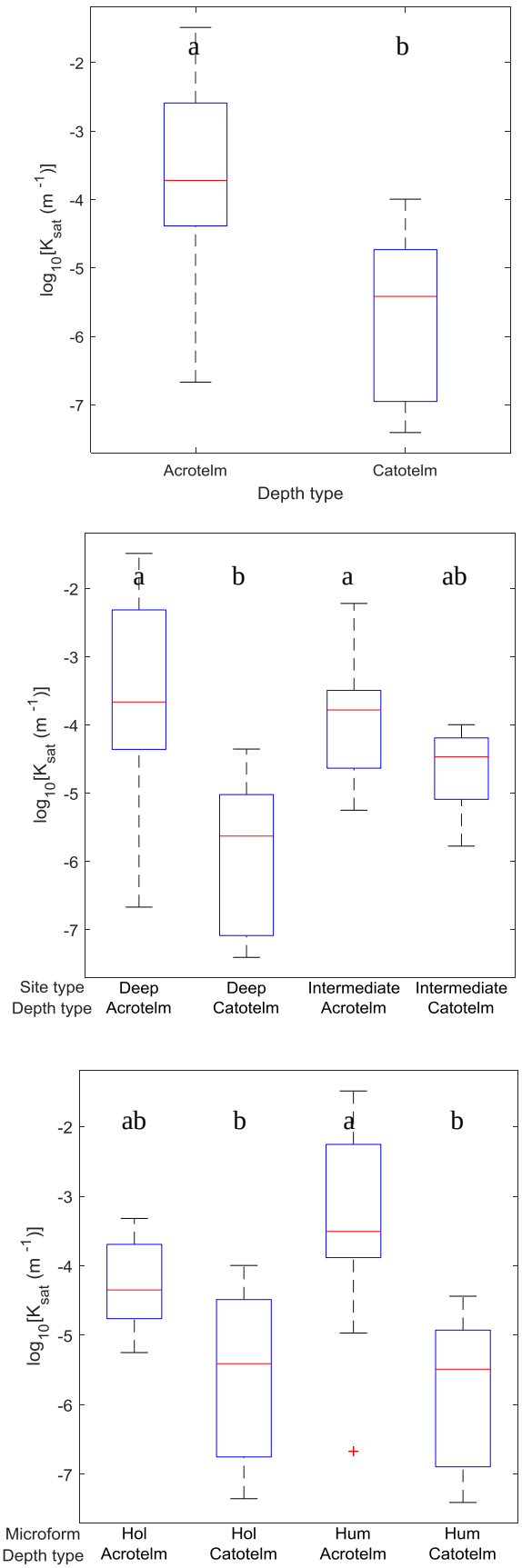

Figure 2.8: Boxplots depict differences in K_{sat} with depth and its interactions with depression size and microform (top to bottom). Boxes display the interquartile range, with crosses indicating outliers. Letters denote significant differences (to $p<0.05$, by Tukey HSD) between groups not sharing a letter.

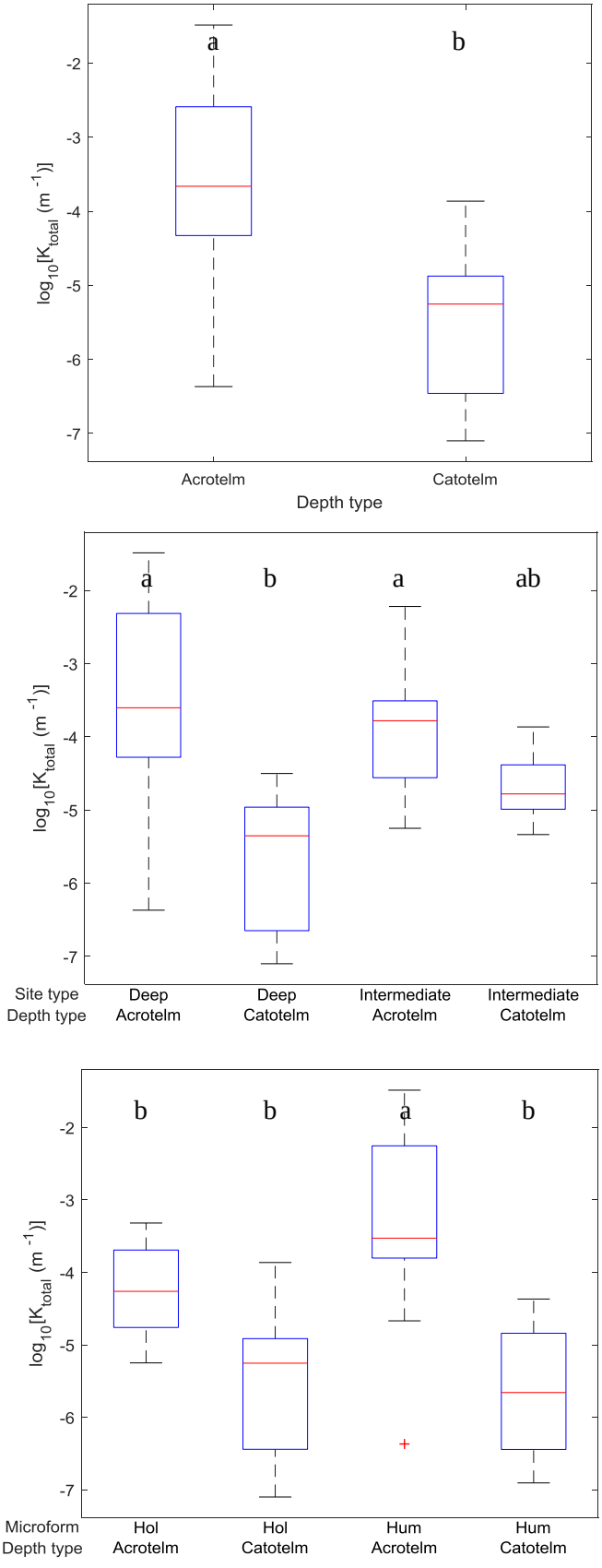

Figure 2.9: Boxplots depict differences in K_{Total} with depth and its interactions with depression size and microform (top to bottom). Boxes display the interquartile range, with crosses indicating outliers. Letters denote significant differences (to $p<0.05$, by Tukey HSD) between groups not sharing a letter.

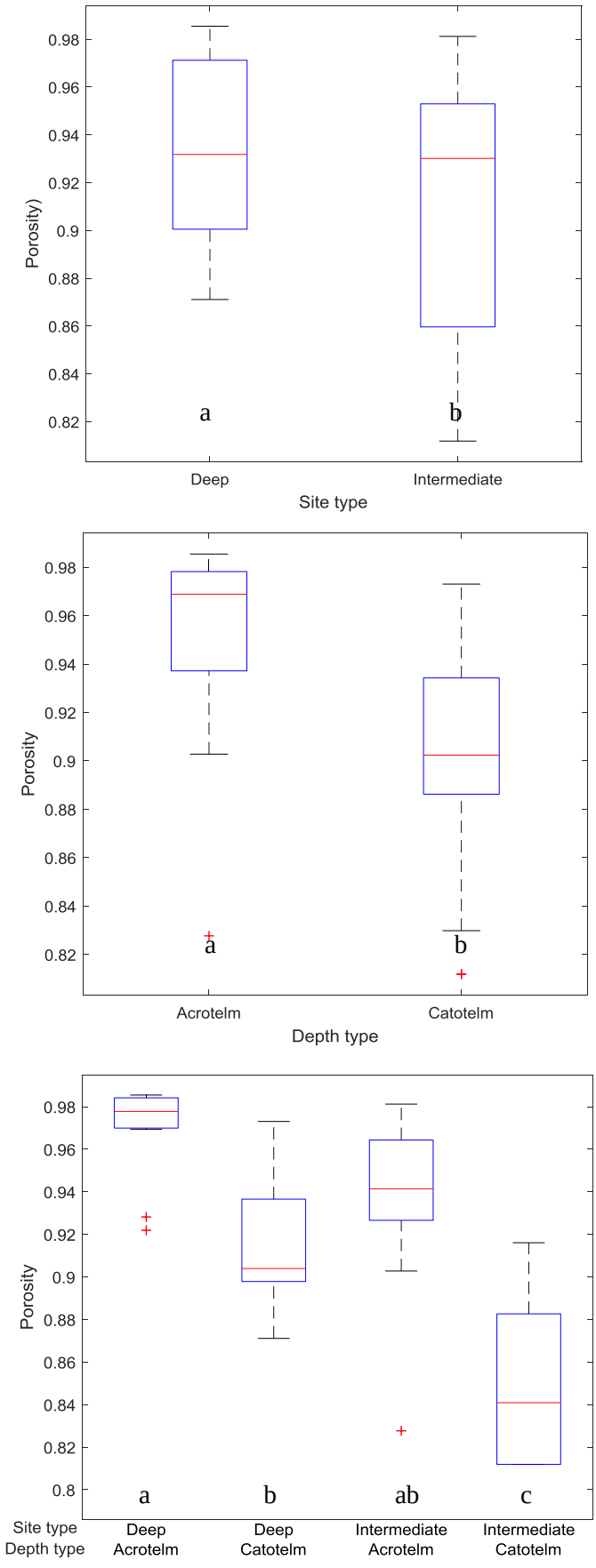

Figure 2.10: Boxplots depict differences in porosity with depth and its interactions with depression size and microform (top to bottom). Boxes display the interquartile range, with crosses indicating outliers. Letters denote significant differences (to $p<0.05$, by Tukey HSD) between groups not sharing a letter.

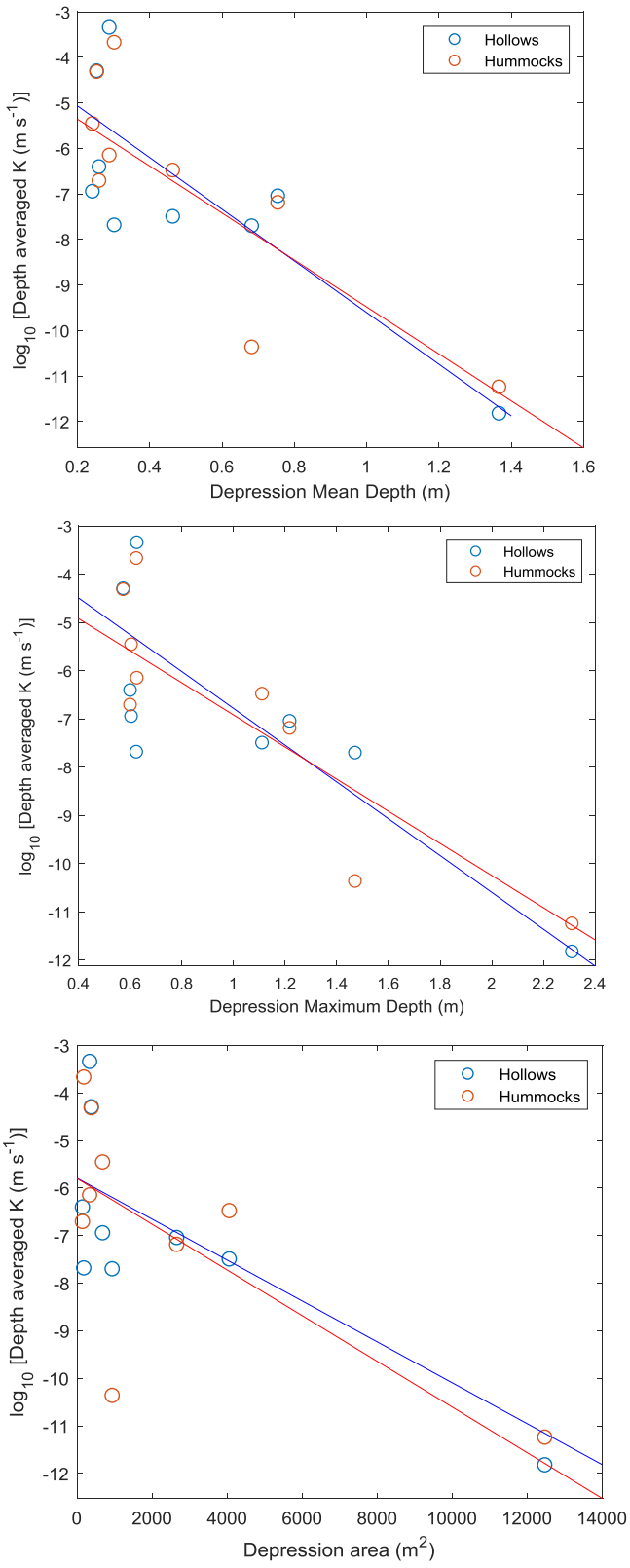

Figure 2.11: Linear regressions were developed between site depth averaged K for hollow and hummock profiles with parameters of overall site size depicted top to bottom; mean depth (R^2=0.604, $p<0.01$ and R^2 = 0.666, $p<0.005$, respectively), maximum depth (R^2=0.63, $p<0.01$ and R^2= 0.765, $p<0.005$, respectively) and area (R^2= 0.597, $p<0.01$ and R^2= 0.388, $p<0.05$, respectively). Depth averaged K was the K_{total} at the most basal layer measured and was log_{10}-transformed.

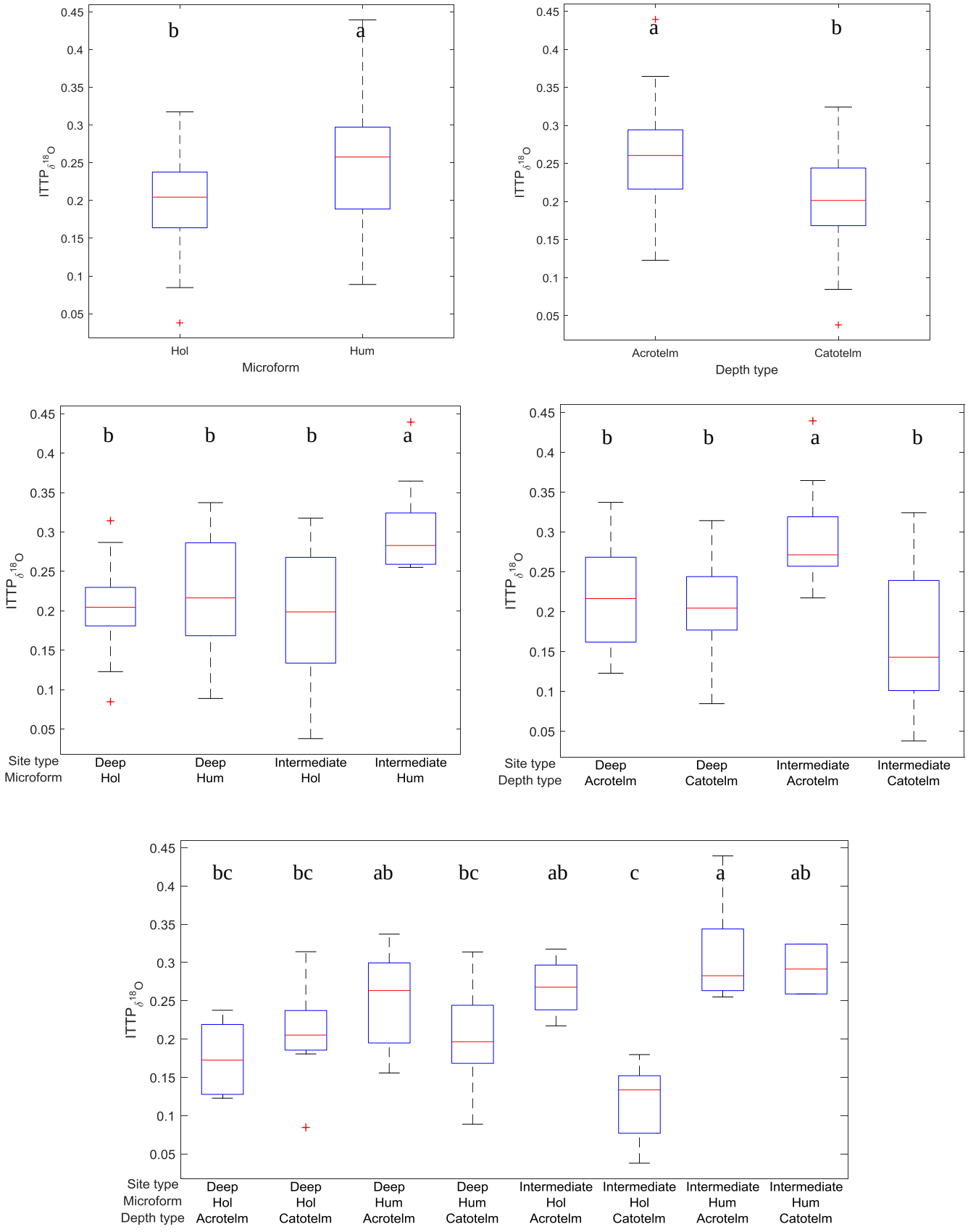

Figure 2.12: Boxplots depict differences in $ITTP_{\delta 18O}$ with microform, depth, site size x microform, site size x depth and three-way interactions between them all (left to right, top to bottom) Boxes display the interquartile range, with crosses indicating outliers. Letters denote significant differences (to $p<0.05$, by Tukey HSD) between groups not sharing a letter.

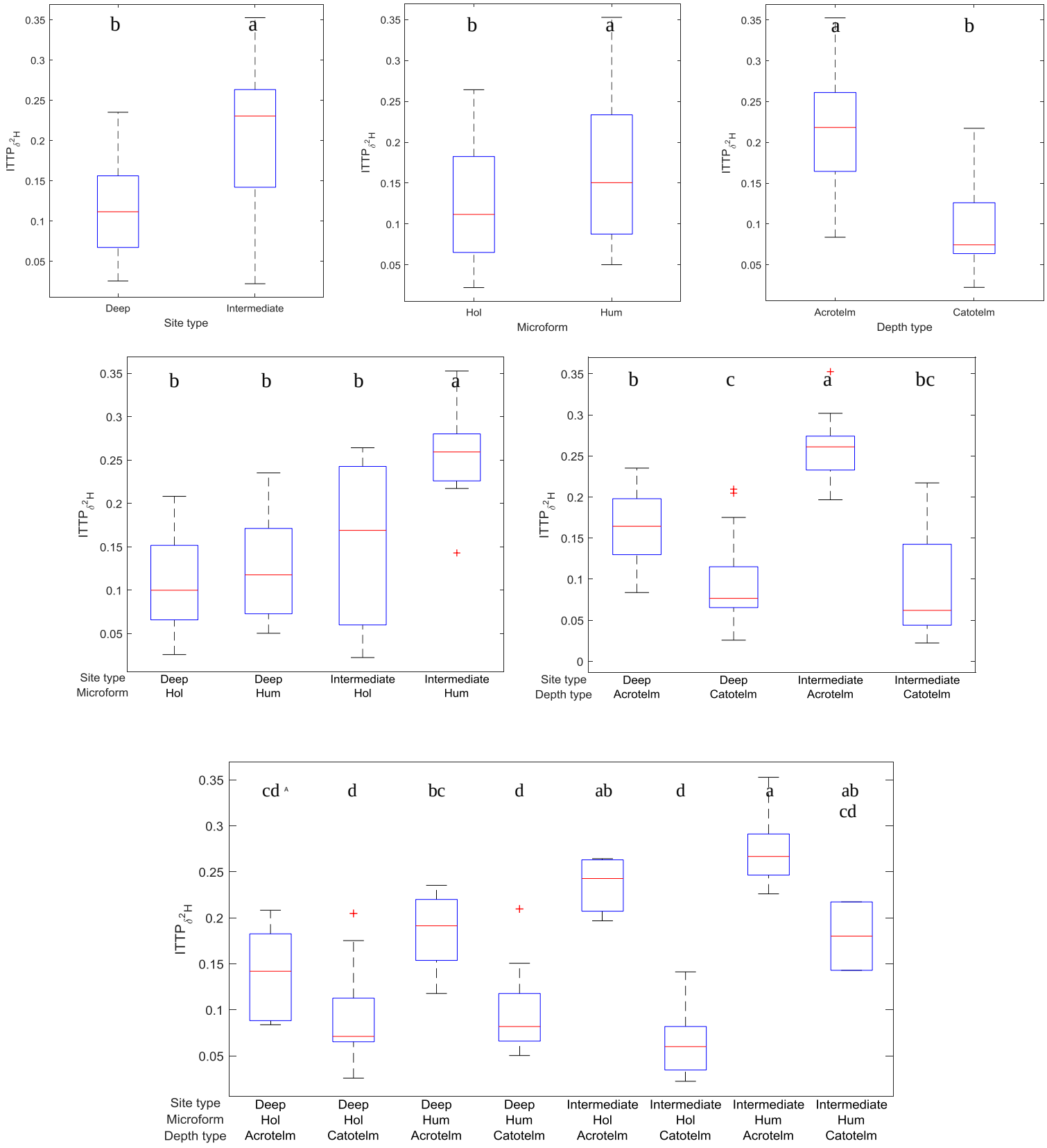

Figure 2.13: Boxplots depict differences in $ITTP_{\delta 2H}$ with site size, microform, depth, site size x microform, site size x depth and three-way interactions between them all (left to right, top to bottom) Boxes display the interquartile range, with crosses indicating outliers. Letters denote significant differences (to $p<0.05$, by Tukey HSD) between groups not sharing a letter.

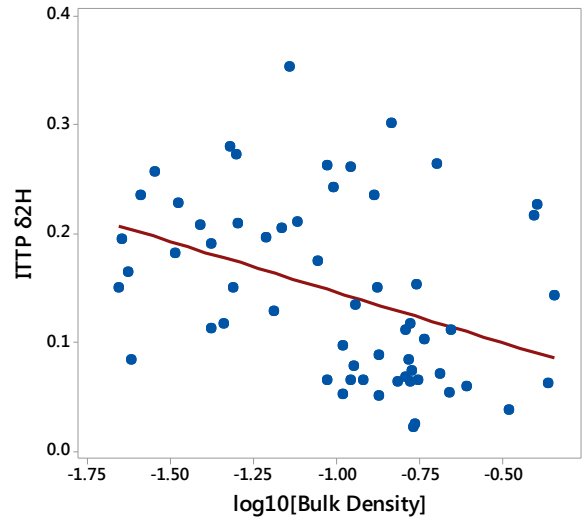

Orthogonal: ITTP δ2H = 0.054 - 0.093 log10[Bulk Density], p<0.005, R2 = 0.1257

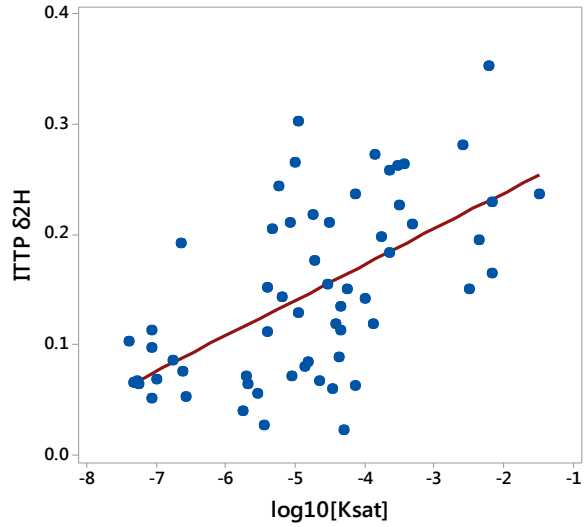

Orthogonal: ITTP_d2H = 0.302 + 0.032 log10Ksat, p<0.001, R2 = 0.3458

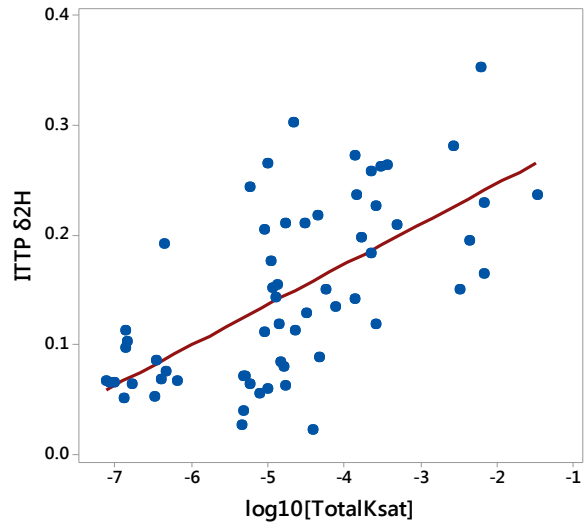

Orthogonal: ITTP δ2H = 0.320 + 0.037 log10[TotalKsat], p<0.001, R2 = 0.3916

Figure 2.14: Orthogonal regression was used to investigate the significant correlations between $ITTP_{\delta 2H}$ and measured hydrophysical properties. Bulk density was significant to $p<0.005$ whereas the measures of hydraulic conductivity were significant to $p<0.001$. Adjusted-R^2 values were 0.1254, 0.3504, and 0.3933 (top to bottom).

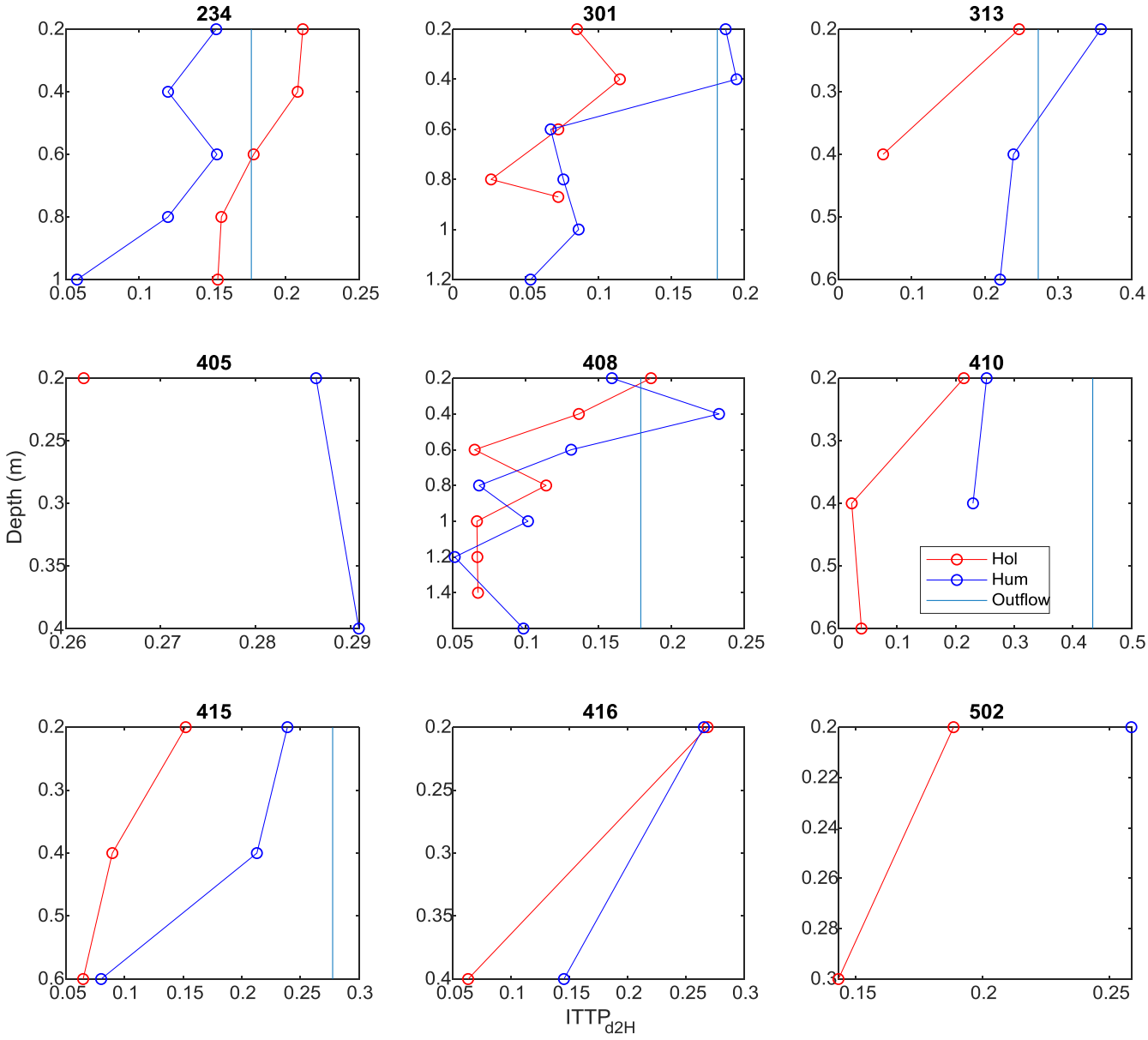

Figure 2.15: Profiles of relative pore water residence time, as estimated by the inverse transit time proxy (ITTP) from δ^2H are compared by microform (Hol and Hum) across four deep sites (234, 301, 408 and 415) and five intermediate sites (313, 405, 410, 416 and 502). Also plotted in cyan are the ITTP$_{\delta 2H}$ of outflow collected at the outlet of sites 234, 301, 313, 408, 410 and 415, which were observed to be 'spilling' for a majority of the 16-week study period.

CHAPTER 3: CARBON ACCUMULATION AND DISSOLVED ORGANIC MATTER (DOM) QUALITY

3.1 INTRODUCTION

3.1.1 C accumulation in peatlands

The original diplotelmic model by Ingram (1978), despite its limitations (see Morris et al., 2011 for critique), offers a good starting point to approaching carbon accumulation in northern peatlands. In this model, the primary production taking place in the upper, periodically saturated acrotelm, is countered by decomposition, the majority of which takes place there (Clymo et al., 1998). Only about 10% of litter reaches the catotelm, which remains permanently saturated throughout the year and permits decomposition two orders of magnitude slower than the acrotelm (Frolking et al., 2001). The upper peat layers may undergo enhanced decomposition due to aeration and warmer conditions, while the deeper layers present cooler, waterlogged and recalcitrant conditions (Yavitt et al., 1997). Due to the constraints on decay, the catotelm has not been observed to play much of an active role in atmospheric carbon exchange (Blodau et al., 2007; Frolking et al., 2001; Lafleur et al., 2001), but nevertheless is an important sink that supports long-term carbon accumulation in peatlands by facilitating transport and geochemical constraints on decomposition. Carbon sequestration is dependent on the peat formation near the surface exceeding any losses from decay (Clymo, 1984). While decomposition in the acrotelm is controlled by more short-term climate and hydrological conditions, the catotelm relies upon feedbacks related to the peat composition and the conditions created deeper in the peat to bestow resistance to decay.

3.1.1.1 Sphagnum peat's resistance to decay

Organic matter decomposition may vary across different types of wetland ecosystems (Thormann et al., 1999); this is the result of qualities of the organic matter undergoing decomposition (and therefore vegetation) as well as the conditions under which they may undergo decay. Ingram (1978) posited that substrate control on decay was only significant in the more active, periodically saturated acrotelm, but there is a considerable body of evidence to support the strength of the control of litter quality on decomposition (Fogel and Cromack Jr., 1977). For northern peatlands, the unique recalcitrant properties of the litter of their ecosystem

engineer *Sphagnum* moss, has received considerable attention. Slow decomposition in *Sphagnum* litter has been associated with lignin-like compounds (Lindberg et al., 1952) and polymerized lipids (Kalviainen and Karunen, 1984; Karunen and Ekman, 1982). It was previously thought to contain lignin but instead has been attributed to its high phenol content (including the genus-specific, stable, Sphagnum acid) (Rudolph and Samland, 1985; van der Heijden, 1994). The basis for *Sphagnum*'s resistance to decay may lie in chemical protection of cell well sugars by polyphenolic network polymers and lipid surface coating (Karunen and Ekman, 1982) as well as tannin-like compounds that may suppress microbial activity (van der Heijden, 1994).

Different varieties of *Sphagnum* moss are found across microforms along the hollow-hummock gradient (Andrus et al., 1983). Hollow species (in particular *S. cuspidatum*) have been found to decay as much as 1.5 times as fast as a hummock species (*S. fuscum*) where the species effect exceeded that of microhabitat (Johnson and Damman, 1991) where microforms may differ in oxygenation, redox chemistry, pH and element mobility (Damman, 1978; Pakarinen, 1978; Zobel, 1986). This was further supported by Turetsky et al. (2008) who also observed hollow *Sphagnum* species producing more labile litter compared to a hummock species that demonstrated greater investment in structural carbohydrates.

In terms of variation in decomposition with depth, decay in the deep, permanently saturated catotelm progresses extremely slowly at 0.1 to 0.001%/year, potentially two orders of magnitude slower than in the acrotelm (Clymo et al., 1998; Frolking et al., 2001; Karunen and Ekman, 1982). The influence of the catotelm environment should not be underestimated despite *Sphagnum* peat's recalcitrant qualities, which is vulnerable to the aeration and decomposition that comes with drainage, as this may alter the hydraulic properties permanently (Schouwenaars, 1988). It is crucial that the conditions in the deep peat layers are maintained, where the saturated conditions only permit anaerobic respiration that is made further energetically unfavourable by the accumulation of decay end-products (Beer and Blodau, 2007) and the availability of more favourable substrates is suppressed by the low conductivity and solute transport in the buried peat (Beer et al., 2008). Despite potential variation across microforms, the deeper layers of peatlands appear to have ubiquitously slow decomposition of organic matter (Beer et al., 2008). This supports earlier work that the catotelm does not typically partake in much atmospheric

exchange (Blodau et al., 2007; Frolking et al., 2001; Lafleur et al., 2001) and its water is effectively disconnected from the surface (Beer and Blodau, 2007) rendering the store of carbon relatively stable and resilient to potential disturbance.

3.1.2 Pore-water chemistry

Dissolved organic matter (DOM) constitutes a mixture of organic compounds found in any waters, from fallen rainfall and surface water to soil pore water and groundwater, that is typically sourced from decomposition and exudates of plants and microbes (Gabor et al., 2014). The distribution, export and quality of dissolved organic matter (DOM) in peat pore-water is controlled primarily by peatland hydrology, such as WTD (Waddington et al., 2008), hydraulic conductivity and gradient (Fraser et al., 2001). Microform type and patterns also play a role (Belyea and Clymo, 2001). In their examination of the peat pore-water chemistry-decomposition feedback, Beer et al. (2008) conducted FTIR (Fourier Transform Infrared) analysis on peat pore-water, where they observed a greater prevalence of aromatics and phenolics with depth and concluded that most DOM in the catotelm is produced and consumed in situ (autochthonous), which mirrored the findings of Fraser et al., (2001) at the Mer Bleue bog in Ontario, Canada.

3.1.3 Fluorescence spectroscopy

The quality, or composition of this DOM is dynamic both spatially and temporally; this in addition to the diversity of potential sources results in it being rather chemically complex, which poses challenges for analysis (Aiken, 2014). One technique that offers a means to address this problem is fluorescence spectroscopy. While not a recently developed technique (Hartley, 1893), it offers a means of analyzing natural organic compounds in a way that facilitates fairly simple and direct data collection to inform on the concentration and composition of DOM (Weishaar et al., 2003). About a century since its origins, fluorescence spectroscopy has seen considerable development and greater application among a variety of aquatic systems (Baker et al., 2008; Cory and McKnight, 2005; Spencer et al., 2007).

The assumption underlying fluorescence spectroscopy is that the compounds that constitute DOM will behave similarly to pure compounds in solution, which predicates that any changes in observed properties such as the intensity, absorbance, peak width and wavelengths of maximum

intensity reflect variation in DOM constituents (Aiken, 2014). However, in order for measurements of fluorescence to be comparable, one must account for other complicating factors such as instrumental biases and environmental variation (Aiken, 2014; Stedmon and Bro, 2008). On the side of instrumental correction, two common techniques are the calibration of signal intensity by Quinine Sulfate (QS) and Raman Signal (RS). The QS standard is measured at an excitation of 350 nm and emission of 450 nm in order to apply spectral corrections to account for deviation in light source output whereas the RS is a pure water sample whose spectrum is subtracted from the sample spectrum to correct for Raman scattering. (Stedmon and Bro, 2008). Inner filter effects (IFE) stemming from the absorption of incoming excitation light (Ohno, 2002) must also be corrected for. Rayleigh scatter corrections are further applied by the removal of areas of the excitation-emission matrix (EEM) that lack any data (Stedmon and Bro, 2008). With regards to analyzing DOM, excitation and emission spectra may range considerably from 250-400 nm and 350–500 nm, respectively (Stedmon and Bro, 2008), though the absorption of certain wavelengths have also proved to be a valuable analytical tool.

3.1.3.1 Absorption and fluorescence of DOM

In the UV to visible spectrum (190–780 nm) of light, absorption entails the excitation of electrons in chemical bonds from a ground to excited energy state (Valeur, 2001). The wavelength absorbed depends on the molecular structure and difference in energy between these energy states of the light-absorbing portion of the molecule called a chromophore (Aiken, 2014). Simpler single-bond molecules such as alkanes and carbohydrates tend to absorb at shorter wavelengths outside of the UV-visible spectrum, whereas more conjugated alkene and aromatic molecules absorb light at longer wavelengths, most strongly with aromatic molecules (Aiken, 2014).

In contrast, the phenomenon known as fluorescence refers to the light emitted when the excited electrons return to their ground state and molecules that are capable of this are referred to as fluorophores (Valeur, 2001). The intensity and wavelength of emission is controlled by the molecular structure as is the case with absorption, with aromatic compounds fluorescing with greater intensity than less conjugated molecules (Aiken, 2014) and the wavelength of emission longer when functional groups are present (Valeur, 2001).

3.1.3.2 Indices of DOM quality

In order to interpret absorption data and the data contained in the EEMs produced by fluorescence spectroscopy, a number of indices have been developed and used to characterize organic material by standardized measures (Gabor et al., 2014). These indices have been used to identify characteristics of organic material including source material (Cory and McKnight, 2005; McKnight et al., 2001), humification (Ohno, 2002; Zsolnay et al., 1999), production processes (Huguet et al., 2009; Parlanti et al., 2000; Wilson and Xenopoulos, 2009) and molecular structure (Chen et al., 1977; De Haan, 1993; Peuravuori and Pihlaja, 1997).

The fluorescence index (FI) was originally developed by McKnight et al. (2001) to indicate the relative contribution of terrestrial vegetation and microbial sources to DOM pool calculated as the ratio of emission at a wavelength of 450 nm to the emission at 500 nm based on excitation at 370 nm (Cory et al., 2010). McKnight et al. (2001) originally investigated lakes and rivers in Antarctica and the United States with microbial-based (~1.9) and terrestrial-based (~1.4) end members and noted a strong correlation with percent aromaticity. This FI was later modified for instrument corrections to be the emission ratio of 470 nm to 520 nm from excitation at 370 nm (Cory and McKnight, 2005).

The humification index (HIX 1999) was originally formulated by Zsolnay et al. (1999) as the area under the emission spectra from 435 to 480 nm divided by the peak area from 300 to 345 nm, at an excitation of 254 nm. Later on, Ohno (2002) modified the index (HIX 2002) to the area under the emission spectra from 435 to 480 nm divided by peak area from 300 to 345 nm and 435 and 480 nm at an excitation of 254 nm, to eliminate potential for IFEs in concentrated samples. Both HIXs indicate the degree of humification of organic matter which is associated with a decrease in the ratio of H/C (Gabor et al., 2014; Ohno, 2002; Zsolnay et al., 1999).

The freshness index was originally developed by Parlanti et al. (2000) as the ratio between the β peak (ratio between maximum intensity for excitation at 310 to 320 nm to maximum intensity between emissions from 380 to 420 nm) and α peak (ratio between maximum intensity for excitation from 330 to 350 nm to maximum intensity for emissions from 420 to 480 nm). This ratio indicates how much DOM was recently produced with greater values being ‘fresher’

(Parlanti et al., 2000; Wilson and Xenopoulos, 2009). Wilson and Xenopoulos (2009) later modified this ratio to emission intensity at 380 nm (β) divided by the maximum emission intensity between 420 and 435 nm, all at an excitation of 310 nm (α). The BIX is another variant of the freshness index developed by Huguet et al. (2009) to indicate autochthonous productivity. It is based on the ratio of emission intensity at 380 nm divided by the intensity at 430 nm, both at an excitation wavelength of 310 nm (Huguet et al., 2009).

While fluorescence is generally considered a more sensitive indicator for organic material than absorbance, ratios based on absorption have also been used extensively as far back as the E4/E6 ratio by Chen et al. (1977) based on the ratio of absorbance at 400 nm to the absorbance at 600 nm. This ratio has been frequently cited as a measure of humification or molecular weight, where higher values indicate lower weights (Moore, 1987; Summers et al., 1987). It has also been noted to indicate the fulvic versus the humic nature of DOM, where higher values denote fulvic and lower values denote humic (Hautala et al., 2000). The ABS ratio (A254/A365) is another index negatively correlated to molecular weight of DOC (Dahlén et al., 1996; De Haan, 1993). Lastly, the E2/E3 ratio by Peuravuori and Pihlaja (1997) calculated as absorbance at 250 nm over absorbance at 365 nm, has been used as an estimation of aromaticity or molecular weight, where high values indicate low aromaticity and small molecules of humic solutes (Grayson and Holden, 2012). The nature of the DOM from these absorbance ratios can be used to infer the source. For example more humic or aromatic DOM from peat compared to vascular plant litter, indicated by lower E2/E3 (Khadka et al., 2016). Inferences with regards to aromaticity and molecular size are relevant to pore-water chemistry through the DOM's quality for microbial degradation (Khadka et al., 2015) and its mobility (Strack et al., 2011).

3.1.4 Hypotheses

To assess the chemistry side of the pore-water chemistry-residence time feedback (see 1.5, Figure 1.1), carbon accumulation was quantified by means of peat cores extracted from peat-filled bedrock depressions, as delineated by carbon stored in the intermittently saturated acrotelm and permanently waterlogged catotelm. Larger depressions should store more carbon and hold a greater proportion in their deeper layers that are more resistant to decomposition. Pore-water chemistry was investigated using fluorescence spectrometry in order to discern spatiotemporal

variability in DOM quality in different sized depressions. It was hypothesized that the pore-water held in the deep layers of larger depressions differs in DOM composition to that found in shallower depressions. In terms of resilience to decay, this organic material should be older, more humified and of a more aromatic character, reflecting the recalcitrant properties of peat that are preserved by lack of turnover of deep peat pore-water.

3.2 METHODS

3.2.1 Water collection

Once a month, the suite of weekly pore-water samples underwent analysis for Fluorescence of Dissolved Organic Matter (fDOM), which required that they all be filtered consistently by 0.45 µm polyethersulfone filters due to the operational definition of dissolved organic carbon (DOC) as being comprised of the molecules that pass through such a filter of such size (Thurman, 1985) The water was then stored in amber glass vials (40 mL) to prevent reactions with light or plastics. With the exception of the first month where samples were filtered in a day's time, all subsequent samples destined for fDOM analysis were filtered in the field within an hour into amber glass vials that were then kept cool and stored in a dark refrigerator at 4 ℃ prior to analysis. Due to concerns about potential changes in DOM from the brief storage (up to one day in HDPE rather than just the ideal glass vials (Yoshimura, 2013), several (n=5) duplicate samples in June and August were intentionally stored in the HDPE bottles for one day to compare the effects on DOM of brief storage in HDPE compared to immediate filtration into amber glass vials.

Water samples collected in May-June were analyzed in early July, whereas samples collected in July-August were analyzed in August. While the common practice for fDOM is to analyze within a day, especially for absorbance, thorough testing in support of this requirement is lacking. Peacock et al. (2014) conducted an absorbance degradation experiment over 12 weeks wherein 0.45 µm filtered peatland ditch water samples were not observed to undergo any consistent change in UV-vis absorbance while being kept in cold and dark storage. While this stability is dependent on a number of other chemical properties, their first rigorous monitoring of

absorbance degradation gives a degree of confidence to assume that analyzing later (for logistical reasons) should not significantly affect the composition of DOM.

3.2.2 Dissolved Organic Matter (DOM) water analysis

Water samples collected for fDOM were analyzed on a Horiba-Jobin Yvon Aqualog Machine (Aqualog) owned by the Watershed Hydrology Group at McMaster University. Methods were adapted from those of Rastelli (2016) who examined DOC quality in reclaimed and natural wetlands in Fort McMurray. After pore-water samples were taken out of the refrigerator and to equilibrate to room temperature while covered, approximately 3 mL of sample was pipetted into a quartz cuvette after it was environmentalized three times. These cuvettes were previously bathed in a 50% nitric acid solution for at least 24 hours and thoroughly rinsed with deionized water before use.

Prior to analyzing samples, two standards tests were run on the Aqualog; the QSU (quinine-sulfate unit) and RSU (Raman scattering units) standard tests. The first was run with a Quinine Sulfate standard at an excitation of 350 nm and emission of 450 nm with the settings: 8 pixel, medium CCD gain and a 0.05 second integration time. The resulting values for integration times of 0.1, 0.5 and 1 second were recorded to check for instrument drift across runs. The second standard test was run with pure water in order to measure the Raman Signal to later be subtracted from the sample spectrum to correct for Raman scattering. The RSU test was run for an integration time of 10 seconds with the same pixel and gain settings as the QSU test. Normalization factors for integration times of 0.1, 0.25, 0.5, 0.75 and 1 second were derived, though others were also interpolated for samples requiring different integration times.

Water samples were run on the Aqualog for an excitation range of 240 nm to 600 nm at 5 nm increments and an emission range of 212.5 nm to 621.38 nm at 3.27 nm increments with settings of medium CCD gain and sum of slit width of 12. IFE, Raman Scattering and first-order Rayleigh Masking corrections were applied. All samples were first run at an integration time of 0.1 s to determine their absorbance at 255 nm as a guide for dilution and discerning appropriate integration times to collect each sample's data as EEMs. In this case, 255 nm was used instead of the standard 254 nm for this diagnostic and for index calculations due to the wavelength

increments selected. Any samples with an absorbance over 1.6 were diluted in a 1:1 ratio and then re-run at the same settings to determine if the absorbance at 255 nm was in the appropriate range. Most samples were well below this threshold with the exception of a few around 1.5. Integration times were adjusted on a sample-by-sample basis (raised to increase counts or lowered to decrease) to achieve sample counts in the range of 20,000-45,000 where the upper end of the range was preferred. This led to integration times varying from 0.05 to 1 s, whereby the appropriate RSU value from the RS standard test needed to be adjusted for each run. Some samples yielded counts consistently above the accepted range (often the maximum of 65535); these were the samples that ended up with dilutions regardless of their initial absorbance values. Analysis of fDOM samples on the Aqualog produced individual EEMs that were visually inspected for any abnormalities such as linearity that could infer scattering. Sample output files for absorbance and emission were then imported into RStudio (version 1.0.153, RStudio, Inc.) for processing.

3.2.3 fDOM indices calculations

Seven fDOM indices were calculated from running water samples on the Aqualog, four based on the EEMs produced and three based on the absorbance of the samples at different wavelengths. These calculations were performed in RStudio using a modified set of codes provided by Dr. Claire Oswald of Ryerson University by way of the McMaster Watershed Hydrology Group.

The fluorescence index based on the formulation by Cory & McKnight (2005) (FI 2005) was calculated as the ratio of the emissions at wavelengths of 470 nm and 520 nm obtained at an excitation of 370 nm. The humification index (HIX 2002) was calculated as the area under the emission spectra from 435-480 nm divided by peak area from 300-345 nm and 435 and 480 nm at an excitation of 254 nm (actually 255 nm with our settings). This was based on the formulation by Ohno (2002) and ranges from 0 to 1. The original humification index (HIX 1999) Zsolnay et al. (1999) was also calculated as the area under the emission spectra from 435-480 nm divided by the peak area from 300 to 345 nm, at an excitation of 254 nm (again, modified to 255 nm). However, since they are directly correlated, only the newer Ohno (2002) formulation was used. The freshness index was calculated as the ratio (β/α) of emission intensity at 380 nm (β) divided by the maximum emission intensity between 420 and 435 nm at an excitation of 310 nm

(α) based on the modified formulation by Wilson and Xenopoulos (2009). The biological index (BIX) was calculated as the ratio of emission intensity at 380 nm divided by the intensity at 430 nm, both at an excitation wavelength of 310 nm (Huguet et al., 2009). The absorbance ratio (ABS ratio) was calculated as the ratio of the absorbance at 254 nm (in our case, 255 nm) to the absorbance of the sample at 365 nm (Dahlén et al., 1996; De Haan, 1993). The absorbance ratio E2/E3 was computed as the absorbance at 250 nm divided by the absorbance at 365 nm (Peuravuori and Pihlaja, 1997). The last fDOM index, E4/E6, was calculated as the ratio of absorbance of the sample at 400 nm to the absorbance at 600 nm (Chen et al., 1977; Moore, 1987).

3.2.4 Carbon accumulation

Carbon accumulation in each depression was calculated based on the properties measured from extracted peat cores. For each sample, the fraction of organic matter from LOI analysis was multiplied by the bulk density (in g cm^{-3}), the sample's representative thickness (in cm), and a literature-derived organic carbon content for Sphagnum peat of 42.3% (Loisel et al., 2014) to determine the carbon accumulation (in g cm^{-2}, later converted to kg m^{-2}) for the peat layer. The acrotelm-catotelm boundary based on one standard deviation below the mean WT for the 2016 growing season (see 2.2.3) was then used to divide the peat profile into more stable C residing in the catotelm and the more active acrotelm C above. The WT data was originally measured relative to the peat surface where the groundwater well was installed, but converted to a relative depth to a common site reference with relative elevations measured at the wells and microforms to frame this boundary in relation to the peat profiles extracted.

3.2.5 Statistical analysis

Data management and statistical analyses were undertaken in MATLAB R2018a (Mathworks, Natick, MA, USA) and Minitab 18 (Minitab Inc., State College, PA, USA). To test the equivalency of fDOM characterization with or without a brief storage period in HDPE, the duplicate samples (n=5) were compared for all assessed fDOM indices using orthogonal regression analysis (error variance=1). Spearman correlation was used to investigate relationships among all fDOM samples to examine the consistency of the qualities they are theorized to indicate. A general linear model was used to assess the relationships between

measured peat carbon properties at a given depth (LOI and carbon accumulation to that depth) with parameters of site (deep or intermediate), microtopography (hollow or hummock) and depth in the profile (acrotelm or catotelm). Similar models were also developed for the seven fDOM indices calculated but with the addition of month of sampling (May to August) as factor. Two-way interactions were also taken into consideration in each case. Models were developed for each response variable and the residuals were assessed visually to determine whether they met model assumptions of normality (histogram and normal probability plot) and constant variance (residuals vs. fits). Carbon accumulation, freshness, E2/E3 and BIX were $\log_{10}$- transformed to meet model assumptions, whereas HIX 2002 had to undergo a Box-Cox transformation (λ=7).

For investigation of carbon accumulation on a whole-site basis, Spearman correlation was used to assess relationships between carbon stored in the acrotelm, catotelm and as a total, with site morphological parameters of site mean depth, maximum depth and depression area. The site parameter with the strongest correlations with the carbon accumulation measures, maximum depth, was then used as a predictor variable for each of these carbon accumulation measures in linear regression analyses on a whole site basis and by microform. Similar linear regression analysis was undertaken to assess the relationship between the proportion of carbon stored in the acrotelm and maximum depression depth, again for the whole site as well as by microform.

3.3 RESULTS

3.3.1 fDOM analysis

Though a small set of paired samples was used, there was no evidence that the Aqualog was measuring pore-water fDOM differently based on prior storage in HDPE for all indices ($p<0.001$) (Figure 3.1). This was based on the 95% confidence intervals for their intercept and slope containing 0 and 1, respectively. All indices of fDOM were significantly correlated with the notable exceptions of HIX 2002 with E2/E3, HIX 2002 with ABS ratio and ABS ratio with E2/E3 (Table 3.1).

The character of the DOM found in the peat pore-water varied significantly by site type for all calculated indices (all $p<0.001$ except for E2/E3 and ABS ratio at $p<0.05$) and depth type ($p<0.001$) (Table 3.3). The interaction of these two factors also explained significant variation in

fluorescence index ($p<0.05$), HIX 2002, E4/E6 and BIX ($p<0.001$). The month of sampling also explained variation in the humification index ($p<0.05$). BIX (R^2-adjusted = 0.5427) and freshness index (R^2-adjusted = 0.5075) were fairly well described by the general linear model, while the absorbance ratios E4/E6 (R^2-adjusted = 0.1575) and ABS ratio (R^2-adjusted = 0.1468) were not.

The pore-water in deep sites had a significantly higher humification index ($p<0.001$, Figure 3.4) as did the catotelm ($p=0.001$, Figure 3.5). Within intermediate sites, it was significantly greater in the acrotelm ($p<0.001$) and greater in the catotelm of within deep sites, but not significantly (Figure 3.6). This index value only significantly differed in the month of May compared to June ($p<0.05$, Figure 3.7). The freshness index of pore-water collected from deep sites was significantly lower than intermediate ($p<0.001$, Figure 3.4) and in all acrotelms compared to catotelms ($p<0.001$, Figure 3.5). The latter pattern held true within deep and intermediate sites (Figure 3.6) and the same trends were observed in the closely correlated BIX. The fluorescence index was higher in pore-water from intermediate ($p<0.001$, Figure 3.4) sites and all catotelms ($p<0.001$, Figure 3.5). It was highest within the catotelm of intermediate sites, while being lowest in the acrotelm of deep sites (Figure 3.6). The absorbance ratios E2/E3 ($p<0.05$, $p<0.001$) and ABS ratio ($p<0.05$, $p<0.001$) were both greater in intermediate sites and the catotelm (Figure 3.4, 3.5). The ratio E4/E6 was higher in the pore-water of deep sites (Figure 3.4, $p<0.001$) and the acrotelm (Figure 3.5, $p<0.001$). This ratio was similarly elevated in the deep sites regardless of depth over the acrotelm of the intermediate sites ($p<0.05$) and even more so compared to the intermediate catotelms ($p<0.001$) (Figure 3.6).

3.3.2 Carbon accumulation

The proportion of organics in the peat as determined by LOI varied significantly by site type and depth in the profile, their interaction, as well as the interaction of site type with microform (Table 3.2). LOI was significantly greater in deep sites as a whole ($p<0.001$) and across acrotelms ($p<0.001$) (Figure 3.2). Within intermediate sites it was greater in the hollows ($p<0.05$) and the acrotelm ($p<0.001$). Variability in C accumulation (as cumulative to a given depth) was significantly explained by depth ($p<0.001$) and its interaction with site type ($p<0.05$) (Table 3.2).

Expectedly, it was significantly greater in the catotelm than the acrotelm ($p<0.001$), which held true within both intermediate ($p<0.05$) and deep sites ($p<0.001$) (Figure 3.3).

Correlations between depression morphological parameters were all positive and significant ($p<0.05$), with the strongest between the two measures of depth ($\rho = 0.917$, $p<0.001$, Table 3.4). Carbon accumulation correlated well between total carbon with carbon stored in the catotelm ($\rho=0.979$, $p<0.001$) but not with acrotelm carbon. Neither did carbon stored in the acrotelm correlate with any site morphological parameters. Catotelm carbon, however, correlated with site mean depth ($\rho=0.711$, $p<0.05$) and site maximum depth ($\rho = 0.762$, $p<0.05$). Total site carbon accumulation only correlated with site maximum depth ($\rho = 0.733$, $p<0.05$).

The total C stored in each peat-filled bedrock depression was strongly related to its maximum depth ($p<0.001$, $R^2= 0.8260$), as was the amount of C stored in the more stable catotelm ($p<0.001$, $R^2 = 0.8551$), but not the acrotelm ($p=0.463$, $R^2 = 0$) (Figure 3.8). These relationships were maintained when considering the peat profiles in the microforms separately, though they were slightly stronger in the hummocks for total carbon ($p<0.001$, $R^2=0.825$) and catotelm ($p<0.001$, $R^2=0.894$) compared to the hollows ($p<0.001$, $R^2=0.818$ and $p<0.001$, $R^2=0.821$, respectively). Considering carbon accumulation as proportions in each defined layer (Figure 3.9), there was an inverse relationship between the proportion stored in the acrotelm and depression maximum depth ($p<0.001$, $R^2=0.583$) which was stronger in the hollows ($p<0.001$, $R^2=0.644$) than the hummocks ($p<0.001$, $R^2=0.464$).

3.4 DISCUSSION

3.4.1 Fluorescence spectroscopy analysis

Agreement between fDOM indices was somewhat variable due to differences regarding what they have been used to indicate as they were first developed and in subsequent studies. The indices that provide information on the molecular structure of DOM did not correlate as anticipated. HIX 2002, an indicator of increasing humification (Zsolnay et al., 1999), positively correlated with the E4/E6 absorbance ratio, which has been associated with decreases in humic character (Moore, 1987) Neither did the humification index have significant correlations with the E2/E3 or ABS ratio (Table 3.1). Within these absorbance ratios, this is further confounded by

negative correlations between E4/E6 and the two latter mentioned, despite all being documented to be have inverse relationships with molecular size (Dahlén et al., 1996; Grayson and Holden, 2012; Summers et al., 1987). While E4/E6 has been used to indicate humification, it may not vary with aromaticity as well the other absorbance ratios (Peuravuori and Pihlaja, 1997). Furthermore, O'Driscoll et al. (2006) expressed caution for the use of E4/E6 to assess between-site differences in DOM quality and structure due to its sensitivity to temporal changes in DOM and small changes in absorbance such as those that may arise from variation in measurements by the spectrofluorometer itself. The authors suggested E2/E3 may be more appropriate for assessing spatial change due its relative stability, typically covering a small range of values in natural waters.

On the other hand, the two indices that have been correlated to biological activity, the freshness index and BIX, were nearly correlated 1:1, likely due to the latter being a derivative of the former. The fluorescence index was unlike the other indices since it has been related more so to the source of organic material, though its strong correlations with freshness and BIX indicate similarities concerning autochthonous production. Potential complications and uncertainty in our fDOM analysis lie in concentration and pH (Gabor et al., 2014) which were not strictly controlled for in our analysis. While we applied a series of corrections for IFE, Raman Scattering and first-order Rayleigh Masking, Stedmon and Bro (2008) conveyed caution that even corrections applied cannot eliminate all uncertainty of instrument-specific and inner filter effects.

3.4.2 DOM composition of peat pore-water

Despite the potential confounding factors on the analysis of DOM composition, fDOM indices varied significantly by similar factors to the residence time estimates of Chapter 2; site size and depth, as well as their interactions (Table 3.3). Interestingly, only the humification index exhibited any temporal changes, with a small decrease from May to June. As it is associated with the decomposition process, humification rates would be expected to be too slow (Karunen and Ekman, 1982) to change in such a short time span. The modelling exercise by Morris and Waddington (2011) highlighted the potential for increased rainfall rates to lead to shorter residence times, even in deeper peatlands, by promoting pore-water turnover. Given the high levels of rainfall of 385-434 mm through the study period in 2017 (Figure 2.3) it is possible that

this influx of water caused dilution of the DOM across sites or alternatively, allowed some DOM from shallower, less humified peat layers to reach deeper layers by vertical pore-water movement (Siegel et al., 1995). Overall, it could be said that the DOM of the deep sites was more humified, older, of more terrestrial origin, and showed signs of less autochthonous activity, based on the indices of fluorescence. The picture based on absorbance; however, is a bit murkier, as the E4/E6 suggests lower molecular weights in deep sites while E2/E3 and the ABS ratio suggest the opposite. Considering some of the caveats of E4/E6 for assess spatial differences (O'Driscoll et al., 2006), it may give the latter two ratios more credence in being in agreement of greater molecular weights and aromaticity in deep sites, albeit slightly.

With depth, the indices of fluorescence characterize catotelm DOM as more humified, but with signs of being of more microbial in origin as well as greater autochthonous activity. The latter is consistent with what was observed by Beer et al. (2008) and Fraser et al. (2001). In these deep layers, the only DOM accumulating is doing so with minimal external inputs due to suppressed advective transport and very slow diffusive transport. The acrotelm that consisted of the upper 0.2-0.4 m of sites would have had the opportunity to receive new terrestrial organic material from newly generated litter at the surface or from inputs from rain or run-in. The absorbance ratios again yield conflicting findings, with E4/E6 suggesting slightly greater molecular weight but the opposite from E2/E3 and ABS ratio. If we are take the latter two with greater confidence however, it presents a differing picture from the expected DOM being more aromatic, structurally complex and thereby less labile.

Considering the interactions between the relevant factors of site size and depth in the profile, deep sites appear have more humified DOM. The intermediate sites' catotelms were observed to be the most microbial in origin by the fluorescence index and have the most autochthonous activity by the BIX, while both decrease in the deep sites, especially the acrotelm. It should be noted, however, that the properties described by the absorbance ratios and HIX; aromaticity, humic fraction and molecular size, need not all correlate in every case, depending on the source of DOM. There is also a notable difference between describing the chemistry of the actual peat material, or solid organic material (SOM) compared to DOM. We typically expect humification (as measured by von Post) to increase through the peat profile, but as observed in some of the

peat cores collected, this is not always a steady increase, with reversals possible. Our simple delineation of the peat profile into acrotelm and catotelm may have obscured such patterns, as decomposition (and therefore degree of humification) may be greatest near the WT (Beer and Blodau, 2007). As was a concern of Beer et al. (2008) the leaching of DOM from overlying peat layers which may be more vulnerable to DOM export by their higher conductivity and as enhanced by greater rainfall (Morris and Waddington, 2011), may carry not only more labile substrates but a less humified signal into the deeper layers.

Some of the unexpected results of DOM composition may be attributed to litter quality, which exerts a strong control on decomposition rates (Fogel and Cromack Jr., 1977) where differences in the quality of *Sphagnum* species may exceed the influence of microtopography (Johnson and Damman, 1991), which presents varying environmental conditions with regards to oxygenation, redox chemistry, pH and element mobility (Damman, 1978; Pakarinen, 1978; Zobel, 1986). The influence of litter quality is extended further as it grows more recalcitrant with time (Clymo, 1965; Malmer and Holm, 1984) as it is buried in the increasingly stable, anoxic conditions of the peat profile. It is unclear whether the lack of differences in DOM across microforms is due to their underdeveloped nature and overlap in *Sphagnum* species composition (see Chapter 2.5, Table 2.2) or from the influence of ecological memory effect (as proposed by Morris et al., 2013) whereby previously buried peat layers continue to exert controls hydrologically and influence further peatland formation despite no longer being reflected on the surface. Differences between the *Sphagnum* moss species prevalent across deep and intermediate sites were not well developed apart from the likes of *S. rubellum* and *S. fuscum* being only observed on the deep sites. *Polytrichum*, which differs considerably in composition to mosses of the genus *Sphagnum*, such as a lower C/N ratio (Toet et al., 2006), was more commonly found in intermediate site hummocks. Furthermore, at the intermediate sites, the vegetation patterns extended to vascular plants, namely trees which were found within several intermediate sites but were limited to the margins in deep sites. The large quantities of litter generated by trees, especially in sites 405 and 313, which were more like wet woodlands, would undoubtedly affect litter composition, and in turn, DOM.

3.4.3 Limits to C accumulation in bedrock depressions

In both intermediate and deep sites, C accumulation was greater within the catotelm (Figure 3.3) and across all sites, catotelm carbon dominated total carbon, both of which increased with site maximum depth. This parameter, however, which did not explain variation in acrotelm carbon accumulation (Figure 3.8) The acrotelm thickness did not vary much across sites; it typically included the top 0.2 m of peat in hollows and the top 0.4 m of hummocks, regardless of site size (see Chapter 2.7, Figure 2.5) The small size of some intermediate sites meant that some were even completely comprised of what could be considered acrotelm; this was the case for sites where only one depth increment was monitored. The proportion of carbon stored in the acrotelm inversely related to site maximum depth. In other words, the proportion of carbon in the catotelm positively related to depth and did so more strongly in the hollows (Figure 3.9). The generally thicker acrotelms of the hummock peat profiles (see Chapter 2.7, Figure 2.5) due to the greater elevation of hummocks above the WT may have accounted for slightly more carbon being stored in the hummock acrotelms. In general however, carbon accumulation was strongly driven by the carbon stored in the waterlogged, more stable catotelm, which grew with greater depression depth.

3.4.4 Implications

Characterization of pore-water DOM was not always clear but was able to elucidate some broad differences between the two size classes of depressions and between the acrotelm and catotelm of all sites. Interpretations should be taken with caution, however, as outliers were relatively plentiful when compared across these categories but were not consistent between indices. This may be due to the indices varying nature in terms of what they were developed to identify as well as variation in source material of the peat, and by extension, the DOM, as the vegetation that acts as such varied within sites, between sites, and may have varied through the peat profile with time as a form of ecological memory (as per Morris et al., 2013). The influence of substrate on decomposition, and by extension the composition of the resulting DOM, cannot be understated, as it may exert stronger effects than even the climatic forces of temperature of moisture and temperature that are of concern for peatlands in the near-future (Bell et al., 2018). Furthermore, the limitations imposed by the constraints of the simple diplotelmic model (such as the criticisms of Morris et al., 2011) may have resulted in similar artefacts as with pore-water residence time

(as discussed in Chapter 2, 2.4.4) whereby samples representative of intermediate catotelms were much fewer in number compared to deep sites, with some intermediate sites lacking a catotelm at all. This makes some comparisons difficult since the DOM was integrated across several depth increments for the deep sites. The diplotelmic model, while having its value in coarsely classifying peat layers in a standardized way across peatlands, may not be the most appropriate in these systems given the hydrological behaviour of the smaller depressions. Even the more continuous-depth models discussed by Morris et al. (2011) may not be suitable given the resolution of depths that one would need to observe in such a small peat profile.

To account further, for potential analytical complications, the use of parallel factor analysis (PARAFAC) (Stedmon and Bro, 2008) may be of value for characterizing DOM within our set of samples, though it does not lend itself as much to intercomparison between studies. Quantifying and standardizing for concentration of DOM (as DOC) as well as the pH of samples, may also reduce further potential sources of variation (Gabor et al., 2014).

While we were able to demonstrate that deeper peat-filled bedrock depressions expectedly accumulate more carbon, and do so in their thicker, more stable catotelms, it remains to be seen whether the shallower depressions simply accumulate carbon more slowly due the elevated decomposition associated with their greater WT fluctuations (as observed by Didemus, 2016), or if they are younger, potentially due to peat accumulation having to 'restart' after wildfire that is known to have shaped the eastern Georgian Bay rock barrens landscape (Catling and Brownwell, 1999, with ash evidence noted by Didemus, 2016). The hydrology of shallower systems suggested that most of the peat fell below the bedrock depression sill compared to deep sites that domed above to some degree (See Chapter 2.3.1), pointing to greater constraints. Carbon accumulation rates are not constant through time, and their changes may be used to infer past climate regimes in the depression's history. Radiocarbon analysis of peat cores (as in Beilman et al., 2009; Turetsky et al., 2004) could be used to address such questions and coupled with macrofossil analysis (as in Loisel and Garneau, 2010), may reveal more detail with regards to past vegetation regimes and ecological memory (Morris et al., 2013) in these smaller peat-forming systems. All we have been able to elucidate is a snapshot of more carbon intuitively held in deeper depressions, with more of it held in the more stable catotelm, but understanding the

temporal carbon dynamics will inform us further on the evolution of these systems by primary peat formation on the Canadian Shield. On the spatial side, there are also opportunities to model carbon accumulation with more detailed depth surveys that are made feasible by the smaller scale of most bedrock depressions. By developing an inventory of peat profiles of the two size classes, empirical relationships between carbon accumulation and depth could be used to estimate the total carbon storage of these depressions and inform management decisions with respect to the carbon footprints that the loss of these systems will have via anthropogenic development. Destruction of these wetlands would be on the order of a few kg m^{-2} of carbon in intermediate depressions to over 70 kg m^{-2} of carbon in the largest depressions (Figure 3.8). In the eastern Georgian Bay region, this is a growing concern due to the prevalence of tourism (and therefore cottage development), as well as recent energy projects being undertaken.

3.6 TABLES

Table 3.1: Spearman rank correlation was used to investigate relationships between fDOM indices calculated from the analysis of monthly pore-water samples by fluorescence spectrometry. Spearman's ρ is displayed, **bolded** where significant to $p<0.001$.

	HIX 2002	Freshness	FI 2005	E4/E6	E2/E3	BIX	ABS Ratio
HIX 2002							
Freshness	**-0.499**						
FI 2005	**-0.424**	**0.911**					
E4/E6	**0.506**	**-0.643**	**-0.631**				
E2/E3	-0.090	**0.516**	**0.488**	**-0.326**			
BIX	**-0.512**	**0.997**	**0.907**	**-0.641**	**0.506**		
ABS Ratio	-0.083	**0.503**	**0.474**	**-0.314**	0.999	**0.493**	

Table 3.2: General linear model of two variables of peat carbon related to site parameters of size, microtopography and depth. Three two-way interactions were included. Carbon accumulation failed to meet model assumptions and so had to be log_{10}-transformed. P-values are **bolded** where significant to p<0.01, *italicized* where significant to p<0.05 and model performance was assessed as adjusted R^2.

	LOI		C Accumulation	
	F	*p*	*F*	*p*
Site type	103.01	**0.000**	0.00	0.955
Microform	2.01	0.162	0.01	0.934
Depth type	93.07	**0.000**	58.83	**0.000**
Site type x Microform	8.67	**0.005**	0.27	0.605
Site type x Depth type	44.86	**0.000**	5.18	*0.027*
Microform x Depth type	0.51	0.478	0.86	0.359
R^2 (adj)		0.7216		0.6290

Table 3.3: General linear models were used to assess the relationships of fDOM indices with parameters of site (deep or intermediate), microtopography (hollow or hummock), depth in the profile (acrotelm or catotelm), and the month of collection (May to August). Six two-way interactions were included. Freshness index, E2/E3 and BIX were $\log_{10}$- transformed to meet model assumptions, whereas HIX 2002 had to undergo a Box-Cox transformation (λ=7). P-values are **bolded** where significant to $p<0.01$, *italicized* where significant to $p<0.05$ and model performance was assessed as adjusted R^2.

	HIX 2002		Freshness		FI 2005		E4/E6		E2/E3		BIX		ABS Ratio	
	F	*p*	*F*	*p*	*F*	*p*	*F*	*p*	*F*	*p*	*F*	*p*	*F*	*p*
Site type	104.10	**0.000**	179.65	**0.000**	67.94	**0.000**	82.41	**0.000**	6.27	*0.013*	204.06	**0.000**	6.53	*0.011*
Microform	1.78	0.184	1.26	0.263	1.51	0.220	1.59	0.208	1.40	0.239	1.74	0.188	1.92	0.168
Depth type	11.12	**0.001**	85.09	**0.000**	43.39	**0.000**	33.87	**0.000**	46.05	**0.000**	94.51	**0.000**	43.14	**0.000**
Month	2.83	*0.039*	2.15	0.095	2.53	0.058	0.45	0.720	0.70	0.553	2.33	0.076	0.51	0.675
Site type x Microform	0.09	0.770	0.64	0.425	0.26	0.612	0.28	0.599	3.38	0.068	1.03	0.310	2.53	0.113
Site type x Depth type	38.92	**0.000**	15.57	**0.000**	6.80	**0.010**	22.18	**0.000**	1.45	0.230	23.20	**0.000**	2.90	0.090
Site type x Month	0.36	0.782	2.20	0.089	0.70	0.551	0.67	0.572	1.59	0.193	2.14	0.096	2.05	0.108
Microform x Depth type	1.40	0.238	0.85	0.359	0.17	0.677	0.15	0.701	0.77	0.382	0.78	0.379	0.53	0.468
Microform x Month	0.42	0.741	0.36	0.782	0.20	0.894	0.27	0.848	0.48	0.697	0.47	0.706	0.36	0.785
Depth type x Month	1.53	0.207	0.83	0.479	0.49	0.686	1.47	0.224	1.62	0.185	0.78	0.507	2.01	0.113
R^2 (adj)		0.4007		0.5075		0.2902		0.3220		0.1575		0.5427		0.1468

Table 3.4: Spearman rank correlation was used to investigate relationships between site carbon accumulation measures and site morphological parameters. Spearman's ρ is displayed, **bolded** where significant to $p<0.001$ and *italicized* where significant to $p<0.05$.

	C acrotelm	C catotelm	Total C	Site mean depth	Site max depth
C catotelm	0.326				
Total C	0.467	**0.979**			
Site mean depth	-0.083	*0.711*	0.650		
Site max depth	0.133	*0.762*	*0.733*	**0.917**	
Site area	-0.117	0.619	0.550	*0.667*	*0.750*

3.7 FIGURES

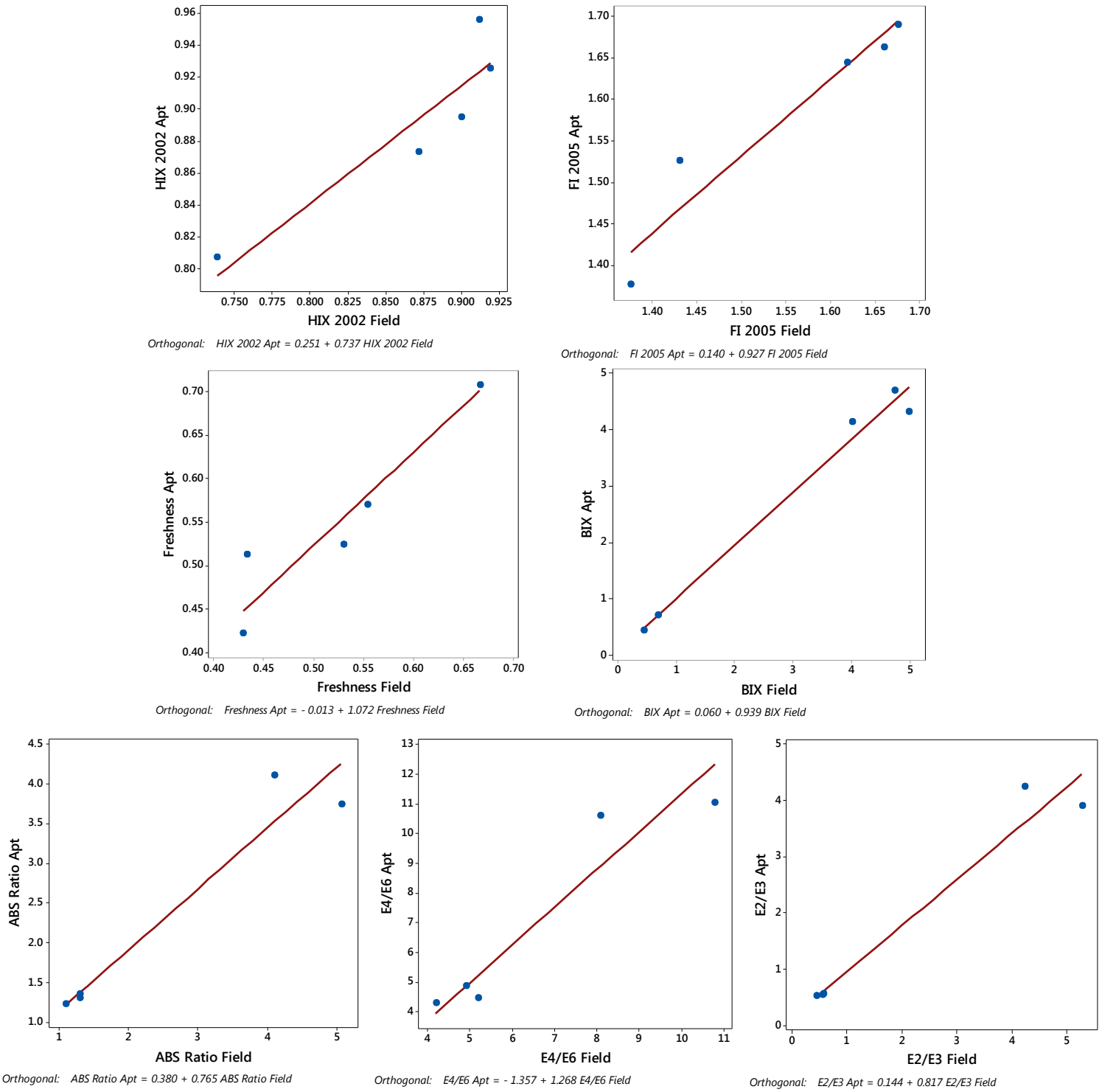

Figure 3.1: Duplicate pore-water samples (n=5) were compared by all seven fDOM indices by orthogonal regression analysis to discern storage in amber HDPE bottles impacted the fluorescence and absorbance signals measured. 'Field' denotes the sample originally collected and filtered in the field in June-August whereas 'Apt' denotes samples intentionally stored refrigerated in HDPE. Orthogonal regression equations are displayed below each plot. Orthogonal regression equations are displayed below plots, where 95% confidence intervals all contained 1 for slope and 0 for the intercept.

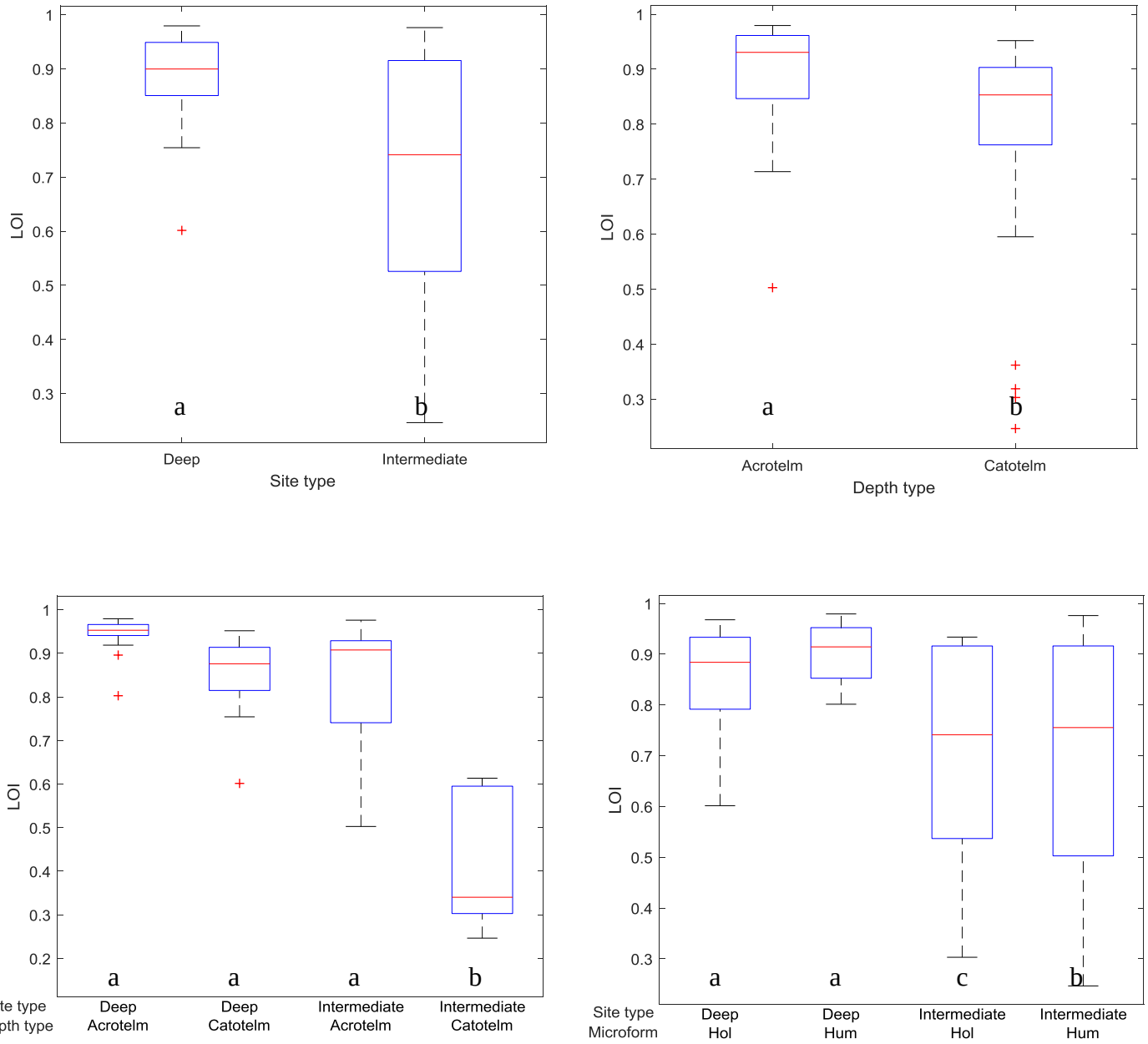

Figure 3.2: Boxplots depict differences in organic matter content as LOI of peat with site size, depth, the interaction between the two and the interaction between site size and microform (left to right, top to bottom) Boxes display the interquartile range, with crosses indicating outliers. Letters denote significant differences (to $p<0.05$, by Tukey HSD) between groups not sharing a letter.

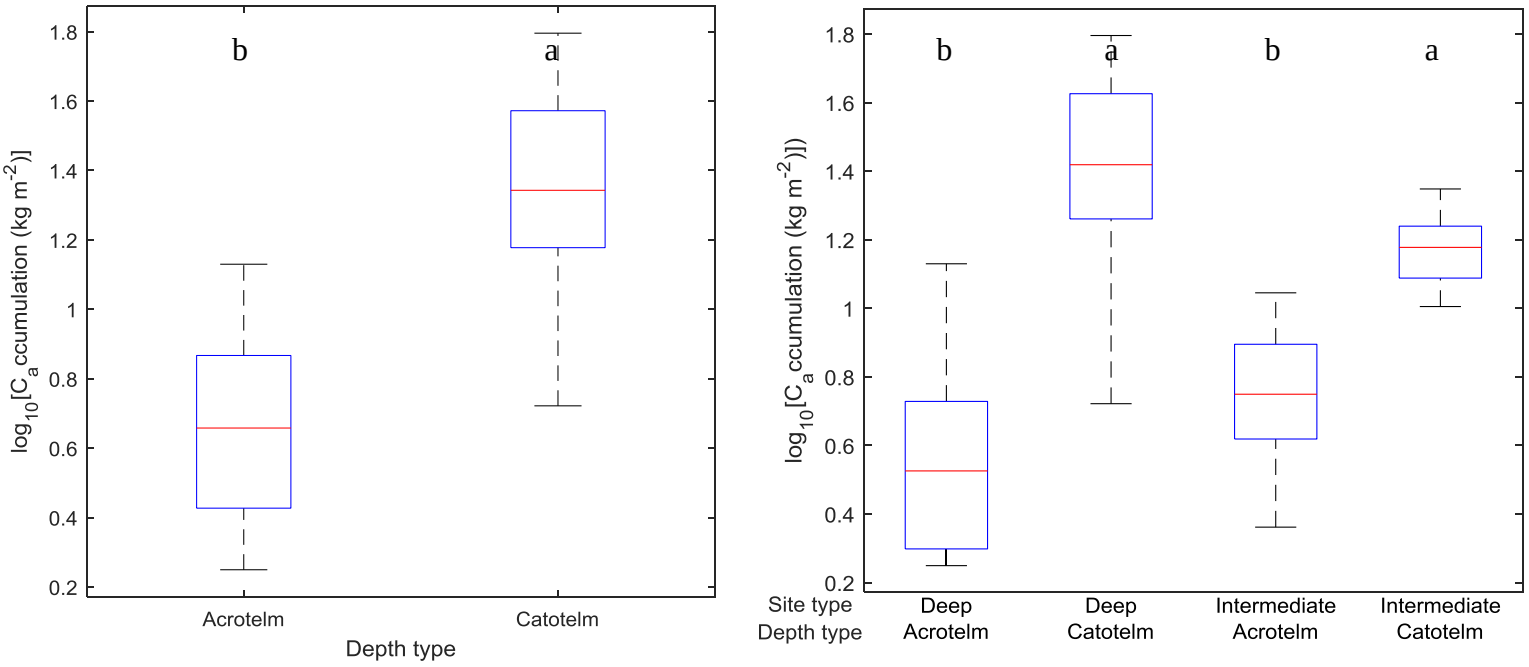

Figure 3.3: Boxplots depict differences of carbon accumulation to a given depth with depth in profile and its interaction with site size (left to right) Boxes display the interquartile range, with crosses indicating outliers. Letters denote significant differences (to $p<0.05$, by Tukey HSD) between groups not sharing a letter.

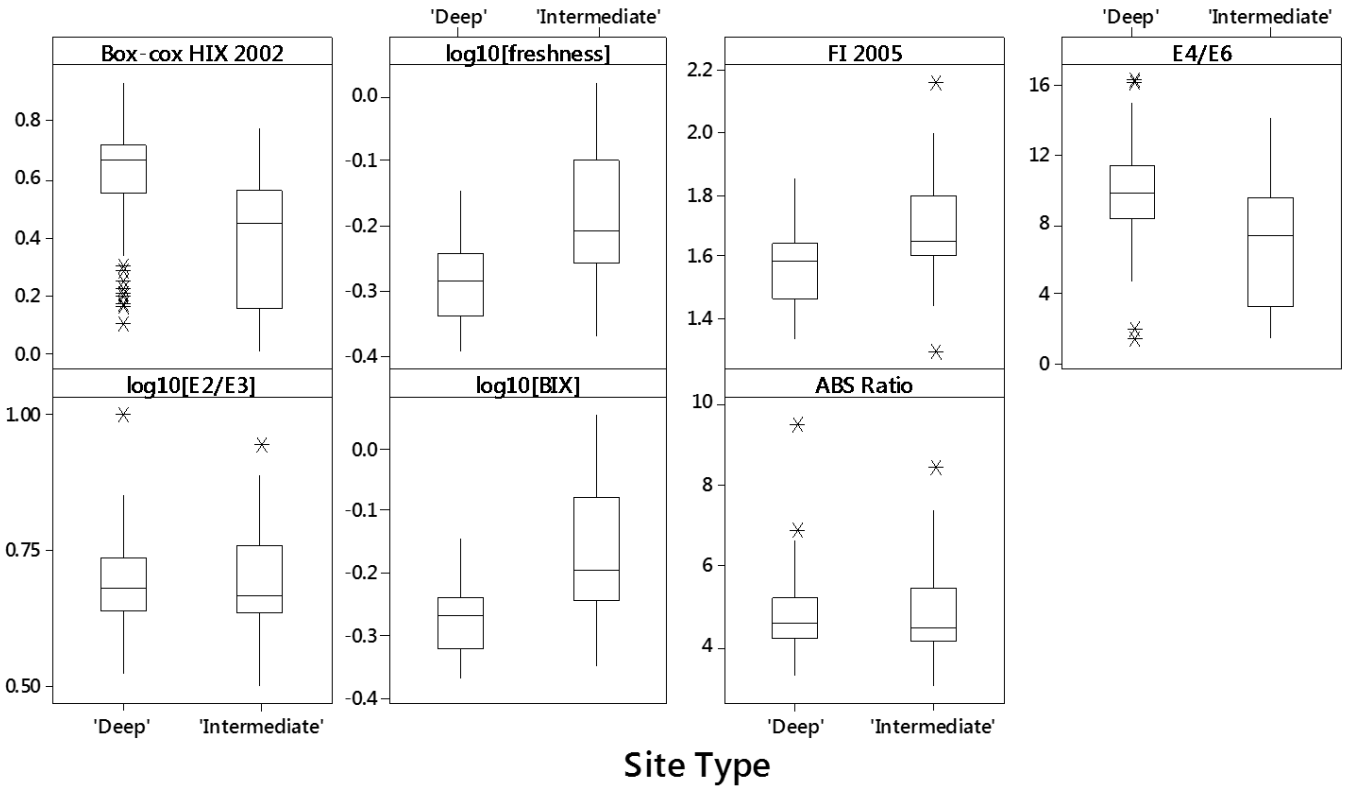

Figure 3.4: Boxplots depict differences in in pore-water DOM character by seven fDOM indices with site size. Boxes display the interquartile range, with asterisks indicating outliers. All comparisons displayed were significantly different by Tukey HSD ($p<0.05$).

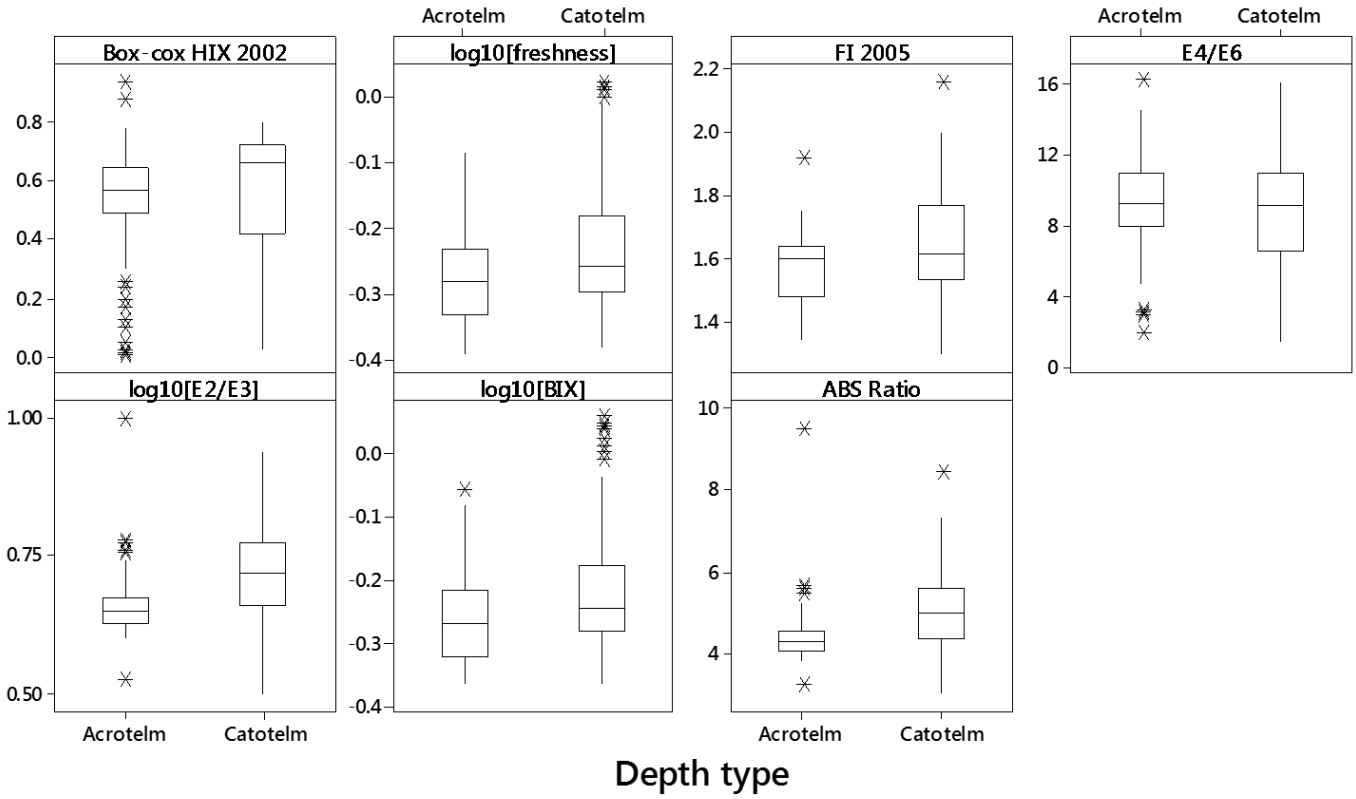

Figure 3.5: Boxplots depict differences in in pore-water DOM character by seven fDOM indices with depth in the peat profile. Boxes display the interquartile range, with asterisks indicating outliers. All comparisons displayed were significantly different by Tukey HSD ($p<0.05$).

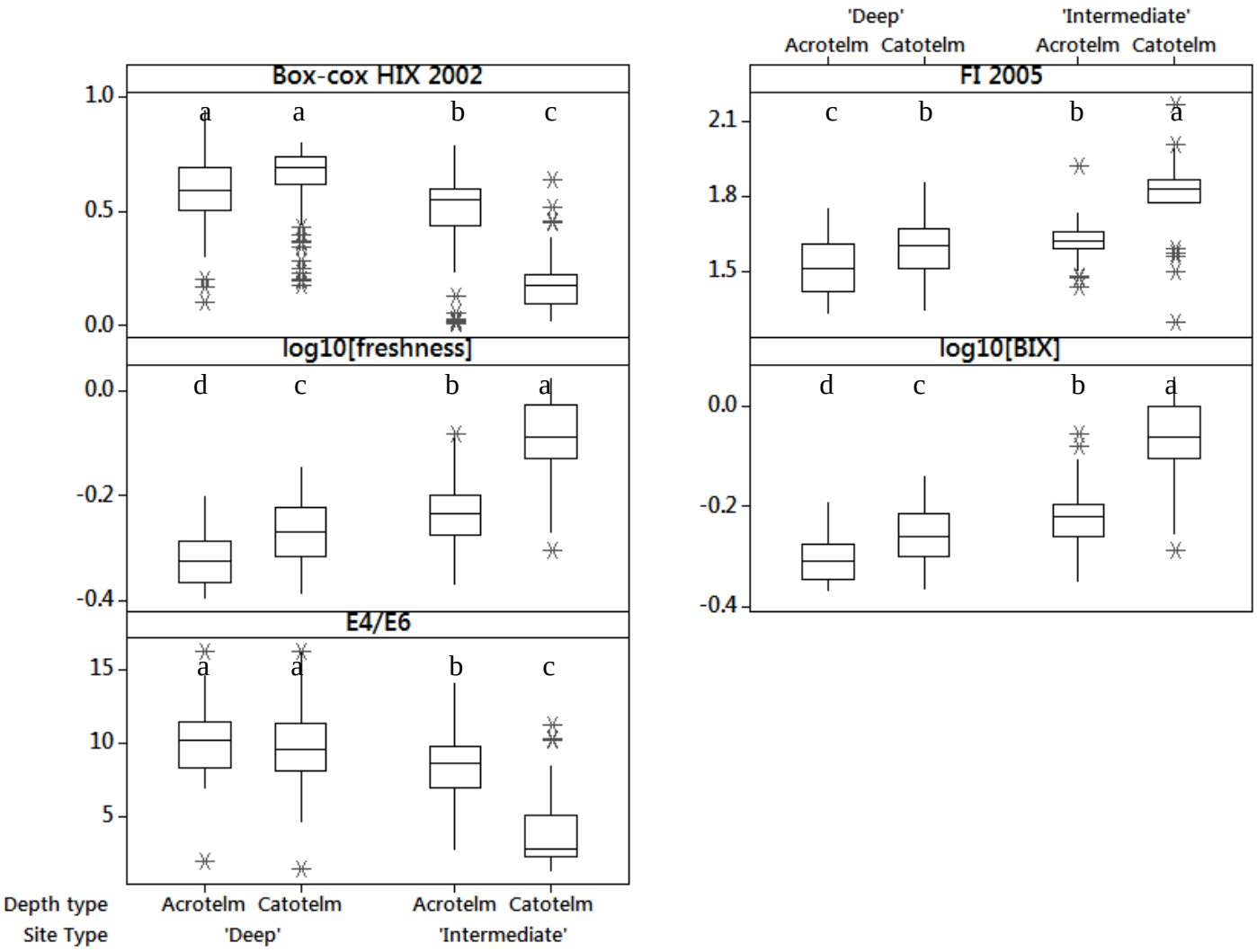

Figure 3.6: Boxplots depict differences in in pore-water DOM character by five fDOM indices determined by general linear model analysis to vary significantly by the interaction between site size and depth. Boxes display the interquartile range, with asterisks indicating outliers. Letters denote significant differences (to $p<0.05$, by Tukey HSD) between groups not sharing a letter.

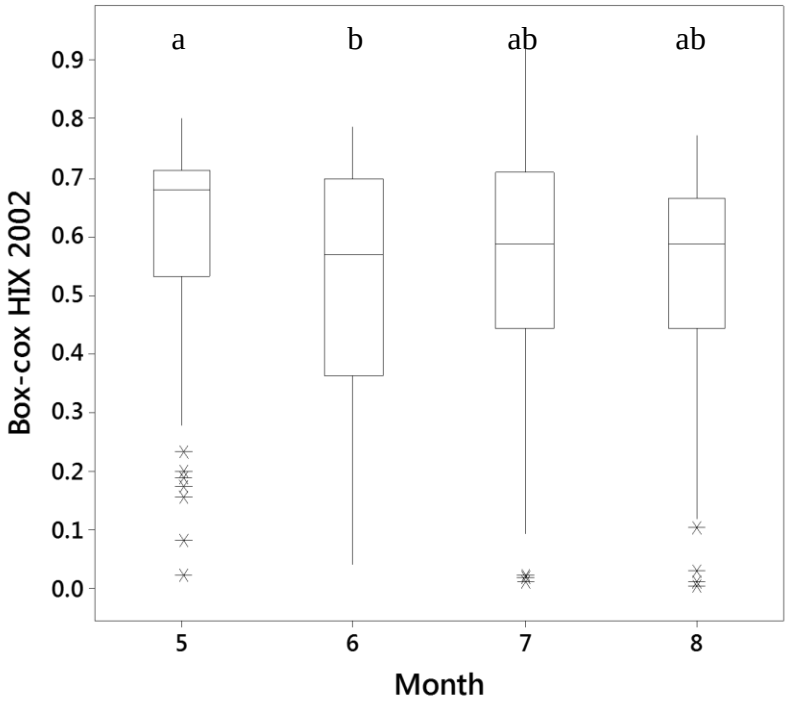

Figure 3.7: Boxplots depict differences in the degree of humification of pore-water DOM humification index (HIX 2002) with month of sampling in 2017. Boxes display the interquartile range, with asterisks indicating outliers. Letters denote significant differences (to $p<0.05$, by Tukey HSD) between groups not sharing a letter.

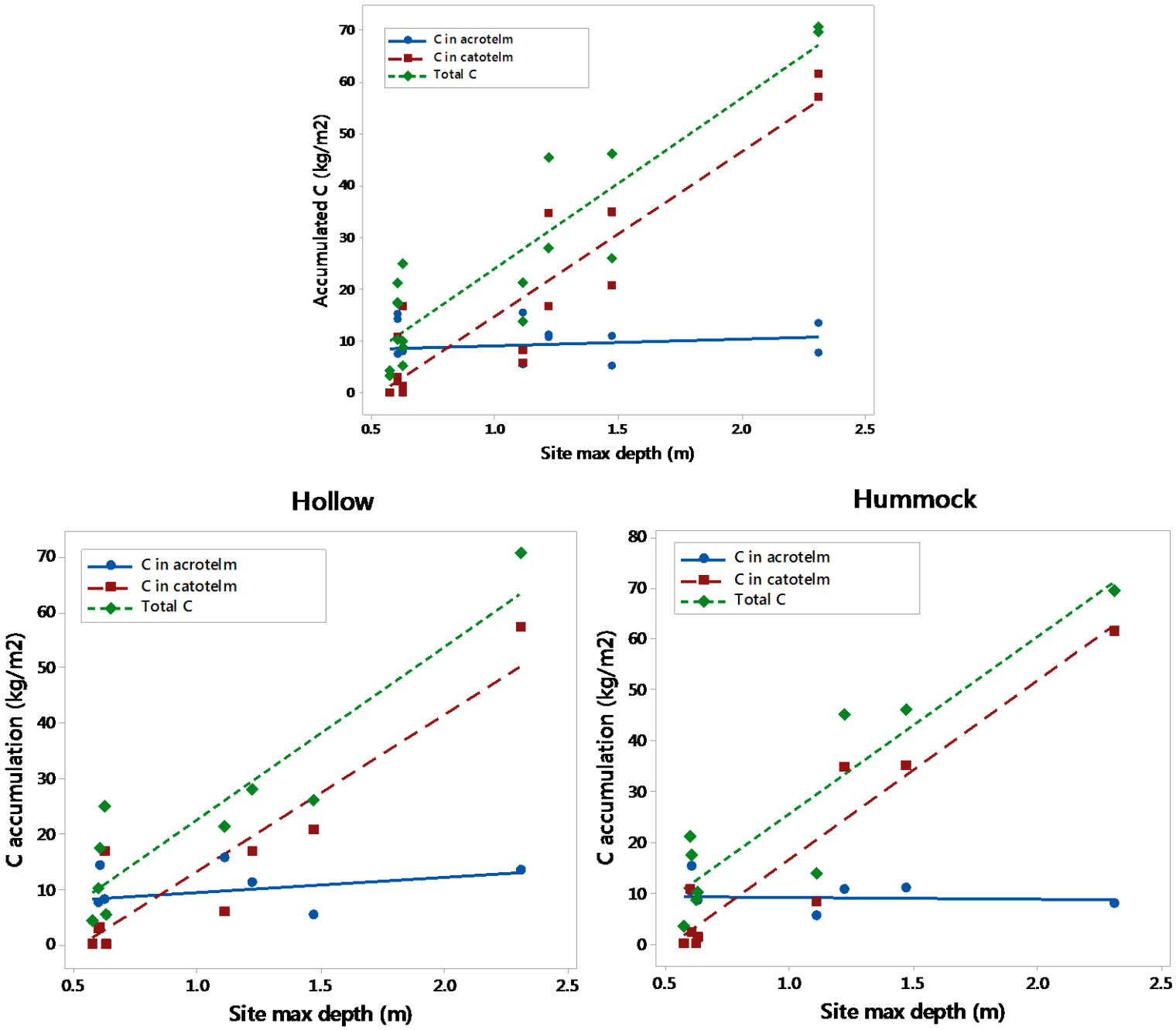

Figure 3.8: Linear regressions between carbon accumulation (in kg m^{-2}) and the maximum depth measured in each depression are displayed as totals ($p<0.001$, $R^2=0.826$) and divided up into the respective site's acrotelm ($p=0.463$, $R^2=0$) and catotelm ($p<0.001$, $R^2=0.855$) (top). This analysis was repeated for the subsets of the hollow (bottom left) and hummock (bottom right) microforms for total carbon ($p<0.001$, $R^2=0.818$ and $p<0.001$, $R^2=0.825$, respectively), acrotelm carbon ($p=0.316$, $R^2=0.02$ and $p=0.888$, $R^2=0$, respectively) and catotelm carbon ($p<0.001$, $R^2= 0.821$ and $p<0.001$, $R^2=0.894$, respectively).

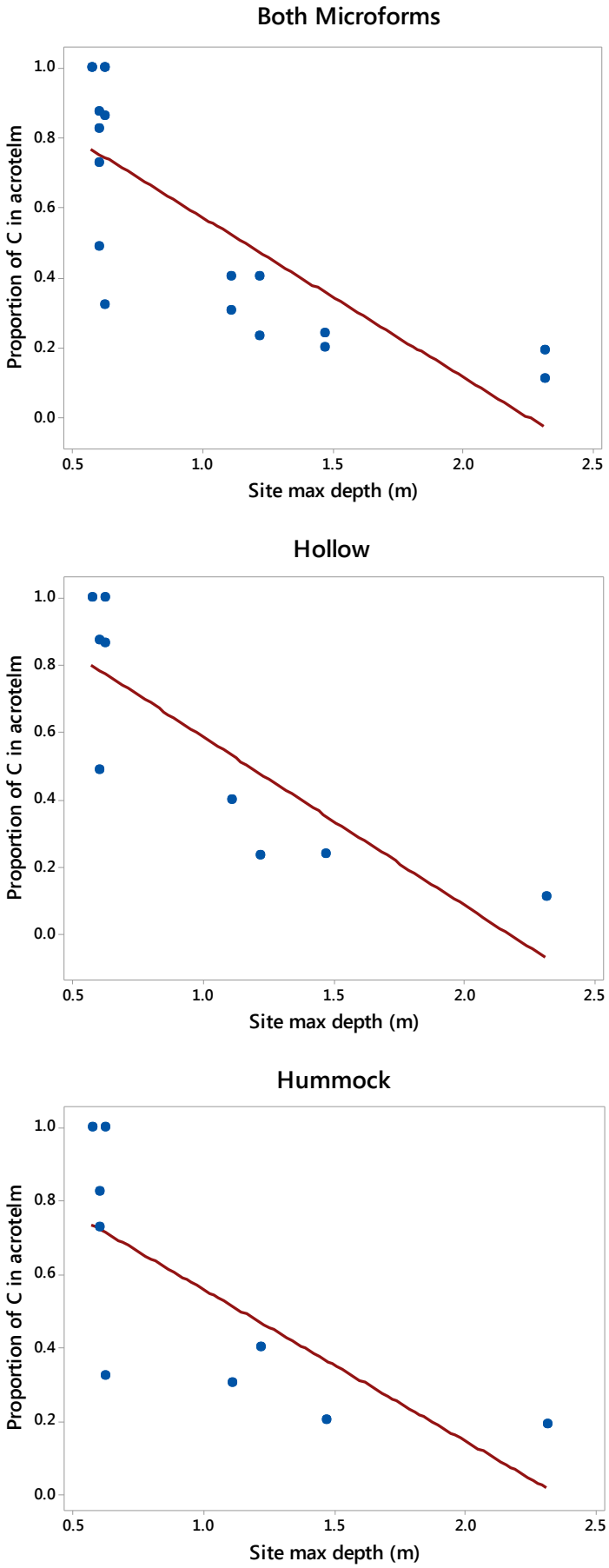

Figure 3.9: The proportion of total carbon stored in the acrotelm of each depression was related to site depth for all peat profiles ($p<0.001$, $R^2=0.583$) and when considering hollows ($p<0.01$, $R^2=0.644$) and hummocks ($p<0.05$, $R^2=0.464$) separately (top to bottom).

CHAPTER 4: CONCLUSION

The overall aim of this study was to investigate the pore-water residence time-chemistry feedback as it pertains to decomposition by approaching the core elements in parallel. The constraints on pore-water transport were first noted by the low conductivity of catotelm peat by Beer et al. (2008). They were later expressed as hydraulic structure (as per Baird et al., 2008) by (Morris and Waddington, 2011) that in turn manifested in longer residence times and were assessed in Chapter 2. Profiles of peat hydrophysical properties were measured along with pore-water residence times estimated by a simple metric based on stable isotope records. It was hypothesized that depression size and depth would serve as the primary controls on hydraulic structure, whereby deeper sites are less conducive to vertical pore-water flux that would allow turnover in the catotelm. Hydraulic structure in peat-filled bedrock depressions was observed to be controlled by site size and depth in the profile, at least in a discrete sense. Measurements of conductivity were observed to be very low in the catotelm of deep sites, similar to the conductivities observed by Beer et al. (2008). This study constitutes the first of its kind in its estimation of the pore-water residence time profiles that have been notably absent, even on larger northern peatland systems (Morris and Waddington, 2011). It was hypothesized that these pore-water residence times, which may indicate the strength of the resilience to decay, would be subject to the same controls as hydraulic structure and thus be longer in the catotelm, particularly in deep depressions where this feedback may be stronger. Residence time estimates through use of the simplified inverse transit time proxy (ITTP) were able to distinguish between the slower turnover in deeper, permanently saturated peat layers and the periodically saturated layers near the surface on a discrete basis. Deep (>0.4 m) residence times exceeded those of intermediate (<0.4 m) peat-filled bedrock depressions when the sites were taken as a whole, but the distinction could not be made between their respective catotelms. Peat hydraulic structure, especially expressed as a depth-averaged conductivity, exhibited a close relationship with residence time estimates. The modelling findings of Morris and Waddington (2011) were generally supported in what constitutes the first study of its kind (to our knowledge) in its estimation of the peat pore-water residence time profiles that were remarked to notably absent by the authors, even in larger northern peatland systems. The choice to study this feedback in smaller, geologically constrained peat forming systems did entail complications concerning spatial and temporal scaling compared to previous work. The nature of these systems and the wet conditions in which they were studied

may have obscured differences in residence time, but the contrasting hydraulic behaviour and potential resilience to decay of the deep and intermediate systems was still observable, at least in a discrete sense. Furthermore, it was possible to further understanding of the hydrological, ecological and biogeochemical functions of these geographically isolated wetlands (GIWs).

In Chapter 3, the potential outcomes of the pore-water residence time-chemistry feedback were hypothesized to be observable in the carbon accumulation facilitated by the resilience to decay and composition of DOM in the pore-water which presents unfavourable conditions for further decomposition in the catotelm. It was hypothesized that the greater strength of this feedback in deeper peat-filled depressions permits greater and more stable carbon accumulation over time. While only a static profile was analyzed, the deep sites were found to store far more carbon than intermediate sites, primarily in their thicker catotelms. The vulnerability of intermediate sites to WT fluctuations, as exhibited in the WT-specific yield feedback observed by Didemus (2016), left them with generally thin catotelms and some lacking any appreciable permanently saturated layers of peat. While the wet season of 2017 kept both classes of depressions fairly wet for most of the study period, the dry conditions of the previous year would have resulted in a near-complete turnover of pore-water compared to the results of Chapter 2, and perhaps more importantly from a carbon storage perspective, permitted accelerated rates of aerobic decomposition throughout the peat profiles of the intermediate sites. Carbon loss may be more prevalent on a seasonal basis for these smaller depressions and may explain why those observed were more geologically constrained than their deeper counterparts. The DOM composition in the catotelm of deep sites was hypothesized to be more humified and autochthonous in nature than the equivalent in the intermediate sites. While the same depression characteristics of site size and depth within the profile, related to hydraulic structure and residence time in Chapter 2, were found to explain variation in seven indices of fluorescence spectroscopy, characterization was not always clear. DOM in deep sites appeared to be more humified than in intermediate sites based on a humification index. This DOM was not as recently produced and showed less indication of autochthonous activity. The uncertain influence of past vegetation on litter quality through ecological memory (Morris et al., 2013) and the similarities between present *Sphagnum* cover potentially confound DOM characterization due to the strong control of litter on decomposition (Fogel and Cromack Jr., 1977; Johnson and Damman, 1991; Turetsky et al.,

2008). Similar to pore-water residence time, the characterization of DOM was somewhat limited by the delineation of depths within the peat profiles based in the traditional diplotelmic model (Ingram, 1978) as some intermediate sites completely lacked a catotelm or otherwise had very few representative samples compared to the deep sites. Their differences with depth may have thus be obscured by the means based on catotelms in deep sites being moderated by samples from the middle of the profile, compared to the intermediate sites where only the very deepest depth increment was sampled.

With consideration to the biogeochemical functions of GIWs, the generally longer residence times of deeper peat-filled bedrock depressions suggest they are better able to provide this ecosystem service (Holland et al., 2004; Werner and Kadlec, 2000). In the context of habitat conservation and restoration, these systems should thereby be a target for management decisions. Facing direct disturbance by anthropogenic development, the loss of these potentially older systems amounts to a far greater loss of carbon compared to shallower depressions. This carbon in particular is stored in the fairly stable catotelm, which otherwise provides resilience to the potentially decay-accelerating effects of climate change. The loss of habitat to the threatened Eastern Massassauga Rattlesnake (Harvey and Weatherhead, 2006; Smolarz et al., 2018) is also greater on a site basis, especially since the hummocks they require for hibernacula are far less developed in shallower depressions. If peat-filled depressions are destroyed and new habitat is to be constructed, the size of the deep sites (mean depth >0.4 m) and observed in this study are a good starting point. The experimental column experiments by Blodau et al. (2011) and Bonaiuti et al. (2017) may further inform restoration from controlled settings as the authors were able to induce the pore-water transport limitations and resulting thermodynamic suppression of anaerobic decay of a homogenous mixture of peat, simply by its burial. Their constructed peat column depths of 1.4 and 0.85 m further suggest that the pore-water residence time-chemistry feedback may operate in shallower peat systems. The hydraulic structure and longer pore-water residence times of deep depressions indicate a resilience to deep peat decomposition by restricted pore-water transport (as per Beer et al., 2008). Their greater carbon accumulation predominantly in their permanently waterlogged catotelms suggest their carbon stores may be more resilient to seasonal WT fluctuations that may intensify with climate change. The categories of depressions imposed revealed some key hydrological differences despite much greater morphological

differences among the deep sites. For the sake of cost-effectiveness in habitat reconstruction, peat deposits need not be excessively deep, as the smallest deep site was on average about half a meter deep with a maximum depth just over a meter, nor extensive, as the smallest was under 1000 m^2 in area.

REFERENCES

Aiken, G., 2014. Fluorescence and Dissolved Organic Matter: A Chemist's Perspective, Aquatic Organic Matter Fluorescence. https://doi.org/10.1017/CBO9781139045452.005

Allan, C.J., Roulet, N.T., 1994. Runoff generation in zero-order precambrian shield catchments: The stormflow response of a heterogeneous landscape. Hydrol. Process. 8, 369–388. https://doi.org/10.1002/hyp.3360080409

Andrus, R.E., Wagner, D.J., Titus, J.E., 1983. Vertical zonation of Sphagnum mosses along hummock-hollow gradients. Can. J. Bot. 61, 3128–3139. https://doi.org/10.1139/b83-352

Aravena, R., Warnert, B.G., Charman, D.J., Belyea, L.R., Mathur, S.P., Dinel, H., 1993. Carbon Isotopic Composition of Deep Carbon Gases in an Ombrogenous Peatland, Northwestern Ontario, Canada. Radiocarbon 35, 271–276.

Baird, A.J., Belyea, L.R., Morris, P.J., 2013. Upscaling of Peatland-Atmosphere Fluxes of Methane: Small-Scale Heterogeneity in Process Rates and the Pitfalls of "Bucket-and-Slab" Models, in: Carbon Cycling in Northern Peatlands. American Geophysical Union (AGU), pp. 37–53. https://doi.org/10.1029/2008GM000826

Baird, A.J., Eades, P.A., Surridge, B.W.J., 2008. The hydraulic structure of a raised bog and its implications for ecohydrological modelling of bog development. Ecohydrology 1, 289–298. https://doi.org/10.1002/eco.33

Baker, A., Bolton, L., Newson, M., Spencer, R.G.M., 2008. Spectrophotometric properties of surface water dissolved organic matter in an afforested upland peat catchment. Hydrol. Process. 22, 2325–2336. https://doi.org/10.1002/hyp

Beckwith, C.W., Baird, A.J., Heathwaite, A.L., 2003. Anisotropy and depth-related heterogeneity of hydraulic conductivity in a bog peat. I: laboratory measurements. Hydrol. Process. 17, 89–101. https://doi.org/10.1002/hyp.1116

Beer, J., Blodau, C., 2007. Transport and thermodynamics constrain belowground carbon turnover in a northern peatland. Geochim. Cosmochim. Acta 71, 2989–3002. https://doi.org/10.1016/j.gca.2007.03.010

Beer, J., Lee, K., Whiticar, M., Blodau, C., 2008. Geochemical controls on anaerobic organic matter decomposition in a northern peatland. Limnol. Oceanogr. 53, 1393–1407. https://doi.org/10.4319/lo.2008.53.4.1393

Beilman, D.W., MacDonald, G.M., Smith, L.C., Reimer, P.J., 2009. Carbon accumulation in peatlands of West Siberia over the last 2000 years. Global Biogeochem. Cycles 23. https://doi.org/10.1029/2007GB003112

Bell, M.C., Ritson, J.P., Verhoef, A., Brazier, R.E., Templeton, M.R., Graham, N.J.D., Freeman, C., Clark, J.M., 2018. Sensitivity of peatland litter decomposition to changes in temperature and rainfall. Geoderma 331, 29–37. https://doi.org/10.1016/j.geoderma.2018.06.002

Belyea, L.R., Clymo, R.S., 2001. Feedback control of the rate of peat formation. Proc. R. Soc. B Biol. Sci. 268, 1315–1321. https://doi.org/10.1098/rspb.2001.1665

Belyea, L.R., Malmer, N., 2004. Carbon sequestration in peatland: Patterns and mechanisms of response to climate change. Glob. Chang. Biol. 10, 1043–1052. https://doi.org/10.1111/j.1529-8817.2003.00783.x

Benjamin, L., Knobel, L.L., Hall, L.F., Cecil, L.D., Green, J.R., 2004. Development of a Local Meteoric Water Line for Southeastern Idaho, Western Wyoming, and South-Central Montana, Usgs.

Berden, G., Peeters, R., Meijer, G., 2000. Cavity ring-down spectroscopy: Experimental schemes

and applications. Int. Rev. Phys. Chem. 19, 565–607. https://doi.org/10.1080/014423500750040627
Bernhardt, E.S., Blaszczak, J.R., Ficken, C.D., Fork, M.L., Kaiser, K.E., Seybold, E.C., 2017. Control Points in Ecosystems: Moving Beyond the Hot Spot Hot Moment Concept. Ecosystems 20, 665–682. https://doi.org/10.1007/s10021-016-0103-y
Blodau, C., Roulet, N.T., Heitmann, T., Stewart, H., Beer, J., Lafleur, P., Moore, T.R., 2007. Belowground carbon turnover in a temperate ombrotrophic bog. Global Biogeochem. Cycles 21, 1–12. https://doi.org/10.1029/2005GB002659
Blodau, C., Siems, M., Beer, J., 2011. Experimental burial inhibits methanogenesis and anaerobic decomposition in water-saturated peats. Environ. Sci. Technol. 45, 9984–9989. https://doi.org/10.1021/es201777u
Bonaiuti, S., Blodau, C., Knorr, K.-H., 2017. Transport, anoxia and end-product accumulation control carbon dioxide and methane production and release in peat soils. Biogeochemistry 133, 219–239. https://doi.org/10.1007/s10533-017-0328-7
Bracken, L.J., Croke, J., 2007. The concept of hydrological connectivity and its contribution to understanding runoff-dominated geomorphic systems. Hydrol. Process. 21, 1749–1763. https://doi.org/10.1002/hyp
Bragg, O.M., 2002. Hydrology of peat-forming wetlands in Scotland. Sci. Total Environ. 294, 111–129. https://doi.org/10.1016/S0048-9697(02)00059-1
Brand, W.A., 2004. Mass Spectrometer Hardware for Analyzing Stable Isotope Ratios. Handb. Stable Isot. Anal. Tech. 835–856. https://doi.org/10.1016/B978-044451114-0/50040-5
Brand, W.A., Geilmann, H., Crosson, E.R., Rella, C.W., 2009. Cavity ring-down spectroscopy versus high-temperature conversion isotope ratio mass spectrometry; a case study on δ 2 H and δ 18 O of pure water samples and alcohol/water mixtures. Rapid Commun. Mass Spectrom. 23, 1879–1884. https://doi.org/10.1002/rcm.4083
Branham, J.E., Strack, M., 2014. Saturated hydraulic conductivity in *Sphagnum* -dominated peatlands: do microforms matter? Hydrol. Process. 28, 4352–4362. https://doi.org/10.1002/hyp.10228
Brooks, R.T., Hayashi, M., 2002. Depth-Area-Volume and Hydroperiod Relationships of Ephemeral (Vernal) Forest Pools in Southern New England. Wetlands 22, 247–255.
Bubier, J.L., Bhatia, G., Moore, T.R., Roulet, N.T., Lafleur, P.M., 2003. Spatial and Temporal Variability in Growing-Season Net Ecosystem Carbon Dioxide Exchange at a Large Peatland in Ontario, Canada. Ecosystems 6, 353–367. https://doi.org/10.1007/s10021-003-0125-0
Bullock, A., Acreman, M., 2003. The Role of Wetlands in the Carbon Cycle. Hydrol. Earth Syst. Sci. 7, 358–389.
Burns, D.A., Plummer, L.N., McDonnell, J.J., Busenberg, E., Casile, G.C., Kendall, C., Hooper, R.P., Freer, J.E., Peters, N.E., Beven, K., Schlosser, P., 2003. The Geochemical Evolution of Riparian Ground Water in a Forested Piedmont Catchment. Ground Water 41, 913–925. https://doi.org/10.1111/j.1745-6584.2003.tb02434.x
Buttle, J., 2006. Mapping first-order controls on streamflow from drainage basins: the T3 template. Hydrol. Process. 20, 3415–3422. https://doi.org/10.1002/hyp
Carey, S.K., Quinton, W.L., Goeller, N.T., 2007. Field and laboratory estimates of pore size properties and hydraulic characteristics for subarctic organic soils. Hydrol. Process. 21, 2560–2571. https://doi.org/10.1002/hyp.6795
Carrer, G.E., Rousseau, A.N., Jutras, S., Fossey, M., 2016. Assessment of the impact of pools on

the water isotopic signature of a boreal patterned peatland. Hydrol. Process. 30, 1292–1307. https://doi.org/10.1002/hyp.10715
Cartwright, I., Morgenstern, U., 2016. Contrasting transit times of water from peatlands and eucalypt forests in the Australian Alps determined by tritium: implications for vulnerability and the source of water in upland catchments. Hydrol. Earth Syst. Sci. 20, 4757–4773. https://doi.org/10.5194/hess-20-4757-2016
Catling, P.M., Brownwell, V.R., 1999. The Flora and Ecology of Southern Ontario Granite Barrens, in: Anderson, R.C., Fralish, J.S., Baskin, J.M. (Eds.), Savannas, BArrens and Rock Outcrop Plant Communities of North America. Cambridge University Press.
Chang, E., Wolf, A., Gerlein-Safdi, C., Caylor, K.K., 2016. Improved removal of volatile organic compounds for laser-based spectroscopy of water isotopes. Rapid Commun. Mass Spectrom. 30, 784–790. https://doi.org/10.1002/rcm.7497
Charman, D.J., Aravena, R., Warnert, B.G., 1994. Carbon Dynamics in a Forested Peatland in North-Eastern Ontario , Canada. J. Ecol. 82, 55–62.
Chason, D.B., Siegel, D.I., 1986. Hydraulic conductivity and related physical properties of peat. Soil Sci.
Chen, Y., Senesi, N., Schnitzer, M., 1977. Information Provided on Humic Substances by E4/E6 Ratios. Soil Sci. Soc. Am. J. 41, 352. https://doi.org/10.2136/sssaj1977.03615995004100020037x
Chesson, L.A., Bowen, G.J., Ehleringer, J.R., 2010. Analysis of the hydrogen and oxygen stable isotope ratios of beverage waters without prior water extraction using isotope ratio infrared spectroscopy. Rapid Commun. Mass Spectrom. 24, 3205–3213. https://doi.org/10.1002/rcm.4759
Clark, I., Fritz, P., 1997. Environmental Isotopes in Hydrogeology, 1st ed. CRC Press, Boca Raton, FL. https://doi.org/10.1002/047147844X.gw211
Clymo, R.S., 1984. The Limits to Peat Bog Growth. Philos. Trans. R. Soc. Lond. B. Biol. Sci. 303, 605–654.
Clymo, R.S., 1965. Experiments on Breakdown of Sphagnum in Two Bogs. J. Ecol. 53, 747. https://doi.org/10.2307/2257633
Clymo, R.S., Turunen, J., Tolonen, K., 1998. Carbon Accumulation in Peatland. Oikos 81, 368–388.
Cohen, M.J., Creed, I.F., Alexander, L., Basu, N.B., Calhoun, A.J.K., Craft, C., D'Amico, E., DeKeyser, E., Fowler, L., Golden, H.E., Jawitz, J.W., Kalla, P., Kirkman, L.K., Lane, C.R., Lang, M., Leibowitz, S.G., Lewis, D.B., Marton, J., McLaughlin, D.L., Mushet, D.M., Raanan-Kiperwas, H., Rains, M.C., Smith, L., Walls, S.C., 2016. Do geographically isolated wetlands influence landscape functions? Proc. Natl. Acad. Sci. U. S. A. 113, 1–9. https://doi.org/10.1073/pnas.1512650113
Conrad, R., 1999. Contribution of hydrogen to methane production and control of hydrogen cocnentrations in methanogenic soils. FEMS Microb. Ecol. 28, 193–202. https://doi.org/10.1111/j.1574-6941.1999.tb00575.x
Cory, R.M., McKnight, D.M., 2005. Fluorescence spectroscopy reveals ubiquitous presence of oxidized and reduced quinones in dissolved organic matter. Environ. Sci. Technol. 39, 8142–8149. https://doi.org/10.1021/es0506962
Cory, R.M., Miller, M.P., McKnight, D.M., Guerard, J.J., Miller, P.L., 2010. Effect of instrument-specific response on the analysis of fulvic acid fluorescence spectra. Limnol. Oceanogr. Methods 8, 67–78. https://doi.org/10.4319/lom.2010.8.67

Craig, H., 1961. Isotopic Variations in Meteoric Waters. Science (80-.). 133, 1702–1703.
Dahlén, J., Bertilsson, S., Pettersson, C., 1996. Effects of UV-A irradiation on dissolved organic matter in humic surface waters. Environ. Int. 22, 501–506. https://doi.org/10.1016/0160-4120(96)00038-4
Damman, A.A.W.H., 1978. Nordic Society Oikos Distribution and Movement of Elements in Ombrotrophic Peat Bogs. Oikos 30, 480–495.
Dansgaard, W., 1964. Stable isotopes in precipitation. Tellus 16, 436–468. https://doi.org/10.1111/j.2153-3490.1964.tb00181.x
de Dreuzy, J.-R., Ginn, T.R., 2016. Residence times in subsurface hydrological systems, introduction to the Special Issue. J. Hydrol. 543, 1–6. https://doi.org/10.1016/j.jhydrol.2016.11.046
De Haan, H., 1993. Solar UV-light penetration and photodegradation of humic substances in peaty lake water. Limnol. Oceanogr. 38, 1072–1076. https://doi.org/10.4319/lo.1993.38.5.1072
De Meester, L., Declerck, S., Stoks, R., Louette, G., Van De Meutter, F., De Bie, T., Michels, E., Brendonck, L., 2005. Ponds and pools as model systems in conservation biology, ecology and evolutionary biology. Aquat. Conserv. Mar. Freshw. Ecosyst. 15, 715–725. https://doi.org/10.1002/aqc.748
Devito, K.J., Dillon, P.J., Lazerte, B.D., 1989. Phosphorus and nitrogen retention in five Precambrian shield wetlands. Biogeochemistry 8, 185–204. https://doi.org/10.1007/BF00002888
DeWalle, D., Edwards, P., Swistock, B., Aravena, R., Drimmie, R., 1997. Seasonal isotope hydrology of three Appalachian forest catchments. Hydrol. Process. 11, 1895–1906. https://doi.org/10.1002/(SICI)1099-1085(199712)11:15<1895::AID-HYP538>3.3.CO;2-R
Didemus, B., 2016. Water storage dynamics in peat-filled depressions of canadian shield rock barrens: implications for primary peat formation.
England, N., 2017. Hydrological Characterization of the Sturgeon River Watershed in Northeastern Ontario: A Hydrometric and Water Isotope Analysis. Nipissing University.
Epstein, S., Mayeda, T., 1953. Variation of O18 content of waters from natural sources. Geochim. Cosmochim. Acta 4, 213–224. https://doi.org/10.1016/0016-7037(53)90051-9
Ferronsky, V.I., Polyakov, V. a, 2012. Isotopes of the Earth's Hydrosphere. https://doi.org/10.1007/978-94-007-2856-1
Fogel, R., Cromack Jr., K., 1977. Effect of habitat and substrate quality on Douglas fir litter decomposition in western Oregon. Can. J. Bot. 55, 1632–1640. https://doi.org/10.1139/b77-190
Fraser, C.J.D., Roulet, N.T., Lafleur, M., 2001. Groundwater flow patterns in a large peatland. J. Hydrol. 246, 142–154. https://doi.org/10.1016/S0022-1694(01)00362-6
Fraser, C.J.D., Roulet, N.T., Moore, T.R., 2001. Hydrology and dissolved organic carbon biogeochemistry in an ombrotrophic bog. Hydrol. Process. 15, 3151–3166. https://doi.org/10.1002/hyp.322
Freeze, R.A., Cherry, J.A., 1979. Groundwater. Prentice-Hall.
Frisbee, M.D., Allan, C.J., Thomasson, M.J., Mackereth, R., 2007. Hillslope hydrology and wetland response of two small zero-order boreal catchments on the Precambrian Shield. Hydrol. Process. 21, 2979–2997. https://doi.org/10.1002/hyp.6521
Frolking, S., Roulet, N.T., Moore, T.R., Richard, P.J.H., Lavoie, M., Muller, S.D., 2001. Modeling Northern Peatland Decomposition and Peat Accumulation. Ecosystems 4, 479–

498. https://doi.org/10.1007/s10021-001-0105-1
Gabor, R.S., Baker, A., McKnight, D.M., Miller, M.P., 2014. Fluorescence Indices and Their Interpretation, in: Coble, P.G., Lead, J., Baker, A., Reynolds, D., Spencer, R.G.M. (Eds.), Aquatic Organic Matter Fluorescence. Cambridge University Press, New York, NY, pp. 190–230. https://doi.org/10.1017/CBO9781139045452.010
Gat, J., 2010. Isotope hydrology : a study of the water cycle. Imperial College Press.
Gat, J.R., Tzur, Y., 1967. Modification of the isotopic composition of rainwater by processes which occur before groundwater recharge. International Atomic Energy Agency.
Gehre, M., Geilmann, H., Richter, J., Werner, R.A., Brand, W.A., 2004. Continuous flow2H/1H and18O/16O analysis of water samples with dual inlet precision. Rapid Commun. Mass Spectrom. 18, 2650–2660. https://doi.org/10.1002/rcm.1672
Ghermandi, A., Van Den Bergh, J.C.J.M., Brander, L.M., De Groot, H.L.F., Nunes, P.A.L.D., 2010. Values of natural and human-made wetlands: A meta-analysis. Water Resour. Res. 46. https://doi.org/10.1029/2010WR009071
Gibbon, J.W., Scott, D.E., Ryan, T.J., Buhlmann, K. a., Tuberville, T.D., Metts, B.S., Greene, J.L., Mills, T., Leiden, Y., Poppy, S., Winne, C.T., 2000. The Global Decline of Reptiles, Déjà Vu Amphibians. Bioscience 50, 653–666. https://doi.org/10.1641/0006-3568(2000)050[0653:TGDORD]2.0.CO;2
Gibbons, J.W., 2003. Terrestrial habitat: A vital component for herpetofauna of isolated wetlands. Wetlands 23, 630–635. https://doi.org/10.1672/0277-5212(2003)023[0630:THAVCF]2.0.CO;2
Gonfiantini, R., 1978. Standards for stable isotope measurements in natural compounds. Nature 271, 534–536. https://doi.org/10.1038/271534a0
Gorham, E., 1991. Northern peatlands: role in the carbon cycle and probable responses to climatic warming. Ecol. Appl. https://doi.org/10.2307/1941811
Grayson, R., Holden, J., 2012. Continuous measurement of spectrophotometric absorbance in peatland streamwater in northern England: Implications for understanding fluvial carbon fluxes. Hydrol. Process. 26, 27–39. https://doi.org/10.1002/hyp.8106
Gröning, M., Lutz, H.O., Roller-Lutz, Z., Kralik, M., Gourcy, L., Pöltenstein, L., 2012. A simple rain collector preventing water re-evaporation dedicated for δ 18O and δ 2H analysis of cumulative precipitation samples. J. Hydrol. 448–449, 195–200. https://doi.org/10.1016/j.jhydrol.2012.04.041
Grover, S.P.P., Baldock, J.A., 2013. The link between peat hydrology and decomposition: Beyond von Post. J. Hydrol. 479, 130–138. https://doi.org/10.1016/j.jhydrol.2012.11.049
Gupta, P., Noone, D., Galewsky, J., Sweeney, C., Vaughn, B.H., 2009. Demonstration of high-precision continuous measurements of water vapor isotopologues in laboratory and remote field deployments using wavelength-scanned cavity ring-down spectroscopy (WS-CRDS) technology. Rapid Commun. Mass Spectrom. 23, 2534–2542. https://doi.org/10.1002/rcm.4100
Hartley, W.N., 1893. XV. - Observations on the origin of colour and on fluorescence. J. Chem. Soc. Trans. 63, 243–256. https://doi.org/10.1039/CT8936300243
Harvey, D.S., Weatherhead, P.J., 2006. Hibernation site selection by eastern massasauga rattlensakes (Sistrurus catenatus catenatus) near their northern range limit. J. Herpetol. 40, 66–73. https://doi.org/10.1670/89-05A.1
Hautala, K., Peuravuori, J., Pihlaja, K., 2000. Measurement of aquatic humus content by spectroscopic analyses. Water Res. 34, 246–258. https://doi.org/10.1016/S0043-

1354(99)00137-2
Hayashi, M., Quinton, W.L., Pietroniro, A., Gibson, J.J., 2004. Hydrologic functions of wetlands in a discontinuous permafrost basin indicated by isotopic and chemical signatures. J. Hydrol. 296, 81–97. https://doi.org/10.1016/j.jhydrol.2004.03.020
Hayward, P.., Clymo, R.S., 1982. Profiles of Water Content and Pore Size in Sphagnum and Peat , and their Relation to Peat Bog Ecology. Proc. R. Soc. London. Ser. B, Biol. Sci. 215, 299–325.
Hoefs, J., 2009. Stable Isotope Geochemistry, 6th ed. Springer-Verlag, Berlin, Heidelberg. https://doi.org/10.1017/CBO9781107415324.004
Holden, J., Burt, T.P., Cox, N.J., 2001. Macroporosity and infiltration in blanket peat: The implicaions of tension disc infiltrometer measurements. Hydrol. Process. 15, 289–303. https://doi.org/10.1002/hyp.93
Holland, J.F., Martin, J.F., Granata, T., Bouchard, V., Quigley, M., Brown, L., 2004. Effects of wetland depth and flow rate on residence time distribution characteristics. Ecol. Eng. 23, 189–203. https://doi.org/10.1016/j.ecoleng.2004.09.003
Hrachowitz, M., Soulsby, C., Tetzlaff, D., Dawson, J.J.C., Dunn, S.M., Malcolm, I.A., 2009. Using long-term data sets to understand transit times in contrasting headwater catchments. J. Hydrol. 367, 237–248. https://doi.org/10.1016/J.JHYDROL.2009.01.001
Hrachowitz, M., Soulsby, C., Tetzlaff, D., Malcolm, I.A., 2011. Sensitivity of mean transit time estimates to model conditioning and data availability. Hydrol. Process. 25, 980–990. https://doi.org/10.1002/hyp.7922
Huguet, A., Vacher, L., Relexans, S., Saubusse, S., Froidefond, J.M., Parlanti, E., 2009. Properties of fluorescent dissolved organic matter in the Gironde Estuary. Org. Geochem. 40, 706–719. https://doi.org/10.1016/j.orggeochem.2009.03.002
Ingram, H., 1978. Soil Layers in Mires: Function and Terminology. J. Soil Sci. 29, 224–227. https://doi.org/10.1111/j.1365-2389.1978.tb02053.x
Ivanov, K.E., 1981. Water movement in mirelands. Water Mov. mirelands.
Ivarson, K.C., 1977. Changes in decomposition rate, microbial population and carbohydrate content of an acid peat bog after liming and reclamation. Can. J. Soil Sci. 57, 129–137. https://doi.org/10.4141/cjss77-017
Johnson, B.D., 2000. The phylogeography of the western hognose snake. Am. Zool. 40, 1079–1079.
Johnson, L.C., Damman, A.W.H., 1991. Species-Controlled Sphagnum Decay on a South Swedish Raised Bog. Oikos 61, 234–242.
Johnson, L.C., Damman, A.W.H., Malmer, N., 1990. Sphagnum Macrostructure as an Indicator of Decay and Compaction in Peat Cores from an Ombotrophic Soouth Swedish Peat Bog. J. Ecol. 78, 633–647.
Johnson, M.G., Granath, G., Tahvanainen, T., Pouliot, R., Stenøien, H.K., Rochefort, L., Rydin, H., Shaw, A.J., 2015. Evolution of niche preference in *Sphagnum* peat mosses. Evolution (N. Y). 69, 90–103. https://doi.org/10.1111/evo.12547
Jordan, S.J., Stoffer, J., Nestlerode, J.A., 2011. Wetlands as Sinks for Reactive Nitrogen at Continental and Global Scales: A Meta-Analysis. Ecosystems 14, 144–155. https://doi.org/10.1007/s10021-010-9400-z
Kalviainen, E., Karunen, P., 1984. On the growth, senescence and decay-resistance of Sphagnum mosses. Proc. 7th Int. Peat Congr. Dublin, Irel. 18-23 June 1984.
Karunen, P., Ekman, R., 1982. Age-dependent content of polymerized lipids in Sphagnum

fuscum. Physiol. Plant. 54, 162–166. https://doi.org/10.1111/j.1399-3054.1982.tb06320.x
Kerrigan, E., 2015. USING THE δ18O-SALINITY RELATIONSHIP TO IDENTIFY FRESHWATER INPUTS TO A NORTH ATLANTIC ESTUARY. Dalhousie University.
Kerstel, E.R.T., Trigt, R. van, Dam, N., Reuss, J., Meijer, H.A.J., 1999. Simultaneous Determination of the 2H/1H, 17O/16O, and 18O/16O Isotope Abundance Ratios in Water by Means of Laser Spectrometry. Anal. Chem. 71, 5297–5303. https://doi.org/10.1021/AC990621E
Khadka, B., Munir, T.M., Strack, M., 2016. Dissolved organic carbon in a constructed and natural fens in the Athabasca oil sands region, Alberta, Canada. Sci. Total Environ. 557–558, 579–589. https://doi.org/10.1016/j.scitotenv.2016.03.081
Khadka, B., Munir, T.M., Strack, M., 2015. Effect of environmental factors on production and bioavailability of dissolved organic carbon from substrates available in a constructed and reference fens in the Athabasca oil sands development region. Ecol. Eng. 84, 596–606. https://doi.org/10.1016/j.ecoleng.2015.09.061
Kreutz, K.J., Wake, C.P., Aizen, V.B., Cecil, L.D., Synal, H.-A., 2003. Seasonal deuterium excess in a Tien Shan ice core: Influence of moisture transport and recycling in Central Asia. Geophys. Res. Lett. 30. https://doi.org/10.1029/2003GL017896
Kuhry, P., Nicholson, B.J., Gignac, L.D., Vitt, D.H., Bayley, S.E., 1993. Development of Sphagnum -dominated peatlands in boreal continental Canada. Can. J. Bot. 71, 10–22. https://doi.org/10.1139/b93-002
Lafleur, P.M., Roulet, N.T., Admiral, S.W., 2001. Annual cycle of CO2 exchange at a bog peatland. J. Geophys. Res. 106, 3071. https://doi.org/10.1029/2000JD900588
Leibowitz, S.G., 2009. Isolated Wetlands and their Functions: An Ecological Perspective. Wetlands 23, 517–531. https://doi.org/10.1672/0277-5212(2003)023[0517:IWATFA]2.0.CO;2
Levy, Z.F., Siegel, D.I., Dasgupta, S.S., Glaser, P.H., Welker, J.M., 2014. Stable isotopes of water show deep seasonal recharge in northern bogs and fens. Hydrol. Process. 28, 4938–4952. https://doi.org/10.1002/hyp.9983
Lindberg, B., Theander, O., Motzfeldt, K., Finsnes, E., Sörensen, J.S., Sörensen, N.A., 1952. Studies on Sphagnum Peat. II. Lignin in Sphagnum. Acta Chem. Scand. 6, 311–312. https://doi.org/10.3891/acta.chem.scand.06-0311
Lis, G., Wassenaar, L.I., Hendry, M.J., 2008. High-Precision Laser Spectroscopy D/H and 18O/16O Measurements of Microliter Natural Water Samples. Anal. Chem. 80, 287–293. https://doi.org/10.1021/AC701716Q
Loisel, J., Garneau, M., 2010. Late Holocene paleoecohydrology and carbon accumulation estimates from two boreal peat bogs in eastern Canada: Potential and limits of multi-proxy archives. Palaeogeogr. Palaeoclimatol. Palaeoecol. 291, 493–533. https://doi.org/10.1016/j.palaeo.2010.03.020
Loisel, J., Yu, Z., Beilman, D.W., Camill, P., Alm, J., Amesbury, M.J., Anderson, D., Andersson, S., Bochicchio, C., Barber, K., Belyea, L.R., Bunbury, J., Chambers, F.M., Charman, D.J., De Vleeschouwer, F., Fiałkiewicz-Kozieł, B., Finkelstein, S.A., Gałka, M., Garneau, M., Hammarlund, D., Hinchcliffe, W., Holmquist, J., Hughes, P., Jones, M.C., Klein, E.S., Kokfelt, U., Korhola, A., Kuhry, P., Lamarre, A., Lamentowicz, M., Large, D., Lavoie, M., MacDonald, G., Magnan, G., Mäkilä, M., Mallon, G., Mathijssen, P., Mauquoy, D., McCarroll, J., Moore, T.R., Nichols, J., O'Reilly, B., Oksanen, P., Packalen, M., Peteet, D., Richard, P.J.H., Robinson, S., Ronkainen, T., Rundgren, M., Sannel, A.B.K., Tarnocai,

C., Thom, T., Tuittila, E.S., Turetsky, M., Väliranta, M., van der Linden, M., van Geel, B., van Bellen, S., Vitt, D., Zhao, Y., Zhou, W., 2014. A database and synthesis of northern peatland soil properties and Holocene carbon and nitrogen accumulation. Holocene 24, 1028–1042. https://doi.org/10.1177/0959683614538073

Malmer, N., Holm, E., 1984. Nordic Society Oikos Variation in the C / N-Quotient of Peat in Relation to Decomposition Rate and Age Determination with 210 Pb. Oikos 43, 171–182.

Maloszewski, P., Rauert, W., Stichler, W., Herrmann, A., 1983. Application of flow models in an alpine catchment area using tritium and deuterium data. J. Hydrol. 66, 319–330. https://doi.org/10.1016/0022-1694(83)90193-2

Markle, C.E., Chow-Fraser, P., 2014. Habitat Selection by the Blanding's Turtle (*Emydoidea blandingii*) on a Protected Island in Georgian Bay, Lake Huron. Chelonian Conserv. Biol. 13, 216–226. https://doi.org/10.2744/CCB-1075.1

Marton, J.M., Creed, I.F., Lewis, D.B., Lane, C.R., Basu, N.B., Cohen, M.J., Craft, C.B., 2015. Geographically isolated wetlands are important biogeochemical reactors on the landscape. Bioscience 65, 408–418. https://doi.org/10.1093/biosci/biv009

Mažeika, J., Guobytė, R., Kibirkštis, G., Petrošius, R., Skuratovič, Ž., Taminskas, J., 2009. The Use of Carbon-14 and Tritium For Peat and Water Dynamics Characterization: Case of Čepkeliai Peatland, Southeastern Lithuania. Geochronometria 34, 41–48. https://doi.org/10.2478/v10003-009-0007-3

McGuire, K.J., McDonnell, J.J., 2006. A review and evaluation of catchment transit time modeling. J. Hydrol. 330, 543–563. https://doi.org/10.1016/j.jhydrol.2006.04.020

McGuire, K.J., McDonnell, J.J., Weiler, M., Kendall, C., McGlynn, B.L., Welker, J.M., Seibert, J., 2005. The role of topography on catchment-scale water residence time. Water Resour. Res. 41, 1–14. https://doi.org/10.1029/2004WR003657

McKnight, D.M., Boyer, E.W., Westerhoff, P.K., Doran, P.T., Kulbe, T., Andersen, D.T., 2001. Spectrofluorometric characterization of dissolved organic matter for indication of precursor organic material and aromaticity. Limnol. Oceanogr. 46, 38–48. https://doi.org/10.4319/lo.2001.46.1.0038

Meehl, G.A., Tebaldi, C., 2004. More intense, more frequent, and longer lasting heat waves in the 21st century. Science (80-.). 305, 994–997. https://doi.org/10.1126/science.1098704

Moore, P.A., Morris, P.J., Waddington, J.M., 2015. Multi-decadal water table manipulation alters peatland hydraulic structure and moisture retention. Hydrol. Process. 29, 2970–2982. https://doi.org/10.1002/hyp.10416

Moore, T.R., 1987. A PRELIMINARY STUDY OF THE EFFECTS OF DRAINAGE AND HARVESTING ON WATER QUALITY IN OMBROTROPHIC BOGS NEAR SEPT-ILES, QUEBEC. JAWRA J. Am. Water Resour. Assoc. 23, 785–791. https://doi.org/10.1111/j.1752-1688.1987.tb02953.x

Moore, T.R., Bubier, J.L., Bledzki, L., 2007. Litter Decomposition in Temperate Peatland Ecosystems: The Effect of Substrate and Site. Ecosystems 10, 949–963. https://doi.org/10.1007/s10021-007-9064-5

Morris, P.J., Baird, A.J., Belyea, L.R., 2013. The role of hydrological transience in peatland pattern formation. Earth Surf. Dyn. 1, 29–43. https://doi.org/10.5194/esurf-1-29-2013

Morris, P.J., Waddington, J.M., 2011. Groundwater residence time distributions in peatlands: Implications for peat decomposition and accumulation. Water Resour. Res. 47, 1–12. https://doi.org/10.1029/2010WR009492

Morris, P.J., Waddington, J.M., Benscoter, B.W., Turetsky, M.R., 2011. Conceptual frameworks

in peatland ecohydrology: lookign beyond the two-layered (acrotelm-catotelm) model. Ecohydrology 4, 1–11. https://doi.org/10.1002/eco
Mountain, N., James, A.L., Chutko, K., 2015. Groundwater and surface water influences on streamflow in a mesoscale Precambrian Shield catchment. Hydrol. Process. 29, 3941–3953. https://doi.org/10.1002/hyp.10590
Mushet, D.M., Calhoun, A.J.K., Alexander, L.C., Cohen, M.J., DeKeyser, E.S., Fowler, L., Lane, C.R., Lang, M.W., Rains, M.C., Walls, S.C., 2015. Geographically Isolated Wetlands: Rethinking a Misnomer. Wetlands 35, 423–431. https://doi.org/10.1007/s13157-015-0631-9
O'Driscoll, N.J., Siciliano, S.D., Peak, D., Carignan, R., Lean, D.R.S., 2006. The influence of forestry activity on the structure of dissolved organic matter in lakes: Implications for mercury photoreactions. Sci. Total Environ. 366, 880–893. https://doi.org/10.1016/j.scitotenv.2005.09.067
O'Keefe, A., Deacon, D.A.G., 1988. Cavity ring-down optical spectrometer for absorption measurements using pulsed laser sources. Rev. Sci. Instrum. 59, 2544–2551. https://doi.org/10.1063/1.1139895
Ohno, T., 2002. Fluorescence inner-filtering correction for determining the humification index of dissolved organic matter. Environ. Sci. Technol. 36, 742–746. https://doi.org/10.1021/es0155276
Ohsumi, T., Fujino, H., 1986. Isotopic exchange technique for preparation of hydrogen gas in mass spectrometric D/H analysis of natural waters. Anal. Sci. 2, 489–490 [1–2]. https://doi.org/10.2116/analsci.2.489
Oswald, C.J., Richardson, M.C., Branfireun, B.A., 2011. Water storage dynamics and runoff response of a boreal Shield headwater catchment. Hydrol. Process. 25, 3042–3060. https://doi.org/10.1002/hyp.8036
Pakarinen, P., 1978. Distribution of heavy metals in the Sphagnum layer of bog hummocks and hollows. Ann. Bot. Fenn. 15, 287–292. https://doi.org/10.2307/23725281
Parlanti, E., Wörz, K., Geoffroy, L., Lamotte, M., 2000. Dissolved organic matter fluorescence spectroscopy as a tool to estimate biological activity in a coastal zone submitted to anthropogenic inputs. Org. Geochem. 31, 1765–1781. https://doi.org/10.1016/S0146-6380(00)00124-8
Payne, R.J., Malysheva, E., Tsyganov, A., Pampura, T., Novenko, E., Volkova, E., Babeshko, K., Mazei, Y., 2016. A multi-proxy record of Holocene environmental change, peatland development and carbon accumulation from Staroselsky Moch peatland, Russia. Holocene 26, 314–326. https://doi.org/10.1177/0959683615608692
Peacock, M., Evans, C.D., Fenner, N., Freeman, C., Gough, R., Jones, T.G., Lebron, I., 2014. UV-visible absorbance spectroscopy as a proxy for peatland dissolved organic carbon (DOC) quantity and quality: considerations on wavelength and absorbance degradation. Environ. Sci. Process. Impacts 16, 1445. https://doi.org/10.1039/c4em00108g
Penna, D., Stenni, B., Šanda, M., Wrede, S., Bogaard, T.A., Gobbi, A., Borga, M., Fischer, B.M.C., Bonazza, M., Chárová, Z., 2010. On the reproducibility and repeatability of laser absorption spectroscopy measurements for δ2H and δ18O isotopic analysis. Hydrol. Earth Syst. Sci. 14, 1551–1566. https://doi.org/10.5194/hess-14-1551-2010
Peuravuori, J., Pihlaja, K., 1997. Molecular size distribution and spectroscopic properties of aquatic humic substances. Anal. Chim. Acta 337, 133–149. https://doi.org/10.1016/S0003-2670(96)00412-6
Phillips, R.W., Spence, C., Pomeroy, J.W., 2011. Connectivity and runoff dynamics in

heterogeneous basins. Hydrol. Process. 25, 3061–3075. https://doi.org/10.1002/hyp.8123
Postila, H., Ronkanen, A.K., Marttila, H., Kløve, B., 2015. Hydrology and hydraulics of treatment wetlands constructed on drained peatlands. Ecol. Eng. 75, 232–241. https://doi.org/10.1016/j.ecoleng.2014.11.041
Price, J.S., Heathwaite, a. L., Baird, a. J., 2003. Hydrological processes in abandoned and restored peatlands:an overview of management approaches. Wetl. Ecol. Manag. 11, 65–83. https://doi.org/10.1023/A:1022046409485
Rains, M.C., Leibowitz, S.G., Cohen, M.J., Creed, I.F., Golden, H.E., Jawitz, J.W., Kalla, P., Lane, C.R., Lang, M.W., Mclaughlin, D.L., 2016. Geographically isolated wetlands are part of the hydrological landscape. Hydrol. Process. 30, 153–160. https://doi.org/10.1002/hyp.10610
Rastelli, J., 2016. Dissolved organic carbon concentration, patterns and quality at a reclaimed and two natural wetlands, Fort McMurray, Alberta. McMaster University.
Redding, T.E., Devito, K.J., 2006. Particle densities of wetland soils in northern Alberta, Canada. Can. J. Soil Sci. 86, 57–60. https://doi.org/10.4141/S05-061
Rock, L., Mayer, B., 2007. Isotope hydrology of the Oldman River basin, southern Alberta, Canada. Hydrol. Process. 21, 3301–3315. https://doi.org/10.1002/hyp.6545
Romanowicz, E.A., Siegel, D.I., Glaser, P.H., 1993. Hydraulic reversals and episodic methane emissions during drought cycles in mires. Geology 21, 231. https://doi.org/10.1130/0091-7613(1993)021<0231:HRAEME>2.3.CO;2
Rudolph, H., Samland, J., 1985. Occurrence and metabolism of sphagnum acid in the cell walls of bryophytes. Phytochemistry 24, 745–749. https://doi.org/10.1016/S0031-9422(00)84888-8
Schmidt, M., Maseyk, K., Lett, C., Biron, P., Richard, P., Bariac, T., Seibt, U., 2012. Reducing and correcting for contamination of ecosystem water stable isotopes measured by isotope ratio infrared spectroscopy. Rapid Commun. Mass Spectrom. 26, 141–153. https://doi.org/10.1002/rcm.5317
Schouwenaars, J.M., 1988. The impact of water management upon groundwater fluctuations in a disturbed bog relict. Agric. Water Manag. 14, 439–449. https://doi.org/10.1016/0378-3774(88)90096-0
Schultz, N.M., Griffis, T.J., Lee, X., Baker, J.M., 2011. Identification and correction of spectral contamination in 2H/1H and 18O/16O measured in leaf, stem, and soil water. Rapid Commun. Mass Spectrom. 25, 3360–3368. https://doi.org/10.1002/rcm.5236
Siegel, D.I., Reeve, A.S., Glaser, P.H., Romanowicz, E.A., 1995. Climate-driven flushing of pore water in peatlands. Nature 374, 531–533. https://doi.org/10.1038/374531a0
Smolarz, A., 2017. Thermal and hydrological conditions of reptile species-at-risk habitat along eastern Georgian bay during critical life stages. McMaster University.
Smolarz, A.G., Moore, P.A., Markle, C.E., Waddington, J.M., 2018. Identifying resilient eastern massasauga rattlesnake (Sistrurus catenatus) peatland hummock hibernacula. Can. J. Zool. https://doi.org/10.1139/cjz-2017-0334
Soulsby, C., Tetzlaff, D., 2008. Towards simple approaches for mean residence time estimation in ungauged basins using tracers and soil distributions. J. Hydrol. 363, 60–74. https://doi.org/10.1016/j.jhydrol.2008.10.001
Spence, C., Woo, M., 2008. Hydrology of the Northwestern Subarctic Canadian Shield, in: Cold Region Atmospheric and Hydrologic Studies. The Mackenzie GEWEX Experience. Springer Berlin Heidelberg, Berlin, Heidelberg, pp. 235–256. https://doi.org/10.1007/978-3-

540-75136-6_13
Spence, C., Woo, M., 2006. Hydrology of subarctic Canadian Shield: heterogeneous headwater basins. J. Hydrol. 317, 138–154. https://doi.org/10.1016/J.JHYDROL.2005.05.014
Spence, C., Woo, M., 2003. Hydrology of subarctic Canadian shield: soil-filled valleys. J. Hydrol. 279, 151–166. https://doi.org/10.1016/S0022-1694(03)00175-6
Spencer, R.G.M., Bolton, L., Baker, A., 2007. Freeze/thaw and pH effects on freshwater dissolved organic matter fluorescence and absorbance properties from a number of UK locations. Water Res. 41, 2941–2950. https://doi.org/10.1016/j.watres.2007.04.012
Stedmon, C. a., Bro, R., 2008. Characterizing dissolved organic matter fluorescence with parallel factor analysis: a tutorial. Limnol. Oceanogr. Methods 6, 572–579. https://doi.org/10.4319/lom.2008.6.572
Stockinger, M.P., Bogena, H.R., Lücke, A., Diekkrüger, B., Cornelissen, T., Vereecken, H., 2016. Tracer sampling frequency influences estimates of young water fraction and streamwater transit time distribution. J. Hydrol. 541, 952–964. https://doi.org/10.1016/J.JHYDROL.2016.08.007
Strack, M., Tóth, K., Bourbonniere, R., Waddington, J.M., 2011. Dissolved organic carbon production and runoff quality following peatland extraction and restoration. Ecol. Eng. 37, 1998–2008. https://doi.org/10.1016/j.ecoleng.2011.08.015
Summers, R.S., Cornel, P.K., Roberts, P.V., 1987. Molecular size distribution and spectroscopic characterization of Humic substances. Sci. Total Environ. 62, 27–37. https://doi.org/10.1016/0048-9697(87)90478-5
Surridge, B.W.J., Baird, A.J., Heathwaite, A.L., 2005. Evaluating the quality of hydraulic conductivity estimates from piezometer slug tests in peat. Hydrol. Process. 19, 1227–1244. https://doi.org/10.1002/hyp.5653
Tekleab, S., Wenninger, J., Uhlenbrook, S., 2014. Characterisation of stable isotopes to identify residence times and runoff components in two meso-scale catchments in the Abay/Upper Blue Nile basin, Ethiopia. Hydrol. Earth Syst. Sci. 18, 2415–2431. https://doi.org/10.5194/hess-18-2415-2014
Tetzlaff, D., Seibert, J., McGuire, K.J., Laudon, H., Burns, D.A., Dunn, S.M., Soulsby, C., 2009. How does landscape structure influence catchment transit time across different geomorphic provinces? Hydrol. Process. 23, 945–953. https://doi.org/10.1002/hyp.7240
Thormann, M.N., Szumigalski, A.R., Bayley, S.E., 1999. Aboveground peat and carbon accumulation potentials along a bog-fen-marsh wetland gradient in southern boreal Alberta, Canada. Wetlands 19, 305–317. https://doi.org/10.1007/BF03161761
Thurman, E.M., 1985. Organic Geochemistry of Natural Waters. M. Nijhoff. https://doi.org/10.1007/978-94-009-5095-5
Tiner, R.W., 2003. Geographically isolated wetlands of the United States. Wetlands 23, 494–516. https://doi.org/10.1672/0277-5212(2003)023[0494:GIWOTU]2.0.CO;2
Toet, S., Cornelissen, J.H.C., Aerts, R., Van Logtestijn, R.S.P., De Beus, M., Stoevelaar, R., 2006. Moss responses to elevated CO2and variation in hydrology in a temperate lowland peatland. Plant Ecol. 182, 27–40. https://doi.org/10.1007/s11258-005-9029-8
Turetsky, M.R., 2003. The Role of Bryophytes in Carbon and Nitrogen Cycling. Bryologist 106, 395–409. https://doi.org/10.1639/05
Turetsky, M.R., Crow, S.E., Evans, R.J., Vitt, D.H., Wieder, R.K., 2008. Trade-offs in resource allocation among moss species control decomposition in boreal peatlands. J. Ecol. 96, 1297–1305. https://doi.org/10.1111/j.1365-2745.2008.01438.x

Turetsky, M.R., Manning, S.W., Wieder, R.K., 2004. Dating recent peat deposits. Wetlands 24, 324–356. https://doi.org/10.1672/0277-5212(2004)024[0324:DRPD]2.0.CO;2
Vail, J., 2013. SESDPROC-301-R3: Groundwater Sampling.
Valeur, B., 2001. Molecular Fluorescence: Principles and Applications, Wiley-VCH. https://doi.org/10.1002/3527600248
van der Heijden, E., 1994. A combined anatomical and pyrolysis mass spectrometric study of peatified plant tissues. University of Amsterdam.
van Geldern, R., Barth, J.A.C., 2012. Optimization of instrument setup and post-run corrections for oxygen and hydrogen stable isotope measurements of water by isotope ratio infrared spectroscopy (IRIS). Limnol. Oceanogr. Methods 10, 1024–1036. https://doi.org/10.4319/lom.2012.10.1024
Vitt, D.H., Halsey, L.A., Bauer, I.E., Campbell, C., 2000. Spatial and temporal trends in carbon storage of peatlands of continental western Canada through the Holocene. Can. J. Earth Sci. 37, 683–693. https://doi.org/10.1139/e99-097
Waddington, J.M., Morris, P.J., Kettridge, N., Granath, G., Thompson, D.K., Moore, P.A., 2015. Hydrological feedbacks in northern peatlands. Ecohydrology 8, 113–127. https://doi.org/10.1002/eco.1493
Waddington, J.M., Roulet, N.T., 1997. Groundwater flow and dissolved carbon movement in a boreal peatland. J. Hydrol. 191, 122–138. https://doi.org/10.1016/S0022-1694(96)03075-2
Waddington, J.M., Tóth, K., Bourbonniere, R., 2008. Dissolved organic carbon export from a cutover and restored peatland. Hydrol. Process. 22, 2215–2224. https://doi.org/10.1002/hyp.6818
Wahl, E.H., Fidric, B., Rella, C.W., Koulikov, S., Kharlamov, B., Tan, S., Kachanov, A.A., Richman, B.A., Crosson, E.R., Paldus, B.A., Kalaskar, S., Bowling, D.R., 2006. Applications of cavity ring-down spectroscopy to high precision isotope ratio measurement of 13 C/ 12 C in carbon dioxide. Isotopes Environ. Health Stud. 42, 21–35. https://doi.org/10.1080/10256010500502934
Weishaar, J.L., Aiken, G.R., Bergamaschi, B.A., Fram, M.S., Fujii, R., Mopper, K., 2003. Evaluation of specific ultraviolet absorbance as an indicator of the chemical composition and reactivity of dissolved organic carbon. Environ. Sci. Technol. 37, 4702–4708. https://doi.org/10.1021/es030360x
Werner, R.A., Brand, W.A., 2001. Referencing strategies and techniques in stable isotope ratio analysis. Rapid Commun. Mass Spectrom. 15, 501–519. https://doi.org/10.1002/rcm.258
Werner, T.M., Kadlec, R.H., 2000. Wetland residence time distribution modeling. Ecol. Eng. 15, 77–90. https://doi.org/10.1016/S0925-8574(99)00036-1
Whitmire, S.L., Hamilton, S.K., 2005. Rapid Removal of Nitrate and Sulfate in Freshwater Wetland Sediments. J. Environ. Qual. 34, 2062. https://doi.org/10.2134/jeq2004.0483
Whittington, P.N., Strack, M., van Haarlem, R., Kaufman, S., Stoesser, P., Maltez, J., Price, J.S., Stone, M., 2007. The influence of peat volume change and vegetation on the hydrology of a kettle-hole wetland in Southern Ontario, Canada. Mires Peat 2, 1–14.
Wickland, K.P., Neff, J.C., 2008. Decomposition of soil organic matter from boreal black spruce forest: Environmental and chemical controls. Biogeochemistry 87, 29–47. https://doi.org/10.1007/s10533-007-9166-3
Wilson, H.F., Xenopoulos, M.A., 2009. Effects of agricultural land use on the composition of fluvial dissolved organic matter. Nat. Geosci. 2, 37–41. https://doi.org/10.1038/ngeo391
Yavitt, J.B., Williams, C.J., Kelman Wieder, R., 1997. Production of methane and carbon

dioxide in Peatland ecosystems across north America: Effects of temperature, aeration, and organic chemistry of peat. Geomicrobiol. J. 14, 299–316. https://doi.org/10.1080/01490459709378054
Yoshimura, T., 2013. Appropriate bottles for storing seawater samples for dissolved organic phosphorus (DOP) analysis: A step toward the development of DOP reference materials. Limnol. Oceanogr. Methods 11, 239–246. https://doi.org/10.4319/lom.2013.11.239
Zobel, M., 1986. Aeration and temperature conditions in hummock and depression peat in Kikerpera bog, southwestern Estonia. Suo 37, 99–106.
Zsolnay, A., Baigar, E., Jimenez, M., Steinweg, B., Saccomandi, F., 1999. Differentiating with fluorescence spectroscopy the sources of dissolved organic matter in soils subjected to drying. Chemosphere 38, 45–50. https://doi.org/10.1016/S0045-6535(98)00166-0